

Developmental and paleontological insights into skull bone homology and evolution

Rui Alexandre Ferreira Castanhinha

Dissertation presented to obtain the Ph.D degree in
Biology,
Evolutionary Biology

Instituto de Tecnologia Química e Biológica | Universidade
Nova de Lisboa



Research work coordinated by: FUNDAÇÃO CALOUSTE GULBENKIAN
Instituto Gulbenkian de Ciência

Oeiras,
November,
2014



INSTITUTO
DE TECNOLOGIA
QUÍMICA E BIOLÓGICA
/UNL

Knowledge Creation



Declaração/Declaration

Esta dissertação é o resultado do meu próprio trabalho desenvolvido entre Março de 2010 e Setembro de 2014 nos laboratórios do Dr. Joaquín Rodríguez-Léon e do Dr. Élio Sucena, no Instituto Gulbenkian de Ciência em Oeiras, Portugal, no âmbito do Programa Doutoral Gulbenkian intitulado *Programme in Integrative Biomedical Sciences*, do Instituto Gulbenkian de Ciência (edição 2009-2010). Este trabalho encontra-se em fase de preparação para ser publicado em revistas da especialidade.

This dissertation is the result of my own research, carried out between March 2010 and July 2014 in the laboratory of Dr. Joaquín Rodríguez-Léon and Dr. Élio Sucena, at the *Instituto Gulbenkian de Ciência* in Oeiras, Portugal, under the *Instituto Gulbenkian de Ciência* PhD programme, entitled *Programme in Integrative Biomedical Sciences* (2009-2010 edition). This work is being prepared for publication in scientific journals.

Apoio Financeiro/Financial Support

O trabalho aqui descrito contou com o apoio financeiro da FCT e do FSE no âmbito do Quadro Comunitário de Apoio, através da bolsa de doutoramento SFRH / BD / 51184 / 2010

Financial support for this thesis was provided by FCT and FSE through the Community Support Framework, via the doctoral scholarship SFRH / BD / 51184 / 2010

Inspirações, Ajudas e Empurrões

Joaquín Rodríguez-Léon, Élio Sucena, Gabriel G. Martins, Ricardo Araújo, António Coutinho, Thiago Carvalho, Patrícia Beldade, José Leal, Vincent Fernandez, Paul Tafforeau, Elisabeth Dupin, Bárbara Fonseca, Nicole LeDouarin, Gerard Couly, Marie-Aimée Teillet, Marcelo Sanchez-Villagra, Dai Koyabu, Torsten, Nelson Nhamutole, Salimo Murrula, Luís Costa Júnior, Alexandra Tomás, Alexandre Leitão, Vítor Faria, Pedro Lima, Inês Trancoso, Alexis Hazbún (Perez), Inês Direito, Joana Rodrigues e Marta Pinto (meninas da histologia), Ânia, Pimpão, Joana Monteiro, Marco Barros, Christine Koppl, GEAL - Museu da Lourinhã, ESRF, Jurassic Foundation, e muitos outros.

Obrigado à minha família, amo-vos.

Aos meus avós Ferreira e Castanhinha,
a uns pelos beijos, aos outros pelos livros

Summary

The *Gallus gallus* (chicken) embryo is a central model organism in evolutionary developmental biology. Its anatomy and developmental genetics have been extensively studied and many relevant evolutionary implications have been made so far. However, important questions regarding the developmental origin of the chicken skull bones are still unresolved such that no solid homology can be established across organisms. This precludes evolutionary comparisons between this and other avian model systems in which skull anatomy has evolved significantly over the last millions of years. A classical example is the disputed origin of the frontal bone. Different lineage tracing studies present dissimilar results. The first hypothesis claims that a population of cells exclusively derived from neural crest forms this bone. Other authors advocate for a double ontogenetic contribution from neural crest and paraxial mesoderm derived cells. In mice the results are unanimous attributing the origin of the entire frontal bone to cells derived from neural crest, while the posteriorly contiguous bone (the parietal) is formed exclusively by paraxial mesoderm derived cells. At the same time the posterior region of bird's adult skull misses one bone when compared with other Archosauria and mammals. This absence has been traditionally interpreted as an evolutionary lost of the interparietal. Nevertheless, it is not obvious whether the bird's frontal is homologous to one (frontal), or to a fusion of two skull bones (frontal + parietal). Here, we present new data from GFP chicken to wt chicken chimeras and a preliminary interpretation is provided. In addition, embryos from quail, chicken, duck and crocodile were incubated and stained for bone and cartilage every four hours. These experiments, in combination with a thorough examination of the published fossil material available, can help

to establish more complete homology relationships between the skull bones of Aves and Mammalia, shedding new light on our understanding of the evolution of development of the amniote skull since their last common ancestor.

We describe a new fossil clutch from the Upper Jurassic of Portugal. The clutch contains 13 eggs almost without any deformation ML 1582. We performed propagation phase contrast X-ray synchrotron microtomography (PPC-SR- μ CT) to all individual eggs and found that inside there were the first Crocodylomorpha embryos ever described. In addition, we performed a detailed anatomical description comparing the fossil embryos with PPC-SR- μ CT data with embryos from extant crocodiles (*Alligator mississippiensis* and *Crocodylus niloticus*). Furthermore, we performed a morphometric analysis between using four different bones in four different species (fossil embryos, *Crocodylus niloticus*, *Tyto alba*, *Centrochelys sulcata*) and the results confirm a close relation of the fossil embryos with the *Crocodylus niloticus* anatomy.

Combining experimental data with anatomical comparisons seems to confirm that both paleontology and evolutionary developmental biology present complementary and independent lines of evidence towards a better understanding of paleobiology and evolution.

Sumário

O embrião de *Gallus gallus* (galinha) tornou-se um organismo modelo central na biologia evolutiva do desenvolvimento. A sua anatomia e genética do desenvolvimento têm sido extensivamente estudadas com diversas implicações evolutivas relevantes. No entanto, questões importantes a respeito da origem do desenvolvimento dos ossos do crânio da galinha ainda não foram resolvidas de forma a que

possam ser estabelecidas relações sólidas de homologia. Isto impossibilita comparações evolutivas entre este e outros organismos modelo visto que a anatomia do crânio evoluiu significativamente nos últimos milhões de anos. Um exemplo clássico é a origem do frontal. Diferentes estudos de mapeamento de destinos celulares têm apresentado resultados díspares. Alguns estudos defendem que o frontal deriva exclusivamente de células da crista neural. Outros autores defendem que existe uma dupla contribuição da crista neural e de células da mesoderme paraxial. Em ratinhos os resultados atribuem a origem de todo o osso frontal a células derivadas da crista neural, enquanto o osso contíguo (parietal) é formado exclusivamente por células derivadas da mesoderme paraxial. A região posterior do crânio da aves adultas não apresenta um osso quando comparada com outros Archosauria ou mamíferos. Essa ausência tem sido tradicionalmente interpretada como uma perda evolutiva do interparietal. No entanto, não é óbvio se o frontal da aves é homólogo a um (frontal) ou a uma fusão de dois ossos do crânio (frontal + parietal). São aqui apresentados novos dados resultantes de transplantes de embriões de galinhas GFP em embriões de galinhas tipo selvagem (wt). Além disso, foram incubados embriões de codorniz, galinha, pato e crocodilo onde foram corados os ossos e cartilagem em intervalos regulares. Estas experiências, em combinação com um exame detalhado do material fóssil publicado, ajudam a estabelecer relações de homologia mais completas entre os ossos do crânio de Aves e Mamíferos, o que melhora a compreensão da evolução do desenvolvimento do crânio amniota desde o seu ancestral comum mais recente.

Descrevemos ainda uma nova postura de ovos fósseis do Jurássico Superior de Portugal. A postura (ML 1582) contém 13 ovos quase sem qualquer deformação. Realizámos microtomografias de

raios-X por contraste de fase usando feixe de sincrotrão (PPC-SR- μ CT) a todos os ovos aqui descritos. Isto permitiu descobrir no seu interior os primeiros embriões atribuíveis a Crocodylomorpha até agora conhecidos. Além disso, foi realizada uma descrição anatômica detalhada comparando os embriões fósseis com dados de PPC-SR- μ CT de embriões de crocodilos actuais (*Alligator mississippiensis* e *Crocodylus niloticus*). Foi ainda realizada uma análise morfométrica entre quatro ossos diferentes em quatro espécies diferentes (embriões fósseis, *Crocodylus niloticus*, *Tyto alba*, *Centrochelys sulcata*). Os resultados confirmam a estreita relação dos embriões fósseis com a anatomia dos embriões de *Crocodylus niloticus*.

Uma combinação de dados experimentais alicerçada em comparações anatômicas clássicas parece confirmar que tanto a paleontologia como a biologia do desenvolvimento podem apresentar dados complementares e independentes de forma a melhor se poder compreender processos evolutivos complexos.

INDEX

INTRODUCTION	1
THE ORIGINS: DEVELOPMENT AND EVOLUTION OF THE SKULL	1
HOMOLOGY: MORE THAN A PROBLEM, A SOLUTION	2
BONE: ANOTHER PROBLEM, A DIFFERENT SOLUTION	6
MELTING THE POT	8
CHAPTER I	11
<u>TOWARDS THE RESOLUTION OF AN EVOLUTIONARY CONUNDRUM: THE AVES</u>	
<u>FRONTAL BONE</u>	11
INTRODUCTION	12
THE PALEONTOLOGICAL RECORD	23
RESULTS	26
ALIZARIN-RED AND ALCIAN BLUE STAINING	27
CHICKEN (<i>GALLUS GALLUS</i>)	28
QUAIL (<i>COTURNIX COTURNIX</i>)	35
DUCK (<i>ANAS PLATYRHYNCHOS</i>)	38
CROCODILE (<i>ALLIGATOR MISSISSIPPIENSIS</i> AND <i>CROCODYLUS NILOTICUS</i>)	42
MOUSE	45
MICRO-CT	48
QUAIL-CHICK CHIMERAS	52
CHICK GFP-CHICK WT NEURAL CREST TRANSPLANTS	62
NEURAL CREST TRANSPLANTS	62
PARAXIAL MESODERM TRANSPLANTS	75
GRAFTS OF THE PARAXIAL MESODERM AT THE MESENCEPHALIC LEVEL	75
OPT	79
DISCUSSION	82
FRONTAL OSSIFICATION	82
PREFRONTAL/LACRIMAL	89
AUTHORS CONTRIBUTIONS	89
ACKNOWLEDGMENTS	90
CHAPTER II	92

THE FIRST FOSSIL CROCODYLOMORPHA EGGS WITH EMBRYOS: A	
PRELIMINARY DESCRIPTION	92
INTRODUCTION	93
GEOLOGY	96
RESULTS	98
CLUTCH AND EGGS	98
EGGSHELLS	100
EMBRYO ANATOMY	102
Dermatocranium	104
Dermal ossifications	111
Chondrocranium	111
Splanchnocranium	113
Dermal bones of the jaw	114
Inner ear ossifications	115
Other ossifications	116
Postcrania	116
PROCRUSTES ANALYSIS	121
DISCUSSION	124
AUTHORS CONTRIBUTIONS	126
ACKNOWLEDGMENTS	126
GENERAL DISCUSSION	128
REFERENCES	135
APPENDIX A	147
METHODS	147
WHOLE-MOUNT ALIZARIN RED AND ALCIAN BLUE STAINING	147
HISTOLOGICAL TECHNIQUES	150
CRYOPRESERVATION AND SECTIONING	150
HEMATOXYLIN EOSINE STAINING	150
FEULGEN – ROSSENBECK STAINING	151
OPTICAL PROJECTION TOMOGRAPHY (OPT)	153
IMMUNOHISTOCHEMISTRY	154
Solutions needed	154

Protocol	154
IN VIVO MANIPULATION TECHNIQUES	157
Transplants of Neural Crest Cells	157
Transplants of Paraxial Mesoderm Cells	163
MICROSCOPY TECHNIQUES	165
CONFOCAL	165
FLORESCENT STEREO MICROSCOPE	165
COMPUTED TOMOGRAPHY	165
SYNCHROTRON RADIATION-BASED MICRO-COMPUTED TOMOGRAPHY	165
TOMOGRAPHY DATA PROCESSING	167
APPENDIX B	170
<hr/>	
CHAPTER I SUPPLEMENTARY DATA	171
NEURAL CREST	171
MESODERM (FIRST PART)	172
MESODERM (SECOND PART)	173
CHAPTER II SUPPLEMENTARY DATA	175
TABLE SHOWING MEASURES OF EGGS CORRESPONDING TO ML 1582.	175
TABLE SHOWING MEASURES OF APPENDICULAR BONES IN ML 1582 AND <i>CROCODYLUS NILOTICUS</i> .	176

Introduction

The origins: development and evolution of the skull

“Nothing was your own except the few cubic centimeters inside your skull.” George Orwell, 1984.

Our life is housed inside a skull. Everything that we perceive, feel and think, everything that we say or hear is only possible because our sensory organs are lodged in a complex structure composed by bones and cartilages that vary in form and function. Cranial morphology is extremely variable between different animals and yet each species usually presents a fixed number of skull bones with a typical topology. Developmental processes are so robust in shaping each species skull that many taxonomists use only morphological skull characters when describing a new taxon. This is particularly true in comparative anatomy and paleontology given that, additionally, the skull presents a complexity that is not present in post-cranial skeleton. High complexity implies more morphological traits that are the basis for taxonomical work. Furthermore, the skull houses multiple sensory organs and the major anterior part of the central nervous system. This allows paleobiological studies to infer, not only morphological traits, but also hypothetical behaviors of extinct forms. All this stresses the importance of understanding in detail the origin, development and evolution of probably the noblest part of the vertebrate skeleton. Still, many questions remain open regarding how this fascinating structure originated and evolved over the last five hundred million years.

Homology: more than a problem, a solution

In any effort to understand the origins of vertebrata, the skull is of paramount importance. To reconstruct the evolutionary history of any living form it is critical to find the traits that correctly reflect a true descent with modification and discard any deceptive similarities that may result from shared constraints instead of shared ancestry (convergence). This is to say that only homologous traits are relevant in constructing phylogenies. Yet, and as intuitive as it may sound, homology must be defined in a way that is clear and operational.

The first clear definition of homology was coined by Richard Owen in 1843, in a time when many concepts and fundamental biological ideas were yet to be firmly established. The notion of heritability, evolution, common ancestry and many others were mere hypotheses far from being tested and even further from being widely accepted by the scientific community. In this environment Owen, probably the most influential anatomist of his time, defended a revolutionary idea: the notion that many (if not all) animal morphological traits were related, either by form or by function. For the first time the notion of homologous structure was clearly defined. According to his definition an homologous trait was “The same organ in different animals under every variety of form and function” (Owen and Cooper 1843). This definition contrasted with the term “analogy” that Owen defined at the same time as “a part which has the same function as another”. To his mind, all this was simply a corollary of many other concepts that he had been defending all his life. Owen’s *Weltanschauung* implied that the body of different animal groups corresponded to different conceptual archetypes initially designed by a divine entity. These basic body plans could be compared and homology established. At that time, Owen imagined that all vertebrates shared a typical archetype composed by repeated segments

along the body axis. In his idealistic morphology, multiple repeated segments could be shaped and vary, forming different parts of the body ranging from vertebrae, to limbs or even the different bones of the skull (see Fig.1). All extant and extinct vertebrates would derive from this ideal archetype. Here “derive” refers only to variation from an original prototype and is not an indication of any ancestry relationship.

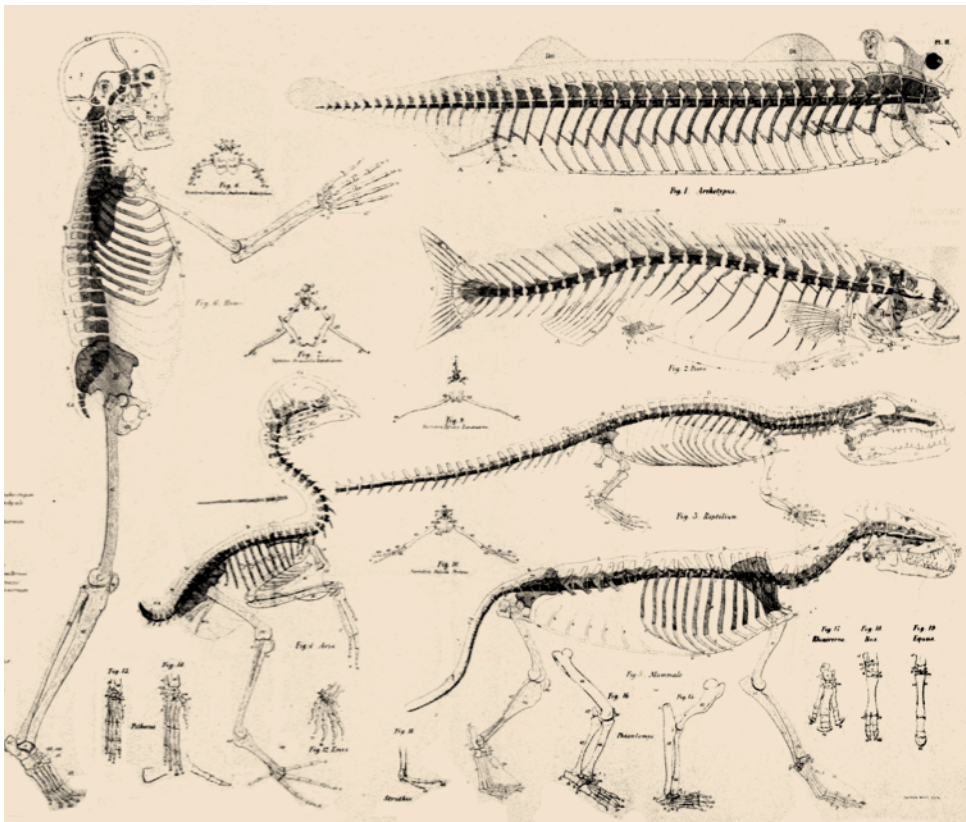


Fig.1 Vertebrata conceptual archetype as idealized by Owen. The body of vertebrates was described as having multiple segments that in combination formed the different elements of the body, from head to tail. Image adapted from (Owen 1848).

Curiously, Owen never concluded that his archetypes could simply represent ancestral stages that give origin to modern forms of life

through evolutionary processes. For him, homologies were indicative of a divine plan and not of common ancestry. Presently, the expression “same organ“ in Owen’s original definition is interpreted, not as an identical structure, but as a trait that is derived from a shared ancestral structure (Raff 1996). Sameness is now viewed as synonym of ancestry.

Since its origins the term “homologous” has been subject of extensive debate and different authors use it with dissimilar connotations (Wagner 2014 and references therein). Actually, Owen (although the first to propose a clear definition) did not invent the concept. The idea that all living organisms could be related either by form or by function had being discussed since Aristotle that recognized dolphins as closely related to mammals, rather than to fish (Panchen 1999). Many others since developed multiple ideas about the concept of unity by form. The XVIII and XIX centuries exploded with new hypotheses and debates over the nature of the living world. In 1830, Étienne Geoffroy de Saint-Hilaire defined *analogie* (referring to homologous structures) as “essential similarity” or “philosophical similarity” thus defining a concept in all aspects equivalent to the notion of homology idealized by Owen almost two decades after. Saint-Hilaire had the opposition of probably the most important anatomist of his time: Georges Cuvier. The two had publicly antagonistic views about the natural world and their disagreements were famous (Rieppel 1994). Cuvier defended the concept that all living forms were predetermined by the Creator’s mind and no animal or plant could be viewed as a variation of a typical plan. Each living being was a perfect match between form and function and without relation, neither under a shared Bauplan nor subject to modification over time.

The concept of homology has had multiple meanings over historical time. Here we here use the term “homologous structure” as “the historical continuity of characters in multiple lineages despite

variations in their character state” (Wagner 1989). This means that a particular trait present in a specific organism is only considered homologous to another trait in another organism if, and only if, this trait was derived from a common ancestor. Essentially, according to this definition, identifying a homology between two organisms implies the existence in the past of the same trait in a common ancestor and the consequent heritability of that trait. Here the notion of a third element (the ancestral) that transmitted the trait to the two organisms under analysis is never a meek hypothesis, rather it is a requirement (and a result) for establishing any homology. This link of causality is vital to infer evolutionary history - or “descent with modification” as Darwin defined it - of organisms, for this is the ultimate goal of evolutionary biology. If not, any other criterion on how to organize the living world would be a mere artificial convention as epistemologically valid as any other.

Although agreement over a definition is required for any rational debate, by itself, it is not sufficient to allow communication. Homology can be challenging to define but it can be even more difficult to diagnose. How can one know if a particular common trait is derived from a shared ancestor and not from shared convergent constraints or even by mere chance? At this stage, it is important to settle the conditions on how to identify homologous characteristics.

Classical comparative anatomy use criteria like topology (relative position), morphology (shape, size and patterning), and some times even function to find homologous bones and compare the same skeletal elements between different taxa (Brigandt 2003). Phylogenetic information should be used with caution given that it can easily create tautological problems (Raff 1996). Homologies are the fuel to phylogenetic analysis and should be defined independently. Thus, we

should pay particular attention when using conclusions from phylogenetic analysis to infer homologies.

As it is obvious, very rarely paleontologists can use data of embryological origin, gene expression patterns or molecular networks to address such homology questions. For example, Rupert Riedl identified three criteria for the establishment of homologies: position, structure and transition. The positional criterion tells us if a particular trait is homologous if it is in the same position (e.g. a bone or gene relative location). The structural criterion says that traits can be presumed homologous if they share a certain amount of characteristics in common (e.g. although male testis may present in different parts of the body, they share structural similarities). The last, transitional criterion, allows inference of homology if a set of commonly shared historical transitions can be demonstrated from its origin (Riedl 1978; Raff 1996). Typically, analyzing the fossil record can help to access the latter criterion. In any case, all criteria are applicable to both anatomical and molecular characters. Although usually without any explicit reference, biologists when referring to homologous traits are recurrently using all (or some of) these principles.

Bone: another problem, a different solution

Other important terms require a prior definition. One such term, that is easily (and wrongly) assumed to be well defined is “bone”. Bones are usually defined as individual parts of the endoskeleton of vertebrates, but at the same time it is extremely probable that a large majority of comparative anatomists never asked the question: what is a bone? The term is usually self-explanatory but it creates uncertainty in situations such as the skull where high bone fusion rates hinder a clear assessment of the number of bones present. An even greater confusion emerges when one dives into ontogeny. Many ossification centers are

transiently formed during early stages of development and are difficult to name and relate to final structures in the skull. To prevent any conceptual misunderstanding, we here use the term bone as an individual piece of calcified tissue present at any stage of the normal development of a species. It can be seen as a synonym of “ossification center” at early stages of development helping to compare transient structures with other structures present in adult animals for other clades.

In attempting to establish homology between different bones, paleontology and evolutionary developmental biology (evo-devo) rarely integrate data from each other. Moreover, although efforts have been made to standardize ontology (Dahdul et al. 2012), it is common in the literature to see the same structure named differently or different structures named with the same term. This lack of interdisciplinary crosstalk results in misperceptions that preclude further comparisons between organisms and impairs any wide range analysis regarding their evolutionary history.

On the other hand, in some cases sound results can be compared but they suggest contradictory conclusions, creating disagreement over the identity of certain structures. This is the case for avian digit homology (Čapek, Metscher, and Müller 2014; Wagner and Gauthier 1999) or vertebrate cranial bones (Koyabu, Maier, and Sánchez-Villagra 2012). In other cases the data obtained by different authors using complementary methods reach opposite conclusions. This is what has been happening over the last four decades regarding the identity and embryological origin of some parts of the avian skull (Gross and Hanken 2008a; Evans and Noden 2006; Couly, Coltey, and Douarin 1993; Couly, Coltey, and Douarin 1992).

Melting the pot

The need to better understand complex evolutionary patterns present in modern living forms demands a greater level of integrative results. Recently, a small but increasing amount of work has been using both types of analysis to test evolutionary hypotheses and propose new conclusions. Particularly, when combined, paleontology and evolutionary developmental biology have shed light onto extremely diverse evolutionary processes. More than competing, the two disciplines often complement each other resulting in important advances across diverse fields such as: developmental plasticity (Standen, Du, and Larsson 2014); bone identity (Botelho et al. 2014; Luo 2011), Bauplan patterning (Müller et al. 2010), deep time embryological evolution (Chen et al. 2014), cell biology processes (Bomfleur, McLoughlin, and Vajda 2014), ecological interactions (Topper, Holmer, and Caron 2014) sexual behavior (Long et al. 2014), and many others (Wilson 2013).

One of the most persistent problems in the evolution of vertebrates is the establishment of correct homologies between skull bones among a wide range of animals (Kuratani 2005). This is particularly true for the tetrapod calvaria. The calvarial bones form the skull roof. The exact list of bones that can be considered calvarial can vary given that in different taxa different combinations of bones cover the dorsal surface of the skull. The bones that can form the skull roof in Amniota are: frontal, postfrontal, postorbital, preparietal, parietal, postparietal, tabular, squamosal and supraoccipital.

Anurans have a particular skull anatomy where a long and flat bone covers the dorsal surface of the head: the frontoparietal. The frontoparietal complex has been assumed to be homologous to the frontal and parietal present in labyrinthodonts (Rocek 1988). In that paper, Rocek combines comparative data from extant and extinct

species of amphibians with some embryological data. Rocek shows that during development the frontoparietal is formed via the fusion of multiple centers of ossification. In addition, Rocek demonstrates that not only the extent of the fusion between the elements that form the frontoparietal complex differs in various extinct lineages but also that the number of elements that contribute to this complex differs within anurans. Collectively, his observations point to the conclusion that the frontoparietal bone in anurans is probably homologous to the frontal and parietal bones of other related species.

In amniotes the skull diversity is even greater and the debate over the skull origin is still alive since Goethe head segmentation hypothesis was published in 1820 (De Beer 1937). In order to explain the morphology and origin of the vertebrate skull, Goethe imagined that the vertebrate head was segmented just like the segments present in the vertebral column. This idea although originally attributed to Goethe had been proposed before by many different authors ranging from Oken (1807), Spix (1815), Bojanus (1819), St. Hilaire (1818), Meckel (1820) and latter by Owen (1846) (De Beer 1937). In any case, debate was long but this hypothesis has been losing ground. Gans and Northcutt published paper in 1983 that settle the new notion that the vertebrate head is a evolutionary innovation. Ever since this idea has gaining global acceptance (Gans and Northcutt 1983). These authors based their hypothesis on the (at that time) new discoveries regarding the contributions of the anterior neural crest to the formation of the vertebrate head and on a wide set of fundamental differences between protochordates and vertebrates. In addition they proposed that a transition from a protochordate filter feeding lifestyle to a (protovertebrate) predatory ecology might have been the driving force that allowed the complex vertebrate head to appear. Under Gans and

Northcutt perspective, the changing of ecology was the driver while the innovative development of the neural crest was the mechanism that permitted the appearance of a “new head”.

In this scenario, homology relationships between complex arrays of bones in the cranium of amniotes are not longer possible to establish with protochordates axial segments. They represent instead an authentic evolutionary innovation.

Within recent vertebrates it is interesting to compare divergent taxa like Synapsida and Sauropsida. These two groups include all extant Amniota and a rich fossil record. These facts present an opportunity to combine experimental data with classical comparative anatomical analysis when trying to reconstruct evolutionary history of living animals.

This thesis will be focused on the importance of finding complementary data to resolve a particular problem in the bone homology of the vertebrate skull, particularly of the archosaurian skull. Over the next chapters we will present two examples, one from experimental developmental biology and another from a paleobiological perspective. Chapter one will address the frontal problem in the avian skull while chapter two will describe a new crocodyliform fossil clutch (with embryos) from the upper Jurassic of Portugal.

Chapter I

Towards the resolution of an evolutionary conundrum: the Aves frontal bone

Introduction

“Canst thou, O partial sleep, give thy repose
To the wet sea-boy in an hour so rude,
And in the calmest and most stillest night,
With all appliances and means to boot,
Deny it to a king? Then happy low, lie down!
Uneasy lies the head that wears a crown.”

W. Shakespeare. King Henry IV. Part II, 1597.

Gallus gallus (chicken) is a central model organism in comparative anatomy and evolutionary developmental biology. Its anatomy and developmental genetics have been extensively studied and many relevant evolutionary implications have been made so far based on diverse experimental analysis (Stern 2005 and references therein). Some examples of unforeseen concepts that have arisen directly from seminal studies using chicken embryos include: the germ layers (ectoderm, mesoderm, endoderm) by the paleontologist Pander (Pander 1817a; Pander 1817b) and its latter elaboration by the embryologist von Baer (von Baer 1828); the neural crest by the anatomist and inventor of the microtome His (His 1868); and the neural tube, somites and capillaries by Marcello Malpighi in the XVII century (Malpighi 1672; Malpighi 1675).

However, important questions regarding the developmental and evolutionary origin of some chicken skull bones are still unresolved such that no solid homology can be established across organisms. This precludes evolutionary comparisons between one of the most widely used model organisms and other animals in which skull anatomy has evolved significantly over million years.

All these questions are even more complex due to the many different cell movements and migrations occurring during embryogenesis of the cephalic region. Different lineage tracing studies present contrasting conclusions, particularly apparent for calvarial bones that lie in the skull region where the boundary between Neural Crest (NC) and Paraxial Mesoderm (PM) derived structures is located. A classical example is the disputed origin of the frontal and parietal bones. It is well known that the frontal and parietal bones cover a wide part of the calvarial region of bird skulls where the frontal is usually the largest bone. Yet, its evolutionary and developmental origins are not well established.

Using techniques developed by Le Douarin (N. M. Le Douarin 1969) Le Lièvre and Noden and co-workers defined the boundary between NC and PM derived cells in the mid supraorbital region of the frontal bone (Le Lièvre 1978; D. M. Noden 1982; D. M. Noden 1984). In contrast, Couly and colleagues concluded that the NC/PM boundary is located more posteriorly between the parietal and supraoccipital (Couly, Coltey, and Douarin 1992; Couly, Coltey, and Douarin 1993) (Fig. 2).

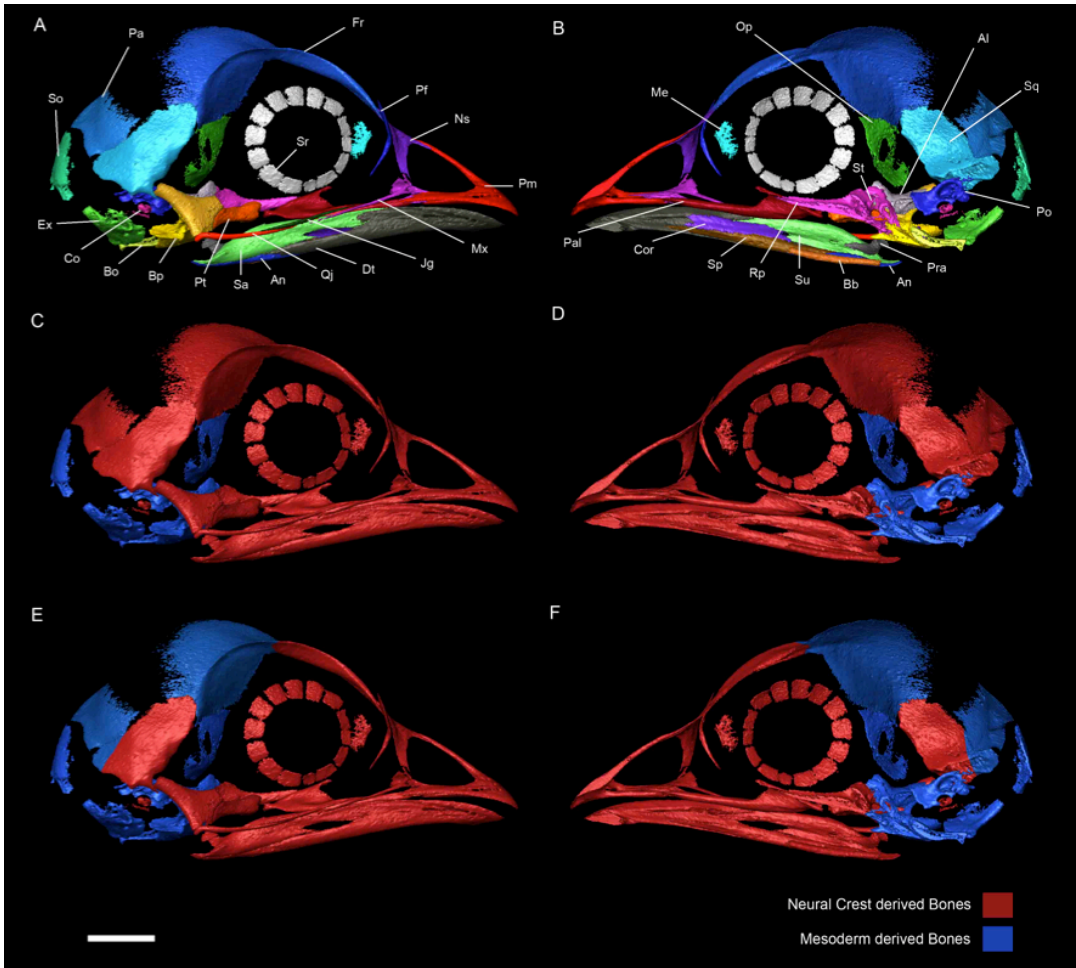


Fig. 2 Right side of a chicken embryo skull at HH40. A, Lateral view with ossification centers identified with different colors. **B,** Medial view with ossification centers identified with different colors. **C** and **D,** respectively lateral and medial views of a chicken skull at HH40 showing in the embryonic origin of each skull element according to Couly et al 1992, 1993. **E** and **F,** respectively lateral and medial views of a chicken skull at HH40 showing in the embryonic origin of each skull element according to (Le Lièvre 1978; D. M. Noden 1982; D. M. Noden 1984;

Evans and Noden 2006). The left side of the skull was removed including the left side of unpaired ossification centers. **Al**, Alisphenoid; **An**, Angular; **Bb**, Basibranchial; **Bo**, Basioccipital; **Bp**, Basisphenoid; **Co**, Columella; **Cor**, Coronoid blade of the splenial; **Dt**, Dentary; **Ex**, Exoccipital; **Fr**, Frontal; **Jg**, Jugal; **Me**, Mesethmoid; **Mx**, Maxilla; **Ns**, Nasal; **Op**, Orbitosphenoid; **Pa**, Parietal; **Pal**, Palatine; **Pf**, Prefrontal; **Pm**, Premaxilla; **Po**, Prootic; **Pra**, Prearticular; **Pt**, Pterygoid; **Qj**, Quadratojugal; **Rp**, Rostroparasphenoid (parasphenoid rostrum); **Sa**, Surangular; **So**, Supraoccipital; **Sp**, Splenial; **Sq**, Squamosal; **Sr**, Sclerotic ring; **St**, Sella turcica.

Using a pioneering technique, Couly and colleagues were able to perform unilateral excisions of neural crest from a host chicken embryo at precise cephalic levels while leaving in situ the neural epithelium. This procedure was repeated in a quail embryo and the resulting piece was inserted in the gap created in the chick embryo. Each transplanted piece of neural fold was about 450 μm in length and was always transplanted from a quail donor to a host chicken embryo of the same stage. Given the early stages used, the neural crest cells had not started to migrate. This ensured that tissues, which presented quail cells, were derived from the neural crest. In addition, these studies presented rigorous histological sections of the operated embryos at several time points post operation showing that the neural crest cells were effectively transplanted and contamination was residual. The identity of the cell type (quail vs chicken) was verified by Feulgen – Rossenbeck staining (Fig. 3). This technique allows a differentiation between the nuclei of quail cells (which present highly condensed chromatin) and chicken nuclei (with a much more diffuse chromatin).

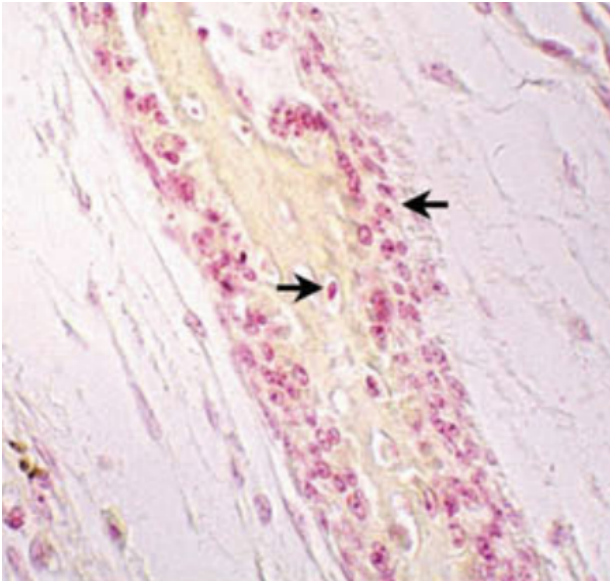


Fig. 3 Sclerotic ossicles (and periosteum) containing cells derived from neural crest (arrows) stained using Feulgen – Rossenbeck protocol. Arrows point to quail cells (image from (Creuzet et al. 2005)).

The results showed that in addition to all anterior bones from the face, cells derived from the donor were present across the whole frontal and parietal bones. Moreover, these authors also performed the complementary experiment where they transplanted the paraxial mesoderm of quail into a chicken host. In these chimaeras they could not find quail cells in any of these bones. These results strongly suggested that the frontal and the parietal bones were (at least in quail and chicken) derived from neural crest cells.

Nevertheless, Evans and Noden criticized these conclusions arguing that two different problems could lead to misinterpretations of the results (Evans and Noden 2006). The first argument pertained to the transplant technique itself. It is known that to produce quail-chick chimeras an extreme precision is needed. In some cases, at least theoretically, the transplanted piece of neural fold may carry over some cells derived from the neural tube, the ectoderm or even of the mesoderm. If the contamination is from the neural tube or of ectodermal origin and given that these tissues do not form bone, no influence in the

results and in their interpretation is expected. On the other hand, if the contamination consists of paraxial mesoderm cells, the identified quail cells in the posterior region of the frontal and in the parietal bones could have a different (mesodermal) origin and point to a distinct ontogeny for those bones. Evans and Noden also noted that these types of transplants are even more difficult to perform in early stages of development. For instance, they claimed that “at stage 8 (three somites) the hindbrain neural folds are vertical and underlying paraxial mesoderm is tightly adherent and, therefore, difficult to exclude from excised pieces of neural fold tissue without the use of proteolytic enzymes to separate epithelial from mesenchymal populations” (Evans and Noden 2006). In addition, it is argued that the Feulgen staining used to distinguish quail and chick cells has been shown to be unstable in angioblasts therefore hindering a correct identification of the mesoderm contribution to the posterior frontal and parietal bones (D. M. Noden 1984; D. M. Noden 1991b).

Specifically, Evans and Noden state that the results obtained by Couly and colleagues (Couly, Coltey, and Douarin 1993) may be misleading because they were based “on the presence of cells containing the quail nuclear marker (Nicole M. Le Douarin 1973) as identified using Feulgen staining, but did not include assays using the QH1 antibody to detect quail endothelial cells. Angioblasts are ubiquitous within early mesodermal populations (D. M. Noden 1984; D. M. Noden 1991a; Borue and Noden 2004) absent only from notochordal and prechordal mesoderm (D. M. Noden 1990). Previous studies have found that the quail nuclear marker is unstable in angioblasts (D. M. Noden 1984; D. M. Noden 1991a). Therefore, Feulgen-based assays often fail to detect these mesodermal cells in chimeric tissues.”

Trying to circumvent these issues, Evans and Noden infected chicken embryos with β -galactosidase-encoding, replication-incompetent retroviruses into the paraxial mesoderm, crest progenitors, and at the interface between mesodermal and the overlying neural crest. This produced alternative fate maps to those generated with the quail–chick grafting technique. These results suggested that the NC/PM boundary was present at the junction of the supraorbital and calvarial regions of the frontal bone (Evans and Noden 2006).

A bone is a complex and dynamic organ. It is known that, during intramembranous ossification, endothelial cells that are always from mesoderm origin will invade the developing osseous tissue to form blood vessels (Couly, Coltey, and Douarin 1993). This contradicts critics made to the quail-chick chimera studies (see Couly et al., 1995 and related papers) simply because all bones should be invaded by blood vessels derived from mesoderm cells. Any staining of endothelial cells would only represent this particular contribution to the bone. On the other hand, blood vessels are composed of two types of cells: an inner layer of endothelial cells and an adjacent external layer of pericytes. Cephalic pericytes are originated anteriorly (forebrain) from neural crest cells and posteriorly (midbrain and hindbrain) from mesoderm cells. At the border between the forebrain/midbrain there should be a mixed population of cells (Etchevers et al. 2001). So any staining of vascular cells would not be conclusive about the origin of a particular bone. It would be important to see the exact origin of osteoblasts and osteocytes when performing fate map studies to understand bone developmental origins.

In addition, Couly and co-workers generated quail-chick mesoderm transplants that never showed donor cells present in the frontal nor parietal bones (Couly, Coltey, and Douarin 1993).

Until now only two experimental works labeling both neural crest and mesodermal tissues were published so far (Couly, Coltey, and Douarin 1993; Evans and Noden 2006). Thus, it would be also legitimate to speculate about any possible imprecision in the retroviral infection studies that could account for the disparate results. Such experiments, although considered by some as offering finer control over cell labeling (Gross and Hanken 2008b) can be imprecise given that it is extremely difficult to control the amount of cells that will be infected. According to the authors themselves the exact depth of injections was hard to determine given that the micropipette ejection force was not defined (Evans and Noden 2006).

Moreover, infections were performed in embryos that range from Hamburger and Hamilton stages (HH stages) 6 to 11, which in some cases, depending on the stage they were performed and on the technique used, resulted in the labeling of mixed cell type populations. Evans and Noden performed three experiments: 1) injection of retrovirus into paraxial mesoderm at HH stages 8–9; 2) washing retrovirus over the surface of the embryo, beneath the vitelline membrane, at stages HH 6 to 9.5; and 3) retrovirus injection at the interface between paraxial mesoderm and overlying neural crest cells at stages HH 10- to 11- (Evans and Noden 2006). This last experiment was specifically designed to label both populations of cells. In the same paper the authors recognize that “each injection typically results in the labeling of some but not all nearby progenitor cells”. For instance “unintended infection of crest cells could occur by virus particles reaching the basal surface of the neural fold or, if they spilled over the surface of the embryo, by reaching the apical surface of the neural fold” (Evans and Noden 2006). In addition, in experiment 1, although the infections were performed at least 6 hours before any neural crest migration, the authors also

recognize that the virus could remain infectious until crest cells start to migrate. This is particularly important given that it is known that chicken cranial NCC migrates via subectodermal streams, immediately dorsal to mesoderm (Serbedzija, Bronner-Fraser, and Fraser 1992; Lumsden, Sprawson, and Graham 1991; N. M. Le Douarin and Kalcheim 1982). Thus cranial NC subectodermal migrating cells could be contaminated with virus. The fact that the frontal and parietal bones were never co-labeled only suggests that the domains (either neural crest or mesoderm or both) are antero-posteriorly separated at early stages of development (HH 6 to 11-). From experimental procedure 3 where both mesoderm and neural crest were infected, it is not possible to draw any conclusion regarding the neural crest:mesoderm origin of these bones. Here, maybe the most important experiment is number 2 but given the fact that the authors do not present the amount of positive cases (out of 66 treatments) for a staining of the anterior region of the frontal, it is hard to extract any conclusion. Moreover, the anterior region of the frontal should be more compact (if not denser) when compared with the posterior sheath of bone that forms the posterior region. Any comparison of a staining should have this into consideration.

Nevertheless it is important to note that in this experiment the authors did not report any cell in neither the posterior region of the frontal or in the parietal bones. In any case, it would be interesting to perform histological cuts in the frontal bone of these embryos and confirm the complete absence of cells labeled in the posterior region of the frontal and in the parietal bone.

On the other hand, in mice a three-bone condition is present in the calvarial region (frontal + parietal + interparietal). The fate map results are unanimous attributing the origin of the entire frontal bone to cells derived from neural crest, while the posteriorly contiguous bone (the

parietal) is formed exclusively by paraxial mesoderm derived cells. The same studies showed that the immediately posterior bone, the interparietal, is composed medially by a portion derived from NC while its lateral parts are PM derived (Gross and Hanken 2008a). The medial and lateral portions have been considered homologous to the postparietal and tabulars of fossil synapsids respectively (Koyabu, Maier, and Sánchez-Villagra 2012).

In sum, currently there are two hypotheses regarding the embryological and evolutionary origin of the calvarial region of the bird skull. The first hypothesis claims that a population of cells exclusively derived from neural crest forms the complete frontal and parietal bones (Couly, Coltey, and Douarin 1993) while other authors advocate for a double ontogenetic contribution from neural crest and paraxial mesoderm derived cells (Evans and Noden 2006).




The implications of these two alternative hypotheses go beyond the avian development realm. As previously mentioned, fundamental questions regarding skull evolution amongst Archosauria are impacted differently by these alternatives.

At this point two alternative evolutionary scenarios can be hypothesized. Hypothesis 1 (H1) corresponds to the classical view where the frontal and parietal bones in birds are homologous to the bones with the same name in mammals and to the frontal and parietal of their last common ancestor. This ancestor should have been a basal amniote similar to *Hylonomus* or *Protoclepsyrops* that lived approximately 300 Ma in the Carboniferous (Tuinen and Hadly 2004). The second hypothesis (H2) calls for a revision of the classical view since the frontal bone in birds would result from a fusion of the frontal and parietal bones during evolution. The resulting bone is a

“frontoparietal”, homologous to the frontal and parietal of mammals. In addition, this would also imply that the classical parietal bone in birds is homologous to the mammalian postparietal (medial portion of the mammalian interparietal) and should also be renamed accordingly.

The two hypotheses entail different and testable predictions. Namely, throughout ontogeny, different observations are expected. If H1 is correct, one should find a single center of ossification in the frontal, developing by intramembranous ossification and completely derived from neural crest cells. If instead H2 is correct, a double center of ossification developing into the frontal should be observed; both centers should develop via intramembranous ossification (if not, it could suggest that one of the centers is an evolutionary novelty rejecting both hypotheses); the ossification centers should be aligned antero-posteriorly; have the correct shape (the anterior should be elongated and the posterior more wide and flat) and the embryological origin should be neural crest anteriorly and paraxial mesoderm posteriorly (see table 1).

Table. 1 Alternative hypotheses and corresponding predictions.

Ossification centers	H1	H2
Number	1	2
Position	-	Anteroposterior
Pattern	-	
Ossification type	2 x Intram.	2 x Intram.
Embryological Origin		

At this point it would be important to consider the fossil record regarding the ancestral condition in modern Archosauria. Is there any reason to consider that the extant crocodiles and birds evolved from an ancestor with a postparietal? And if yes, how can the fossil record help us test the previous hypotheses?

The Paleontological record

“If there has been a first man he must have been born without father or mother – which is repugnant to nature. For there could not have been a first egg to give a beginning to birds, or there should have been a first bird which gave a beginning to eggs; for a bird comes from an egg” Aristotle (384–322 BC)

As it is widely known, the posterior region of the bird's adult skull misses one bone when compared with the most probable ancestor condition conserved in other Archosauria, namely *Alligator mississippiensis* (Klembara 2001). Other closely related Diapsida such as *Euparkeria capensis* and most sinapsids (Koyabu, Maier, and Sánchez-Villagra 2012) do possess a postparietal. The non-archosaurian archosauriform *Euparkeria capensis*, found in the Middle Triassic of South Africa is a very curious fossil in this particular case. It has been considered as representative of the ancestral pattern to all Archosauria (Romer 1956) and, not only that, but nearly all phylogenetic analyses done so far have placed *Euparkeria* as the closest sister group of Archosauria (crown group definition) when analyzing non-archosaurian archosauriforms (Sookias and Butler 2013). In addition to *Euparkeria* and some phytosaurs like *Machaerops* ((Romer 1956) although disputed by Nesbitt) present a postparietal. The presence of a postparietal bone can also be seen within Archosauromorpha (*Mesosuchus browni*) and in multiple Archosauriformes (Nesbitt 2011).

Namely, the basal achosauriforms *Proterosuchus fergusi* and the erythrosuchians *Erythrosuchus africanus* and *Shansisuchus shansisuchus* (Nesbitt 2011). All this is suggestive that any possible loss of this bone could be an autapomorphy of Archosauria (exception made to *Alligator mississippiensis* (Klembara 2001) (Fig. 4).

Other fossil diapsids also show the presence of a paired postparietal (also referred as interparietal), for example *Araeoscelis*, *Protorothyris*, *Milleretta*, *Youngina*, *Petrolacosaurus* and even the anapsid *Labidosaurus* shows a unpaired interparietal (Koyabu, Maier, and Sánchez-Villagra 2012; Nesbitt 2011 and references therein).

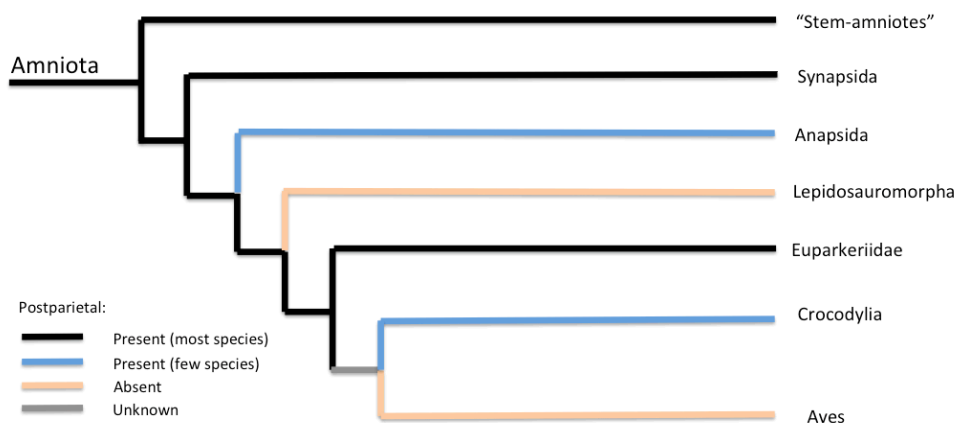


Fig. 4 Phylogenetic distribution of postparietal in Amniota. Tree simplified from (Reisz 1997; Nesbitt 2011).

The absence of a postparietal bone (*sensu* (Koyabu, Maier, and Sánchez-Villagra 2012)) in birds and in the wide majority of extant Sauropsida has been traditionally interpreted as an evolutionary loss of this bone. Nevertheless, until further evidence is presented it is not

obvious whether the bird's frontal is homologous to one bone (frontal), or whether it results from a fusion of two skull bones (frontal and parietal). This doubt makes it difficult to find a definitive terminology for the calvarial bones of birds and it has been proposed that the frontal bone of birds should be called "frontoparietal" (Drew M. Noden and Trainor 2005).

Alternatively the postorbital bone is present in almost all members of Amniota with exception of Aves. This phylogenetic distribution might also suggest that this bone, rather than being lost simply fused to the frontal bone and is still present was a transient calvarial center of ossification (Erdmann 1940).

In this chapter, we will test these competing hypotheses from different angles using comparative anatomy, developmental studies and molecular approaches. Embryos from quail, chicken, duck and crocodile were incubated and stained for bone and cartilage. These experiments, in combination with a thorough examination of the published fossil material available, will serve to establish more complete homology relationships between the skull bones of Aves and Mammalia, shedding new light onto our understanding of the evolution of development of the amniote skull since their last common ancestor.

Results

Alizarin-red and Alcian blue staining

Chicken (*Gallus gallus*)

We incubated 503 chicken eggs at 38 °C in a humid environment and opened 22 eggs at regular 4-hour intervals starting at day 6 plus 23 hours, cleared and stained all embryos with no apparent defect (for detailed protocol see methods section). The staining performed showed cartilage (Alcian blue) and bone (Alizarin red). The sequence of ossification is presented in Table 2. The onset of ossification was only considered to be positive if any red stain was visible under a binocular microscope.

The quadratojugal, surangular and angular are the first bones to appear stained by alizarin red immediately followed by the squamosal at day 7 plus 19 hours and day 7 plus 23 hours respectively. In contrast, the epiotic, mesethmoid, vomer, articular and the hyoid apparatus (except the ceratobranchial) only start ossification at day 11 plus 3 hours.

The premaxilla is stained red just 4 hours after the squamosal and is then followed by the jugal and pterygoid. Four hours later, at 8 days plus 11 hours, the palatines start to appear stained and at 8 days plus 15 hours the prootic, maxilla and dentary start to be ossified. The two latter bones appear to be formed from multiple centers of ossification that will eventually fuse into one.

Table 2. (next page) Chicken skull bone onset of ossification. Skull development was monitored over 4 days using Alizarin Red and Alcian Blue staining to assess ossification timing in the skull of *Gallus gallus*.

	Egg ID																								
	1 - 22	23 - 44	45 - 66	67 - 88	89 - 110	111 - 132	133 - 154	155 - 176	177 - 198	199 - 220	221 - 242	243 - 264	265 - 285	286 - 307	308 - 329	330 - 351	352 - 373	374 - 397	398 - 419	420 - 441	442 - 463	464 - 485	486 - 503		
	Time (Days + Hours + Minutes)																								
	6 + 23	7 + 3	7 + 7	7 + 11	7 + 15	7 + 19	7 + 23	8 + 3	8 + 7	8 + 11	8 + 15	8 + 19	8 + 23	9 + 3	9 + 7	9 + 11	9 + 15	9 + 20 + 30	9 + 23	10 + 3	10 + 7	10 + 11	...	11 + 3	
Skull Bones																									
Occipital																									
Basioccipital																									
ExoOccipital																									
SupraOccipital																									
Sphenoid																									
ParaSphenoid																									
BasioSphenoid																									
OrbitoSphenoid																									
Temporal																									
Squamosal																									
ProOtic																									
Ampulla ?																									
OpisthOtic																									
EpiOtic																									
Parietal																									
Frontal (2 O.C.)																									
Frontal (1 O.C.)																									
Prefrontal																									
Mesethmoid																									
Trabeculae																									
Nasal																									
PreMaxilla																									
Maxilla																									
Palatine																									
Vomer																									
Pterygoid																									
Jugal																									
Quadratojugal																									
Quadrate																									
Mandible																									
Dentary																									
Supra-Angular																									
Angular																									
Splénial																									
PreArticular																									
Articular																									
Mandibular																									
Hyoid Apparatus																									
Entoglossal																									
Basihyal																									
Urohyal																									
Ceratobranchial																									
Epibranchial																									
stapes																									
otolith (lagner)																									

Although it is rare, some bones start to ossify from more than one center of ossification. For instance, the prefrontal ossifies from the combination of a larger, dorsally erected center and a ventral needle-like center. The prefrontal starts to ossify at day 8 + 19 hours but at least until day 11 + 3 hours it was still possible to observe some embryos with two unfused centers of ossification. Also, some embryos present a significant fluctuating asymmetry, displaying one side fused while the other still appears completely separated.

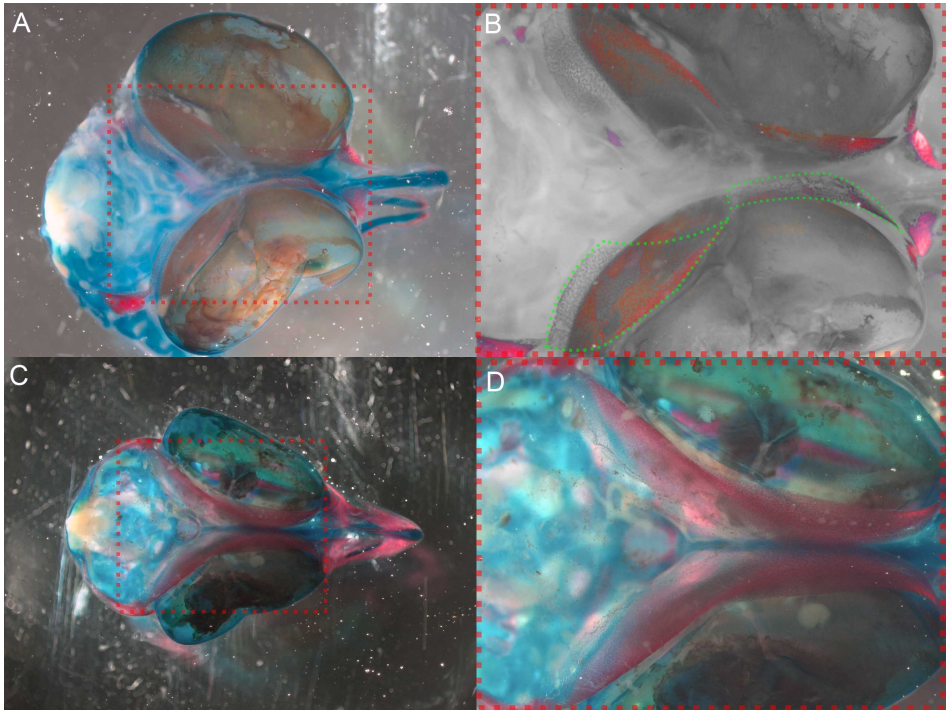


Fig. 5 Chicken embryos (339 and 496) in dorsal view stained with Alizarin red and Alcian blue, anterior towards right side. **A)** Dorsal view of a chicken embryo with 9 days and 3 hours showing two centers of ossification. **B)** Magnification of the dashed line square in A. Except red color all colors were removed. **C)** Dorsal view of a chicken embryo with 11 days and 3 hours showing the ossification centers completely fused. **D)** Magnification of the dashed line square in B. Green dotted line highlights the contours of the right frontal (double center of ossification).

Frontal

At 8 days plus 19 hours it is already possible to observe two embryos (out of 16) with a double center of ossification in the frontal. The anterior center is fusiform curving dorsally along the dorsal surface of the eye presenting approximately symmetrical anterior and posterior

ends. The posterior center is much more expanded posteriorly and tapers anteriorly (Fig. 5). These two centers will expand and eventually fuse in the supraorbital region. During development the fusion of these two centers occur between the beginning of day 9 (9 days plus 3 hours) and the start of day 10 (day 10 plus 3 hours, see Fig 6). This fusion occurs without leaving any scar or suture. After this the frontal continues to grow thickening at its anterior end and expanding posteriorly to cover the brain laterally and dorsally.

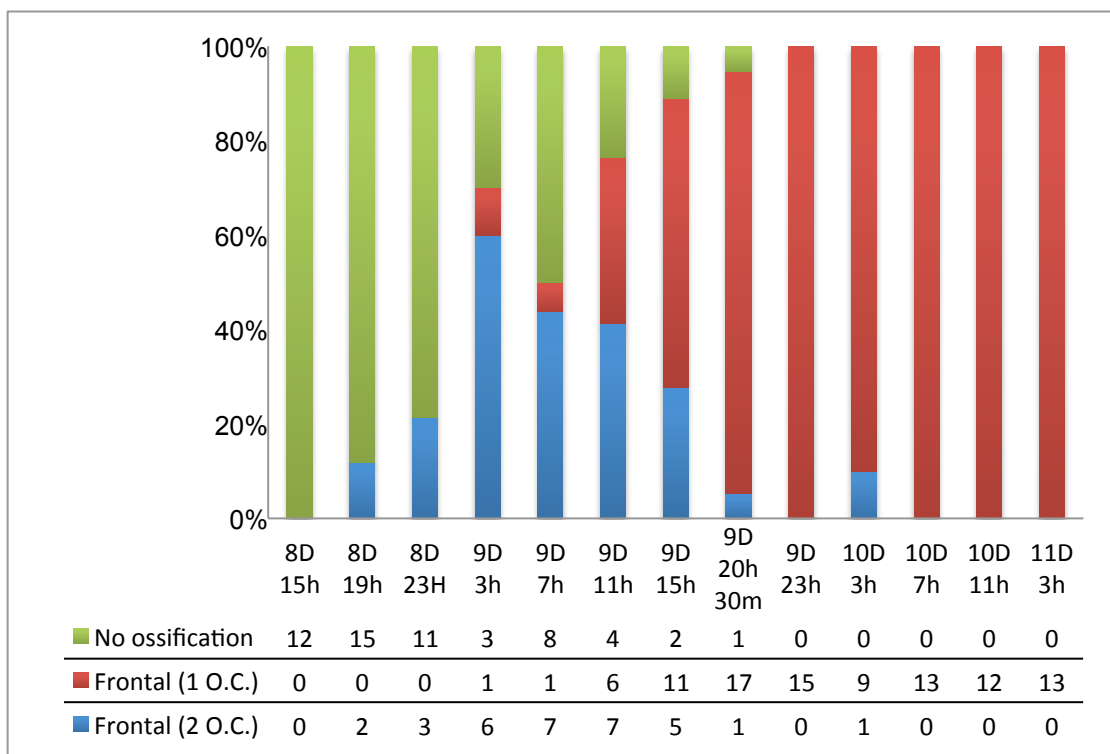


Fig. 6 Percentage of chicken embryos scored as having 0, 1 or 2 ossification centers in the frontal after alizarin red/alcian blue staining. The X-axis shows times points at which embryos were collected.

Parietal

The first embryos that show some staining of the parietal bone were collected after 10 days and 7 hours of incubation. At this time point

5 out of 13 embryos collected presented a faint alizarin red staining in the parietal. After this point the parietals starts to develop as thin stripes of bone perpendicular to the antero-posterior axis. Each side of the skull presents a single center of ossification. These ossification centers continue to develop in the subsequent days expanding anteriorly in the direction of the posterior region of the frontal and posteriorly approaching the anterior border of the supraoccipital. We only observed a single center of ossification for each parietal bone.

The otoliths, splenials and quadrates start to ossify at day 9 plus 7 hours. After this the next bones to appear are the exoccipital, orbitosphenoid, opisthotic at day 9 plus 20 hours. The nasal, parasphenoid and basisphenoid ossify at day 10 plus 3 hours.

The embryos opened at 11 days plus 3 hours presented in addition some ossification in the basioccipital,

Some authors describe the development of the chick parasphenoid has having 7 centers of ossification: an anterior rostral (rostromparasphenoid), a pair below the sella turcica (sellaparasphenoid), a pair extending out from the dorsal margins of the sella (alaparasphenoid), and a posterior pair of basitemporals or basicranials (basiparasphenoid) (Jollie 1957). However, in what concerns birds, other authors refer five (De Beer 1937) or even three ossification centers ((Parker 1890) cited in (Jollie 1957)). Our results are in agreement with Jollie regarding the number of ossification centers, but they differ in the onset. Our embryos showed the ossification centers of the sphenoid complex at the end of the 9th day, this represents one day earlier the data described before (Jollie 1957). After this point the pattern of ossification was equivalent to the one described by Jollie.

Quail (*Coturnix coturnix*)

We started by performing a preliminary experimental test where we incubated 240 eggs and opened every 4 hours to find the interval where the frontal bone was forming in quail. This preliminary experiment showed that the frontal starts to ossify around the seventh incubation day. Then, to increase resolution over the time period where the frontal is forming we incubated 120 quail eggs. From these, subsets of 20 eggs were opened every 4 hours between day 7 and 8 days plus 4 hours. The first embryos to show any ossification in the frontal were sacrificed at 7 days plus 12 hours. Eight hours later all embryos removed from the eggs presented some degree of staining in the frontal center and no secondary center formed after this period (Fig. 7 and 8). Two independent replicas of this experiment were done in parallel and the results were consistent. In virtually all cases the frontal started to ossify as a single center. The very few embryos where a putative double center in the frontal could be hinted were all too faintly stained to allow interpretation. Moreover, in these cases, the double center was only present unilaterally. We only scored a double center when it was conspicuous and bilaterally symmetrical. We used the same criterion in the other experiments carried in the other species.

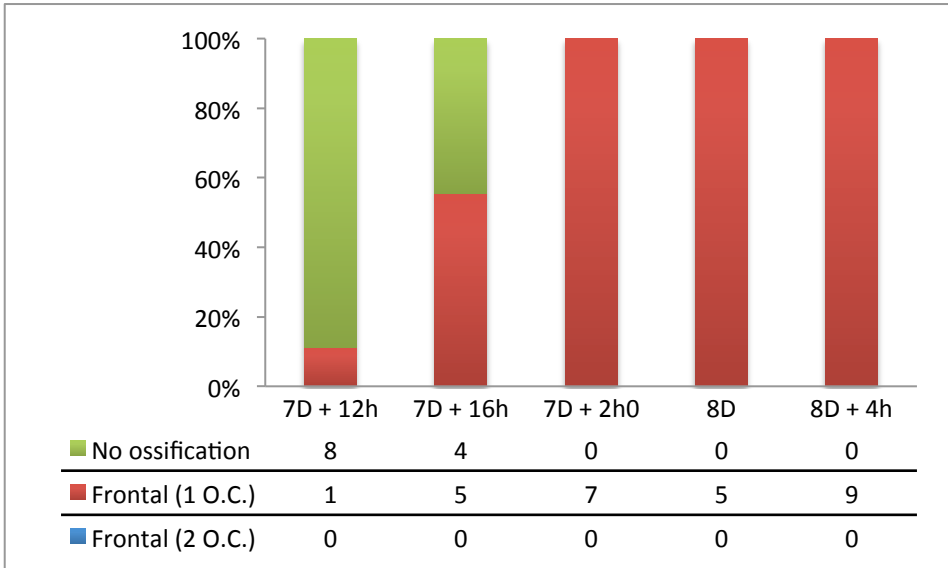
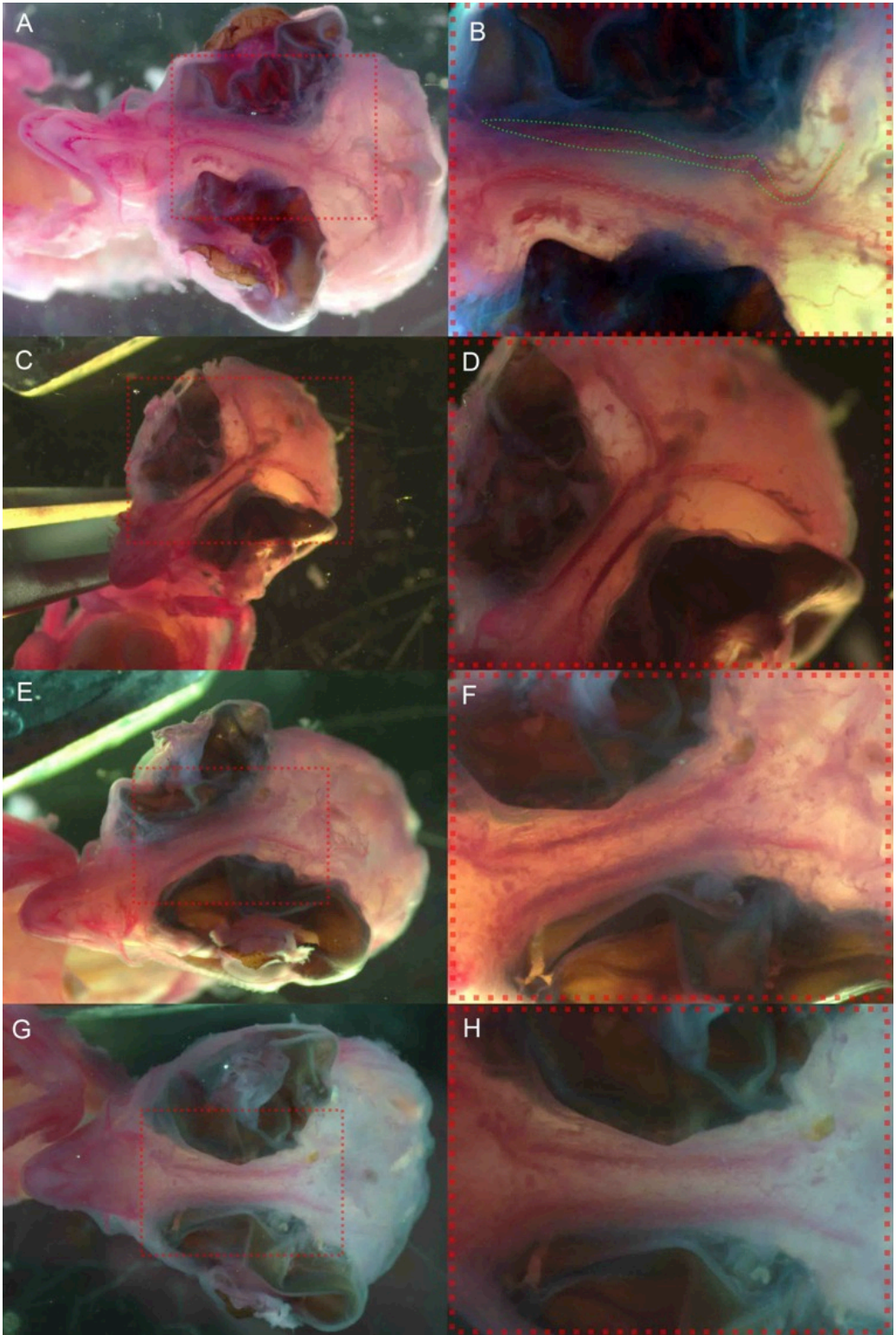


Fig. 7 Percentage of quail embryos scored as having 0, 1 or 2 ossification centers in the frontal after alizarin red/alcian blue staining. The X-axis shows time points at which the embryos were collected.

Fig. 8 (next page) Dorsal views of quail embryos with 8 days and 4 hours of incubation stained with Alizarin red. **A, C, E, G** heads in dorsal view. **B, D, F, H** zoom in showing the frontal centers of ossification in dorsal view. In **B**, green dotted line surrounds the center of ossification of the right frontal.



Duck (*Anas platyrhynchos*)

In a preliminary test, we incubated 200 eggs and opened approximately 12 eggs every 8 hours to find the interval where the frontal bone was forming in the duck. This showed that the frontal bone was being formed around the beginning of the 10th day of incubation. After this, we incubated 120 eggs opening groups of 12 every 4 hours starting at day 9 plus 8 hours and ending at day 10 plus 16 hours. This revealed that the frontal bone in duck is formed by two centers of ossification as in the chicken. However, the posterior center only appears almost 12 hours after the anterior one. The first embryos to show an ossification center in the frontal were collected at 10 days plus 1 hour and the first embryos with the two centers visible were only collected at 10 days plus 12 hours (Fig. 9 and 10). At 10 days plus 16 hours the percentage of embryos with two centers increased but it was not possible to continue the tracing of the frontal ossification dynamics due to lack of embryos. However, in older embryos at 12 days of incubation is already visible that the two centers are completely fused.

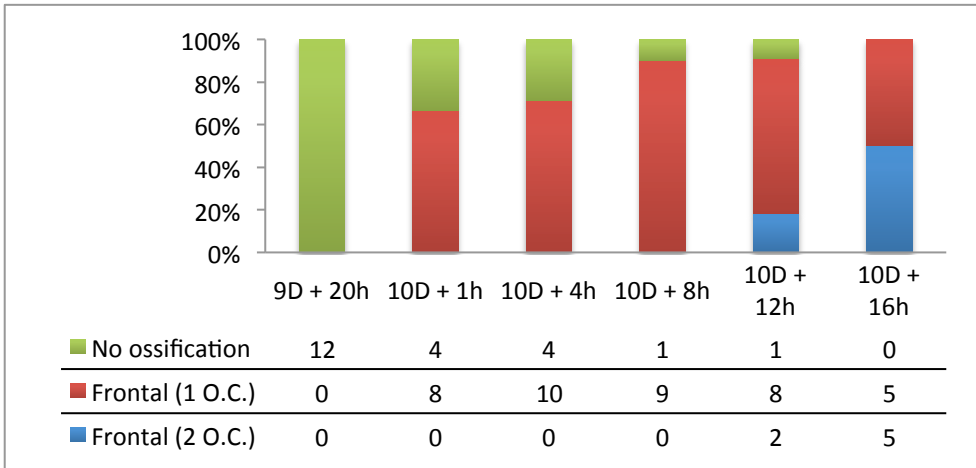


Fig. 9 Percentage of duck embryos scored as having 0, 1 or 2 ossification centers in the frontal after alizarin red/alcian blue staining. The X-axis shows time points at which the embryos were collected.

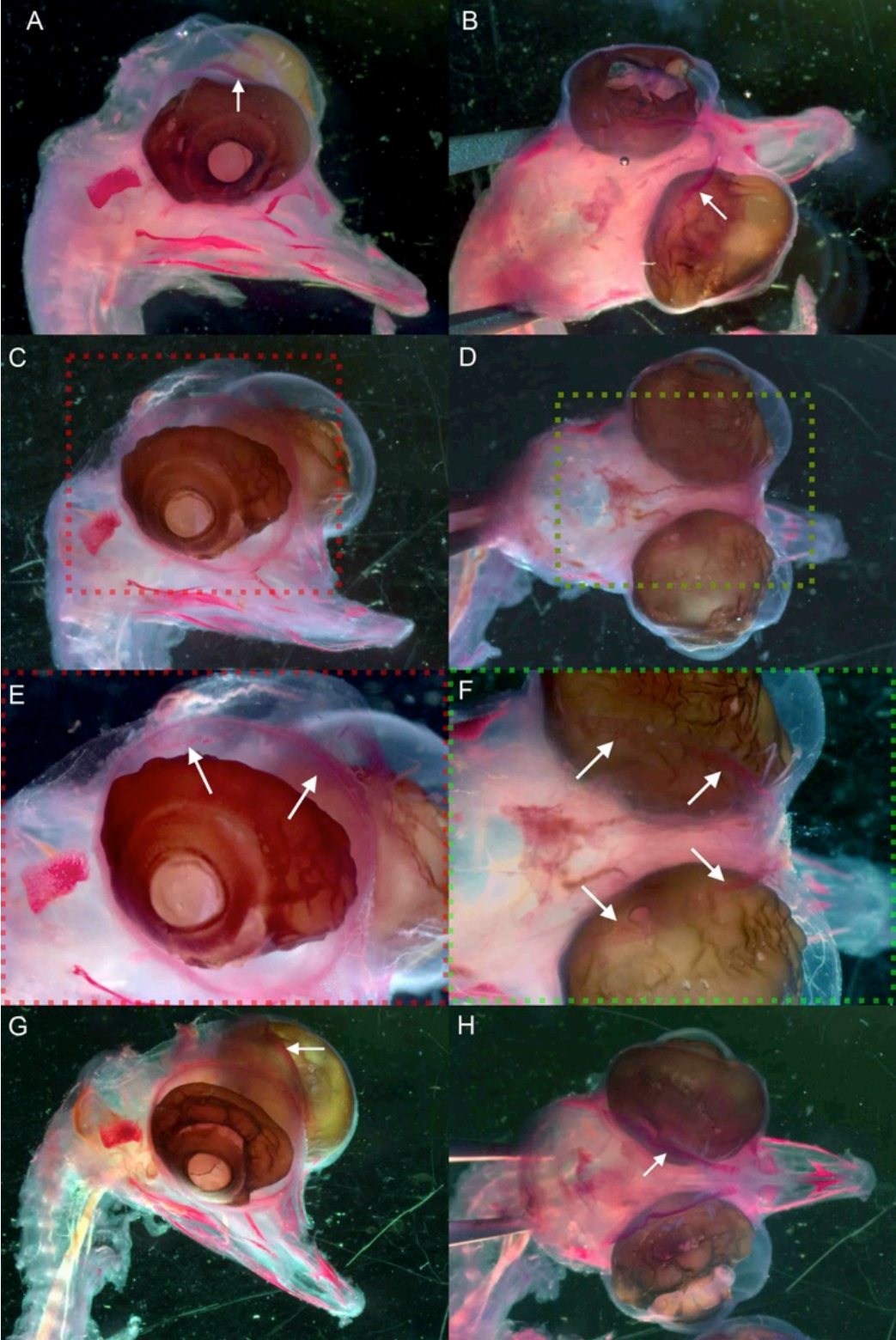


Fig. 10 Duck embryos stained with Alizarin red. (previous page)
A, right lateral view of an embryo with 10 days and 12 hours of incubation. **B**, dorsal view of an embryo with 10 days and 12 hours of incubation. **C**, right lateral view of an embryo with 10 days and 16 hours of incubation. Arrows point to centers of ossification of the frontal bone.

Crocodile (*Alligator mississippiensis* and *Crocodylus niloticus*)

The *Alligator* embryos were staged according to (Ferguson 1987) and the *Crocodylus* embryos were staged in days and ranged from 33 to 93 days of incubation. It was not possible to identify a double center of ossification in the frontal. The same is true for the parietal, postorbital and supraoccipital.

The frontal bone starts to ossify anteroposteriorly. This long and sheath-like ossification center tapers anteriorly and expands posteriorly to contact the parietal. The lacrimal presented two centers of ossification, one lateral and another medial to the lacrimal duct but all other bones appear to be formed from only one center of ossification. This pattern of ossification was observed in both *Alligator* (Fig. 11 and 12) and *Crocodylus* embryos. These results

were mainly extracted from synchrotron micro-CT and micro-CT data for the *C. niloticus* and *A. mississippiensis* respectively. Although Alizarin staining might be able to detect earlier stages of osteogenesis all

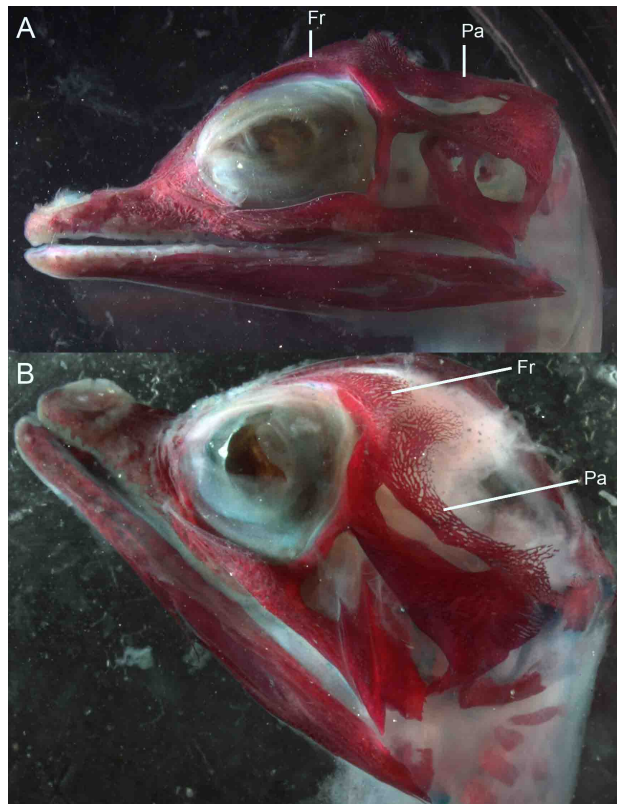


Fig. 11 *Crocodylus niloticus* embryo stain with alizarin red. A, left lateral view; B, dorsolateral view. Fr, frontal; Pa parietal.

embryos that could be used for this particular staining corresponded to more advanced ontogenetic stages Fig. 11. It is possible that the resolution of the CT data was not sufficient to detect the ossification centers when these were small anlagen. Thus, the contrast might be better ascertain using Alizarin red / Alcian blue staining in younger stages.

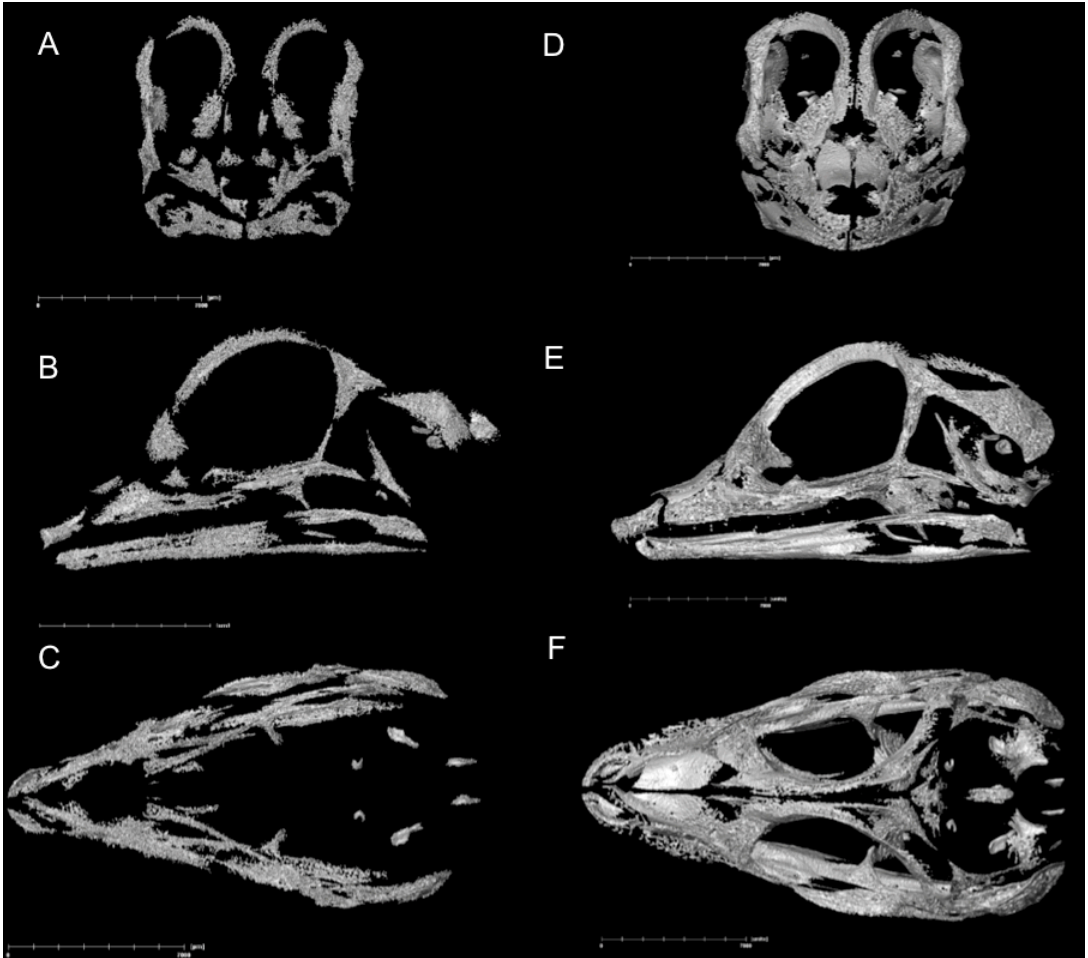


Fig. 12. *Alligator mississippiensis* embryos after digital segmentation. Skulls in: **A**, anterior; **B**, left lateral and **C**, dorsal views. Ferguson Stage 21: **A**, **B** and **C**. Ferguson stage 23: **D**, **E** and **F**.

Mouse (*Mus musculus*)

We cleared and stained multiple embryos (n=17) from different females. The embryos had between 17 days and 19 days of gestation. All embryos recovered from sacrificed females were wild type and did not present any type of malformation. The least developed litter did already have a very developed skull showing one ossification per bone. This means that the frontal and parietal presented only one center of ossification each but it is hard to be sure about what was the pattern during early development. The younger embryos approximately E17 did not present an ossified supraoccipital. However, the more developed litter presented embryos with this bone already stained red (see Fig 13 and 14). In all embryos observed each bone had only one center of ossification.

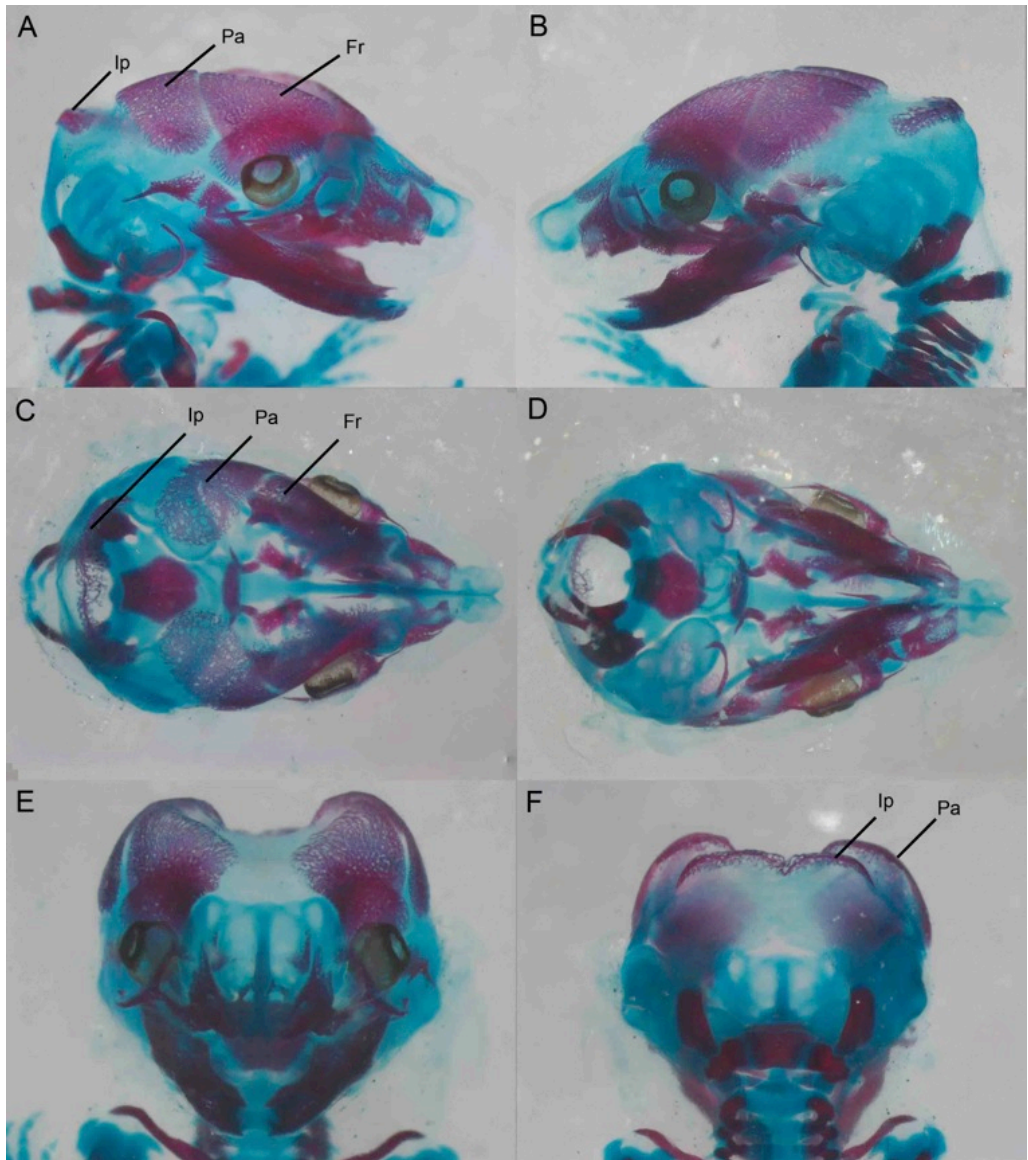


Fig 13 Mouse skull E17 stained with alizarin red and alcian blue. **A**, right lateral, **B**, left lateral, **C**, dorsal, **D**, ventral, **E**, anterior and **F**, posterior views. **Fr**, frontal bone; **Ip**, interparietal; **Pa**, parietal.

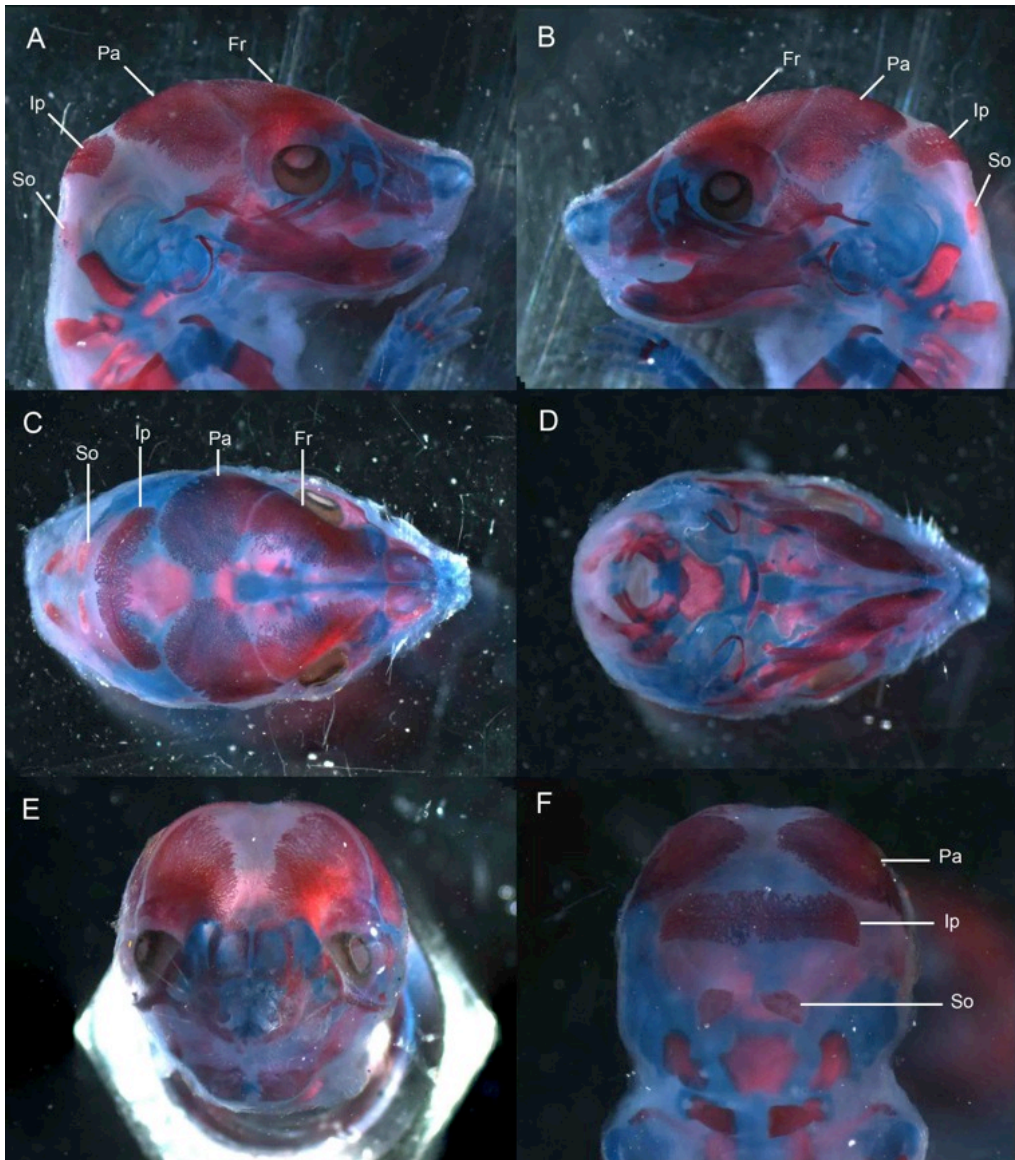


Fig 14 Mouse skull E19 stained with alizarin red and alcian blue. **A**, right lateral, **B**, left lateral, **C**, dorsal, **D**, ventral, **E**, anterior and **F**, posterior views. **Fr**, frontal bone; **Ip**, interparietal; **Pa**, parietal, **So**, supraoccipital.

Micro-CT

We analyzed CT scans from *Crocodylus niloticus* (n=7), *Alligator mississippiensis* (n=5), *Tyto alba* (n=4), *Gallus gallus* (n=1). Regarding *Crocodylus* and *Tyto* we performed a synchrotron radiation-based micro-computed tomography. The data from *Gallus* and *Alligator* was done in a micro-CT. We scanned multiple embryos at different stages from each species. We segmented all embryos using Amira a VGStudio automatic (threshold) and manual tools. We attributed artificial colors to the resulting 3D volumes based on different intensity levels. This allowed a detailed identification of the bones of interest. Additional experimental details are described in the methods section. The following descriptions will be centered in the frontal, postorbital and parietal bones. Further description, morphological analysis and figures can be seen in chapter II.

Although the resolution might be same the density resolution of both micro-CT and synchrotron micro-CT is different. The latter detects smaller differences in contrasts in the medium than the former technology. This is important when trying to visualize structures under development like ossifying bones. Particularly as a result of calcium deposit during ossification there is a marked difference between bone, cartilage and all other tissues that the synchrotron micro-CT was able to detect (Fig. 15). The micro-CT data was also useful especially in the older embryos. Using this virtual data, the bones could be clearly segmented and separated from each other. As a result, individual developmental dynamics could be followed and correlated. However, the very early stages of development of some particular bones could not be clearly identified. This was the case of the frontal bone. Using micro-CT data, it is not possible to distinguish mesenchymal condensations and reconstruct bone anlagen before any ossification. Even if it was possible

to detect ossifying bones at its very early stage (where only few extracellular matrix is secreted) it would be needed a high sample size to be sure that there are no embryos with two ossification centers. For that reason, we could not confirm nor disprove the existence of a double ossification center during development of the frontal in *Tyto alba* without further analysis.

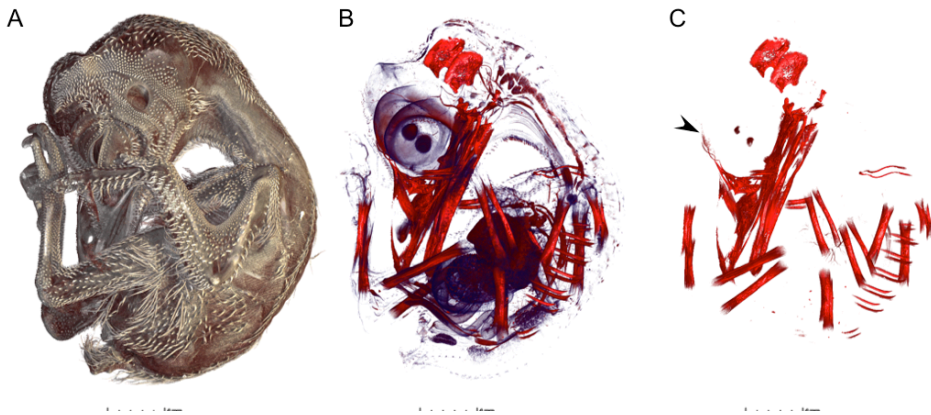


Fig. 15 *Tyto alba* embryo scanned using synchrotron micro-CT. A, full embryo in left lateral view. B, bones in red, cartilage and tissues with equivalent density in blue. C, Only bones and crystalline lens. Black arrow points to frontal ossification center.

Given that the frontal bone starts to ossify as an extremely thin sheath of bone, and given that quickly after is inception the two centers of ossification fuse without leaving any suture or mark, it was not possible to visualize the two centers of ossification of the frontal. In addition, the amount of embryos in each species scanned might not have been enough to detect embryos at the stage of two centers of ossification.

Nevertheless, it was possible to observe that the frontal starts to ossify anteroposteriorly in *Tyto* in contrast with *Gallus*, where the two ossification centers develop almost synchronously. It would be interesting to define if this is the case with by repeating the alizarin red staining experiment but increasing the number of embryos a time points between 9 and 10 days of incubation. The parietal forms latter in development. It appears as two square shaped bones that curve around the hindbrain. Latter this bone will contact at its posterior end, the supraoccipital and at its anterior border the frontal while it will be fused to the squamosal laterally.

In *Alligator* the frontal development is extremely similar to the *Crocodylus*. The frontal starts to ossify at the supraorbital region forming a fusiform and curved ventrally sheath of bone. This thin bone opens dorsally bifurcating and forming two small edges along its dorsal border. The parietal forms as a crescent shaped bone that will close completely medially but will eventually form the supratemporal fenestra given that it will not fuse completely with the squamosal and postorbital, laterally. The parietal contacts: the frontal and the postorbital anteriorly, the squamosal and supraoccipital posteriorly and the laterosphenoid and prootic ventrolaterally. Early in development the postorbital appears as a triangular bone with the characteristic three rami that will fuse with the frontal anteriorly, the squamosal posteriorly and the jugal ventrally. In addition the postorbital contacts the laterosphenoid, the quadrate and the quadratojugal laterally. From the *Crocodylus* embryos scanned both frontal and postorbital develop at the same time (day 39) while the parietal is only detected at day 45.

Quail-Chick chimeras

We performed a total of 41 transplants in embryos ranging from 3 to 11 somite stage. From these 10 embryos survived at least until 8th incubation day. The transplants we done unilaterally according to the protocol and fate map described by previous authors (Couly, Coltey, and Douarin 1993). In addition we only carried out unilateral isotopic transplants between quail and chicken embryos at an equivalent developmental stage. All grafts had approximately 500 µm in length, however it was not possible to measure the exact dimensions of all quail-chick transplants.

Some embryos presented small malformations in the head where the posterior region of the skull was not perfectly symmetrical (Fig. 16). Other embryos had no scar or imperfection displaying only dark feathers in the transplanted side. The macroscopic observation allowed to select the best candidates to be sectioned.

The embryo chosen to be sectioned had 11 days and 12 hours of incubation. The neural crest transplant involved a piece of neural fold from the mesencephalic and rhombencephalic region as was carried at 8 somite stage.

We performed Feulgen-Rossenbeck stain (as described in the methods section). Although multiple protocols were tried and different variations in some timings and reagents were tested, we were never able to differentiate the quail from the chicken nuclei. For this reason we tried a second technique to distinguish quail from chicken cells: immunohistochemistry (IHC).

We used QCPN monoclonal antibodies in order to detect the quail (donor) cells that were present in the embryo. The results were positive and showed that the frontal was not stained at its posterior region (Fig.

17 to 21). At the anterior region the frontal presented many positive cells for the QCPN antibody (Fig. 21). However there seemed to have been some contamination of ectoderm given that a significant portion of epiderm was also positive (FIG. 21). Other maxillary and mandibular bones were also formed by donor quail cells showing that the transplant worked properly. In addition the ear reagon, particularly the cartilagineous otic capsule presented cells from quail origin (Fig. 18 and 19).



Fig. 16 Embryos Y and AB. Quail-chick chimeras. A, right lateral view of embryo Y. **B,** posterior view of embryo Y. **C,** right lateral view of embryo AB. **D,** left lateral view of embryo AB. In all views black feathers are from donor (Quail) origin.

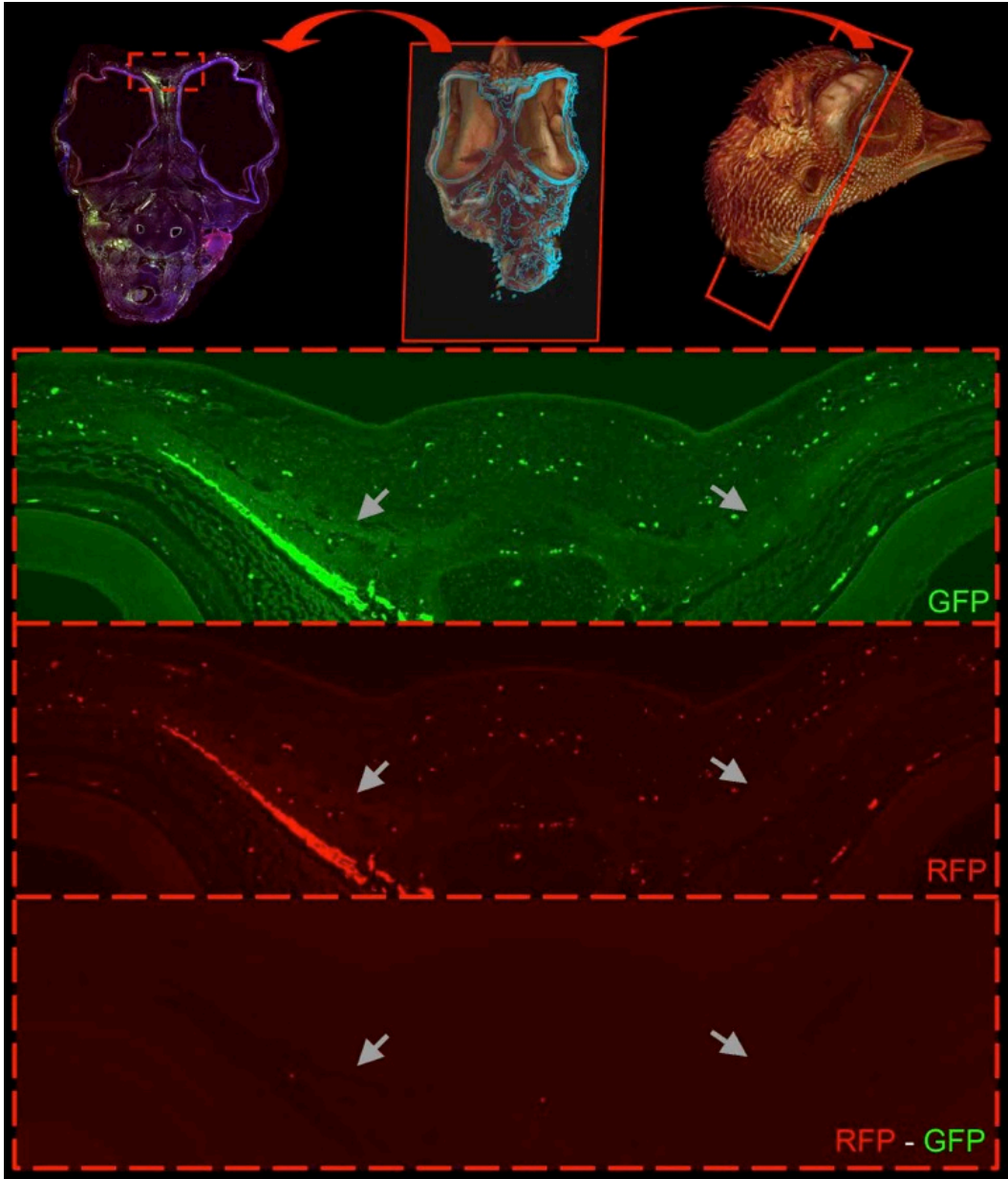


Fig. 17 Absence of cells transplanted to chicken embryo on the frontal bone (embryo HU1504_14, AM, 11D + 11,5h, slide 100). .
A, autofluorescence under GFP channel (green). **B**, QCPN staining under RFP channel (red) **C**, RFP channel after subtraction of GFP

channel. Note that there is no staining in the frontal. Grey arrows point to left and right frontal bones.

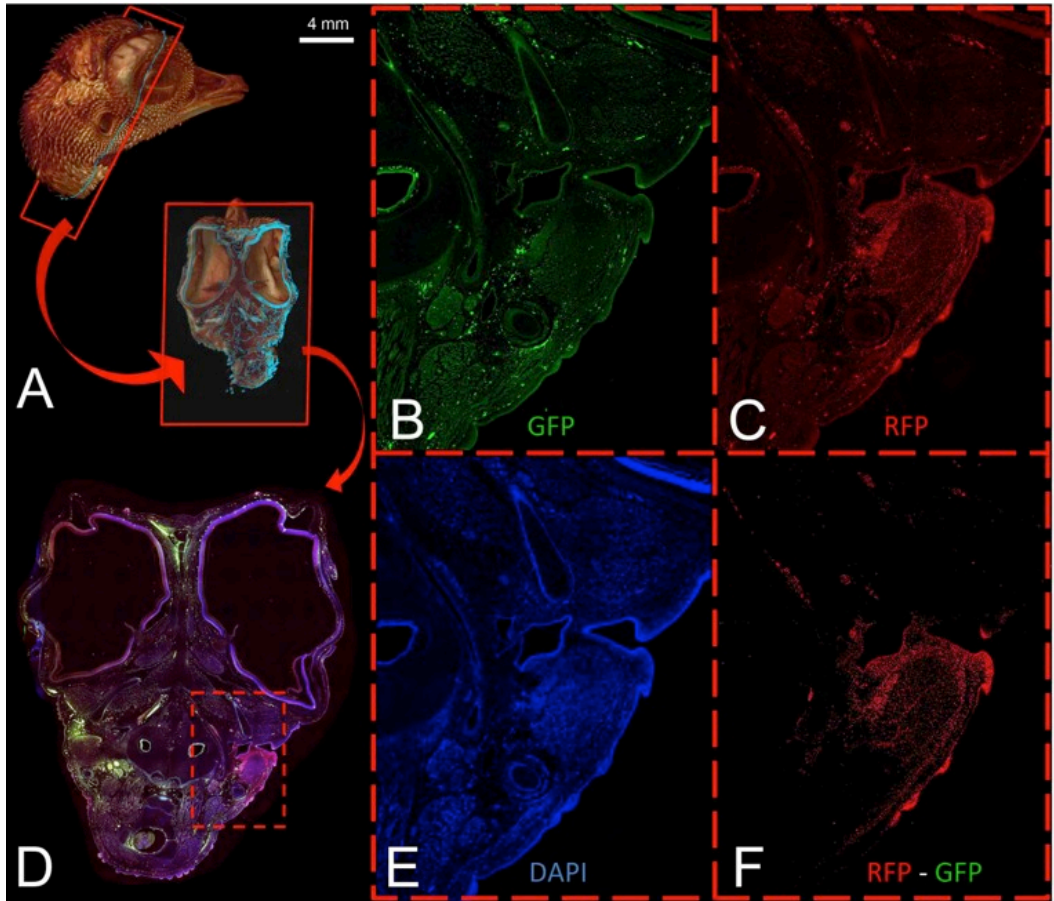


Fig. 18 Quail cells transplanted to chicken embryo (embryo HU1504_14, AM, 11D + 11,5h, slide 100). **A**, virtual section to show a quail head. **E**, DAPI staining (blue). **B**, autofluorescence under GFP channel (green). **C**, QCPN staining showing quail cells transplanted to chick embryo present in the epidermis and in dermis, epidermis and cartilage. **E**, DAPI. **F**, RFP channel after subtraction of GFP channel.

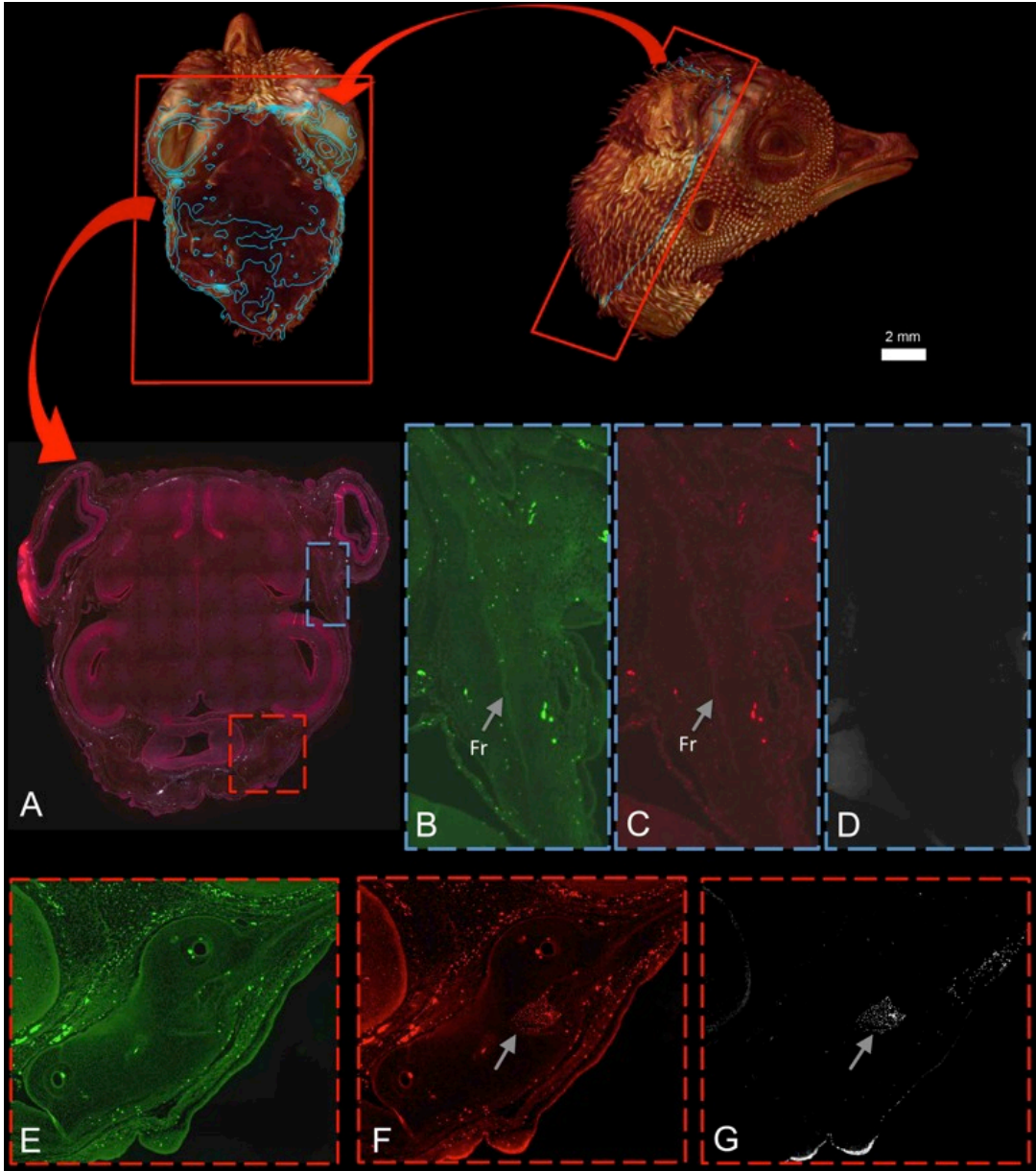


Fig. 19 Quail cells transplanted to chicken embryo (embryo HU1504_14, AM, 11D + 11,5h, slide 151). **A**, Head coronal section. **B**, **C**, and **D**, frontal bone section under GFP, RFP and RFP after subtraction of GFP channel respectively. **E**, **F** and **G** internal ear section under GFP, RFP and RFP after subtraction of GFP channel respectively

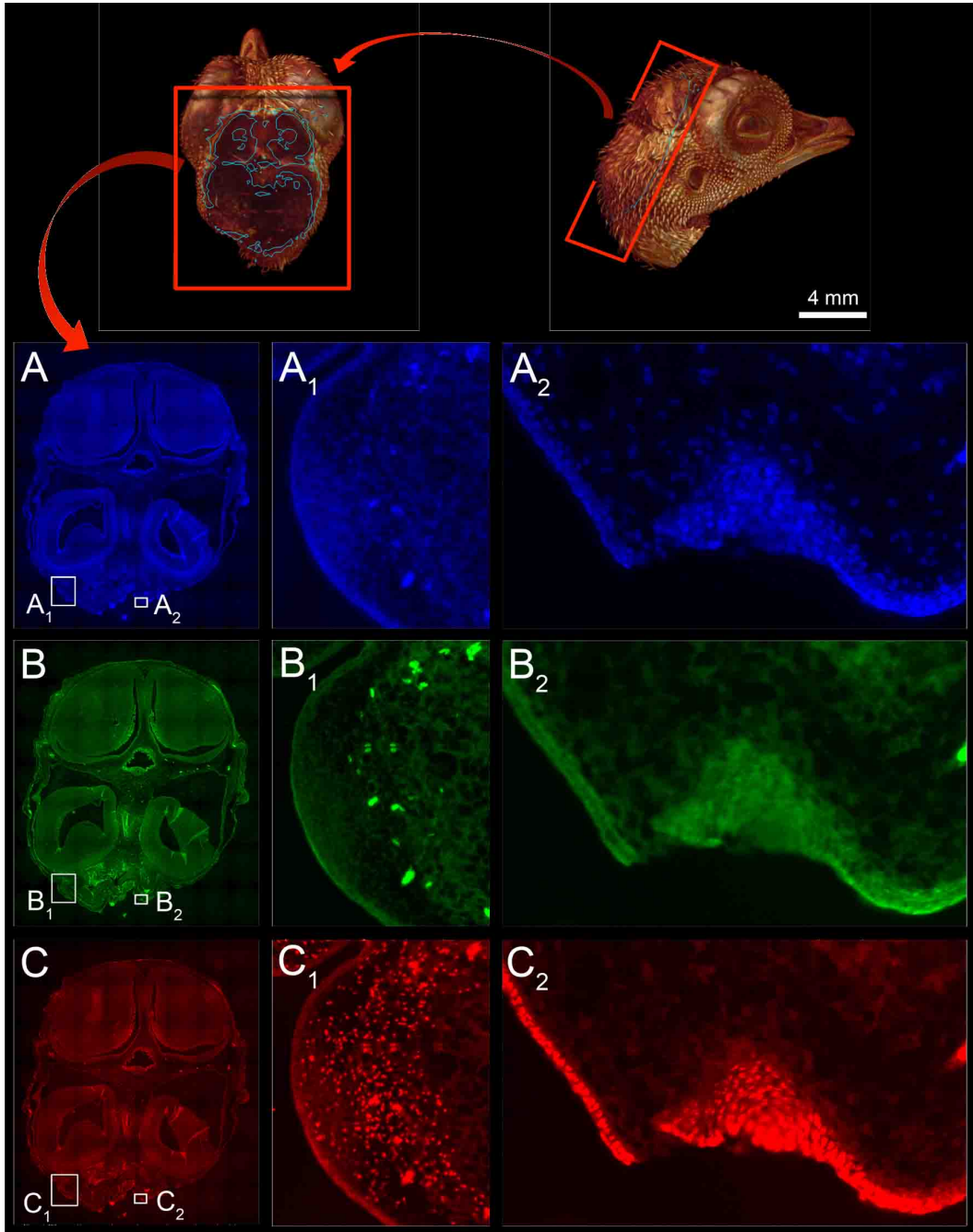


Fig. 20 Quail cells transplanted to chicken embryo (embryo HU1504_14, AM, 11D + 11,5h, slide 168). **A**, DAPI staining (blue). **B**,

autofluorescence under GFP channel (green). **C**, QCPN staining showing quail cells transplanted to chick embryo present in the dermis C1 and epidermis C2. **A₁**, **A₂**, **B₁**, **B₂**, **C₁** and **C₂**, magnifications of the corresponding regions signalized by rectangles in **A**, **B** and **C**.

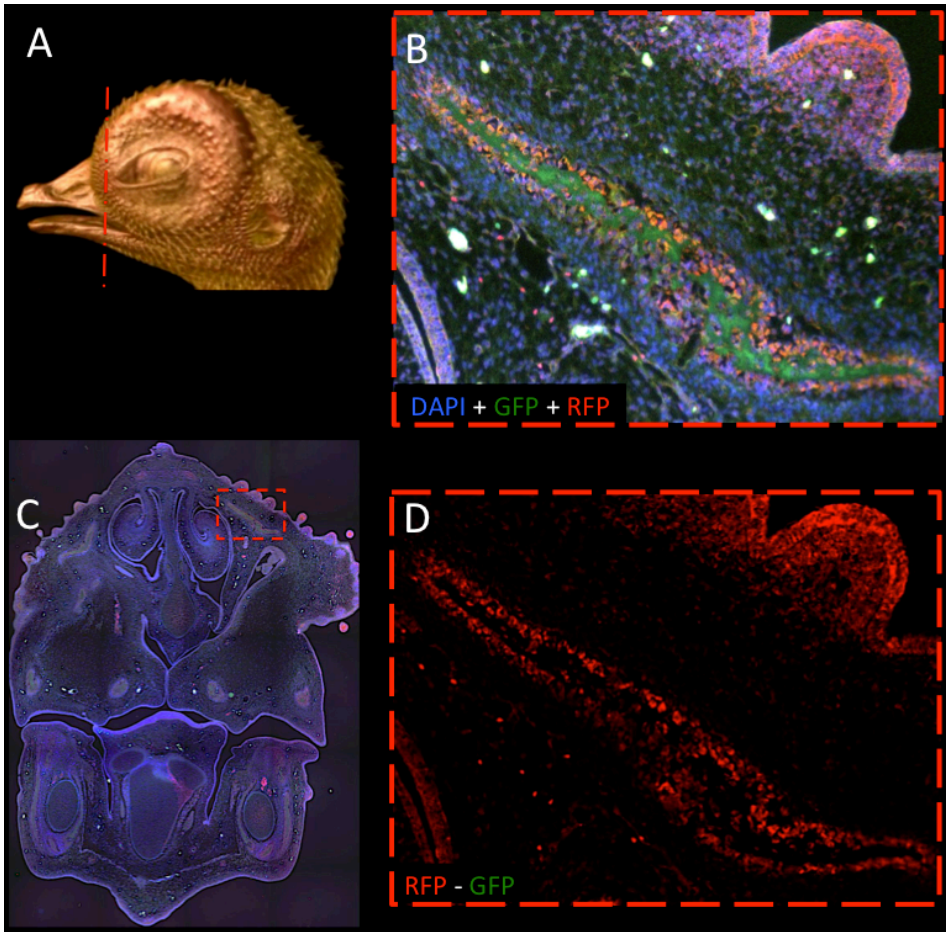


Fig. 21 Quail cells transplanted to chicken embryo (embryo HU1504_14, AM, 11D + 11,5h, slide 39). **A**, cutting plane. **B**, The frontal bone (DAPI plus GFP plus RFP channels). **C**, Whole section correspondent to the cutting plane in **A**. **D**, same as in **B** but with the RFP channel after subtraction of the autofluorescence capture using GFP channel. **B** and **D** correspond to the same zone marked in **C** with a red rectangle.

Chick GFP-Chick wt Neural Crest transplants

A total of 173 transplants were done in embryos ranging from 2 to 10 somite stage. The transplants we done unilaterally according to the

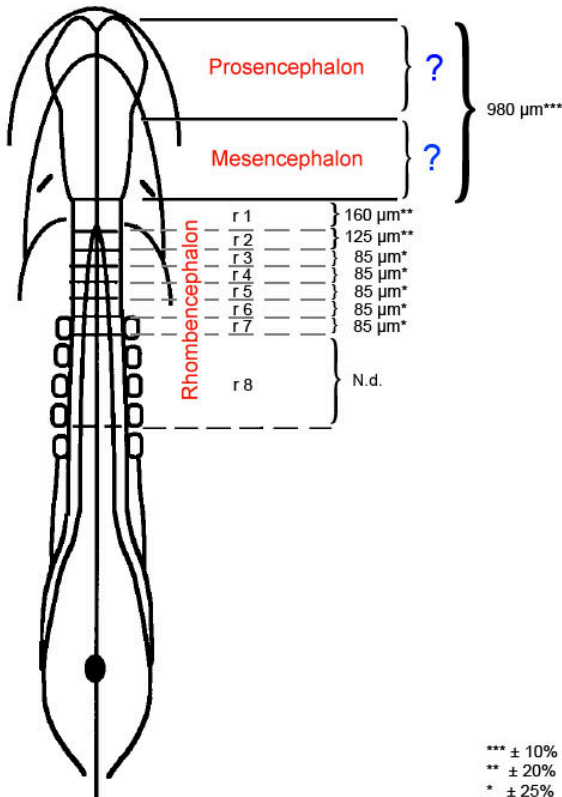


Fig. 22 Fate map of the presumptive territories of the Cephalic Neural Crest at the 5-somite stage (adapted from (Grapin-Botton et al. 1995)). Note that the boundary between Prosencephalon:Mesencephalon was never described nor the posterior limit of the rhombomere 8

fate map described by previous authors (Couly, Coltey, and Douarin 1993; Grapin-Botton et al. 1995) (Fig. 22). In addition we only carried out unilateral isotopic transplants between embryos at an equivalent developmental stage.

Neural crest transplants

We made 86 neural crest transplants of which 28 survived more than one week and were sacrificed at different time points ranging from day 7 and 12 hours to 19 days and 13 hours. The exact position of each graft was registered using a micrometer scale. All

sacrificed embryos were photographed in a fluorescent binocular microscope and some embryos were selected for sectioning either in

cryostat or microtome for histological analysis. Some embryos were also 3D imaged using optical projection tomography (see methods section for detailed protocol).

Transplants of mesencephalic and anterior rhombencephalic (r1 and r2) neural crest

The left-right asymmetry in the expression patterns of the GFP chimeras is easily visible when comparing both sides of the head under fluorescent light (Fig. 23 and 24). The GFP signal was more intense in the lower jaw than in the calvarial region of the head.

Under the fluorescence dissecting microscope it was possible to observe a strong GFP signal in the ventro-posterior region of the head (Fig. 24). Thus, prior to dissection it was possible to tentatively identify some bones in the regions presenting GFP expression. There was a marked stain in the viscerocranium, namely: dentary, splenial, angular, prearticular, jugal, quadratojugal, nasal, prefrontal, maxilla and premaxilla (Fig. 24). The premaxillar region was only stained in the embryos that resulted from the most anterior neural crest transplants. Given that only few transplants were carried in this NC region the premaxilla, nasal and prefrontal were only stained in a small portion of the total embryos. The replication and consistency in these results suggests that the contribution of the neural crest region that will produce the premaxilla/maxilla boundary is already defined at 3-5 somite stages and is located anteriorly to the diencephalon/anterior mesencephalon region.

Some embryos emitted strong green fluorescent light from the posterior region of the head (Fig. 24) corresponding to the place where the posterior frontal and parietal bones should lie. However, after histological analysis this GFP signal proved to be derived from

mesenchymal cells and neurons (probably resulting from a small part of the neural tube that was transplanted attached to the NC grafts). On histological slides, it was possible to observe very few and isolated GFP cells near the parietal (periosteum) and posterior frontal (periosteum and osteocytes). These results contrast with the higher amount of GFP cells present in the immediately adjacent tissues, namely: mesenchyme, meninges, brain, cranial nerves, epidermis, feather follicles and multiple cranial bones (Fig. 25 to 28).

Donor GFP cells invade the anterior part of the frontal and the complete squamosal. The latter presents a higher (average 39,2% GFP cells) concentration of GFP cells than the frontal at any level (average 3,66%) (Fig. 27). Our cell count confirmed that the distribution of GFP cells in the frontal was not homogeneous. A proportion of 5,2% of the cells present at the anterior region of the frontal bone expressed GFP, while only 0,25% were GFP positive at the posterior part.

There was a small portion of cells that crossed towards the side where we did not transplant any piece of neural fold. The fraction of cells crossing was estimated by dividing the percentage of GFP cells present in the right squamosal by the percentage present at the left squamosal. This results showed that approximately 6,7% of cells cross from one side to the other of the neural crest.

Noteworthy, at his dorso-posterior region the squamosal present high concentration of GFP cells in its lateral surface while its medial surface is almost free of GFP cells (Fig.28). Bones and cartilages derived from first pharyngeal arch expressed GFP signal, namely: maxilla, palatine, pterygoid, squamosal, quadrate, entoglossum, dental, splenial, surangular, angular, articular. All these bones presented not

only osteocytes (completely encased inside osteoid matrix) but also osteoblast and mesenchymal cells in the periosteum expressing GFP.

Interestingly, the squamosal bone appears to be formed from neural crest origin but the osteoblasts and osteocytes expressing GFP are present predominantly on the lateral surface of the periosteum (Fig. 28 C).

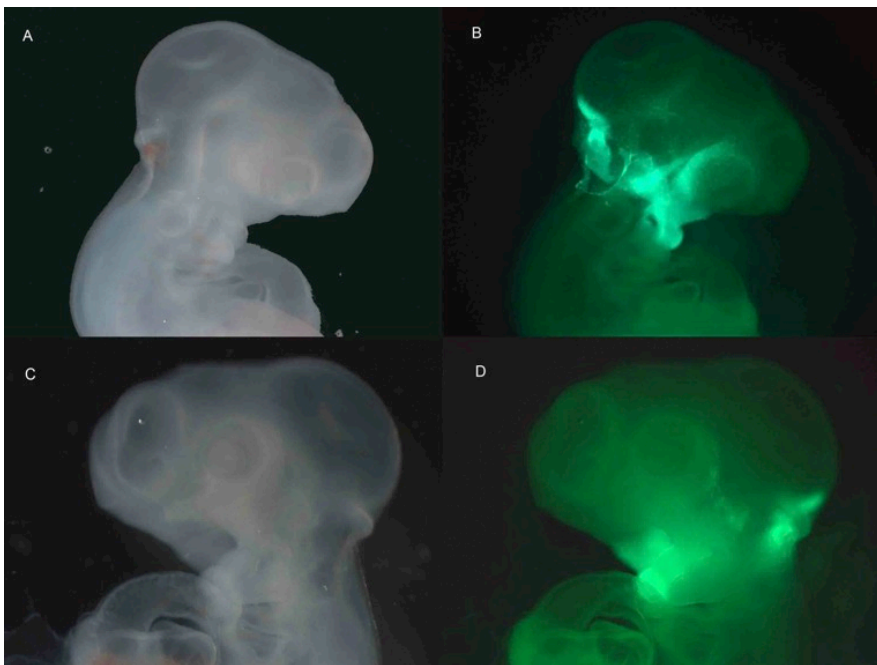


Fig. 23 Embryo 102. (2 days and 18 hours of incubation). **Right side Neural Crest transplant, Chick GFP to Chick Wt.** **A**, Right lateral view under bright field. **B**, Right lateral view under fluorescent light. **C**, left lateral view under bright field. **D**, left lateral view under fluorescent light.

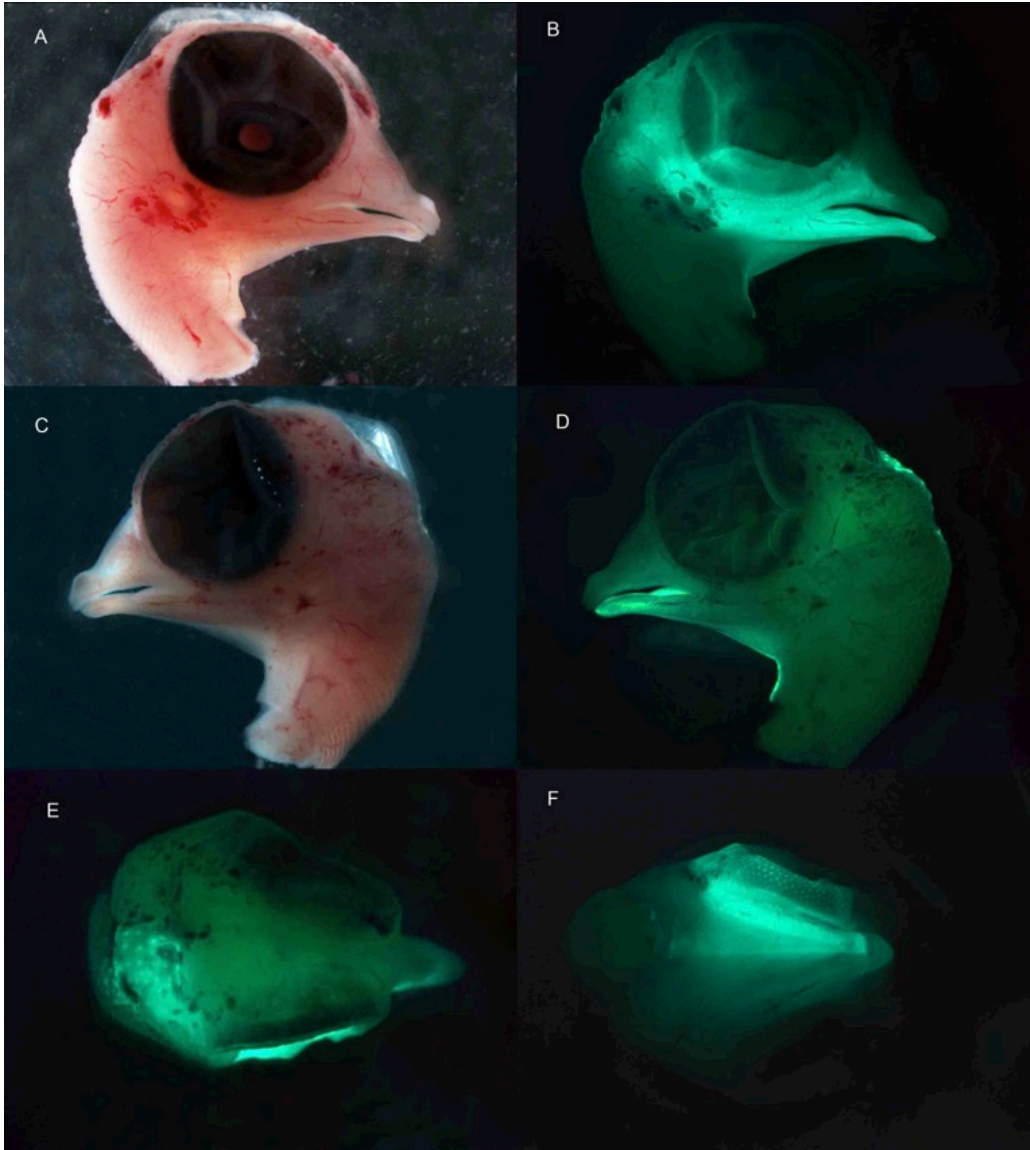


Fig. 24 Right side Neural Crest transplant, Chick GFP to Chick Wt. Embryo 12 (10 days and 8 hours of incubation). **A**, Right lateral view under bright field. **B**, Right lateral view under fluorescent light. **C**, left lateral view under bright field. **D**, left lateral view under fluorescent light. **E**, dorsal view under fluorescent light (beak towards right). **F**, ventral view under fluorescent light (beak towards right).

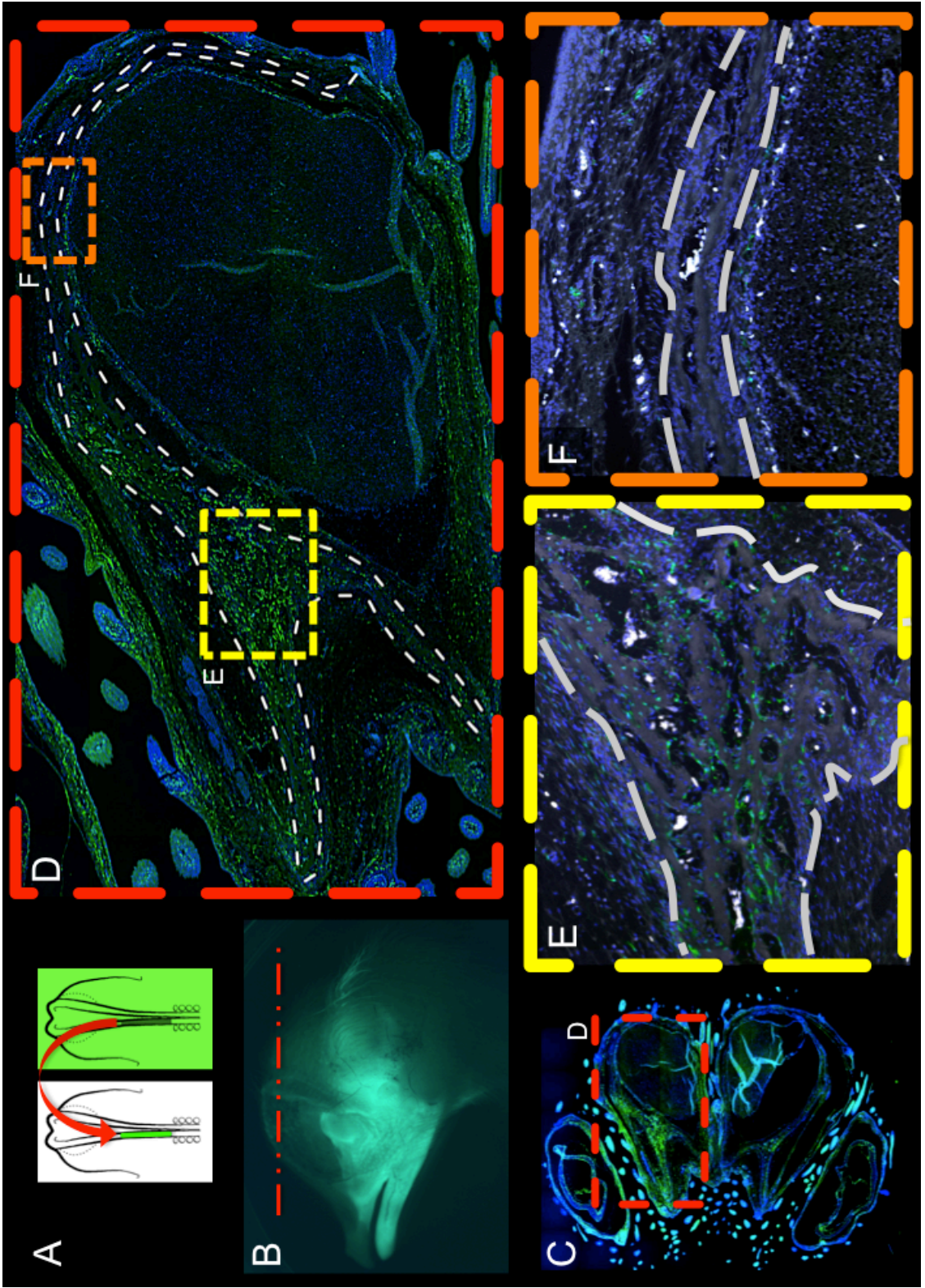


Fig. 25 (previous page) Transverse histological section of the head of a GFP-wt chicken chimera (embryo 27). **A**, schematic draw of the neural crest transplant performed. **B**, head of the GFP-wt chicken chimera under fluorescent light showing section plane of the histological section shown in **C-F**. **C**, Result of 150 stitched fluorescence microscope images (using 10X objective). Blue: DAPI. Green: GFP after subtraction of autofluorescence captured with RFP channel. **D**, enlargement of the area framed in **C**. **E and F**, enlargement of the areas framed in **D**. **E** shows anterior part of the frontal while **F** show posterior region. Dashed grey lines: frontal bone profile.

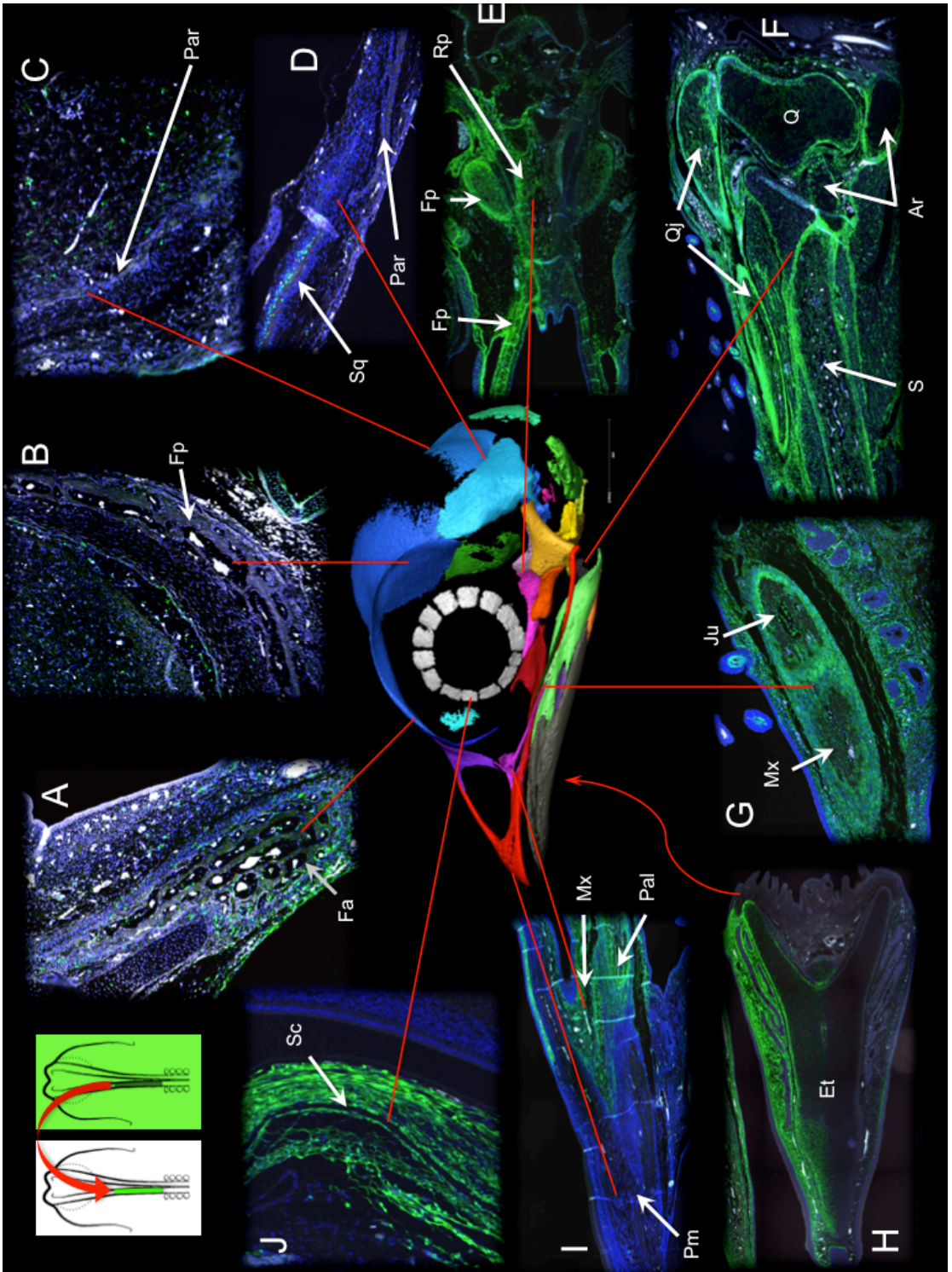


Fig. 26 (previous page) Transverse histological sections of the head of a GFP-wt chicken chimera (embryo 27). **A**, anterior frontal bone region; **B**, posterior frontal region; **C**, parietal bone; **D**, squamosal-parietal suture; **E**, sphenoid region; **F**, articulation quadrate-articular; **G**, jugal and maxilla; **H**, entoglossum; **I**, maxilla-premaxilla suture; **J**, sclera. Upper left corner: schematic draw of the neural crest transplant performed. Central image is a virtual segmentation of a micro-ct performed to a chicken embryo where each bone as a different color. Images **A-D** correspond to the same coplanar section.

Abbreviations: Ar, articular; Et, entoglossum; Fa, Fp, frontal posterior; Ju, jugal; Mx, maxilla; Par, parietal; Pm, premaxilla; Rp, rostromparasphenoid (presphenoid); Qj, quadratojugal; Q, quadrate; S, surangular; Sq, squamosal; Sc, sclerotic bone.

Blue: DAPI. Green: GFP after subtraction of autofluorescence captured with RFP channel.

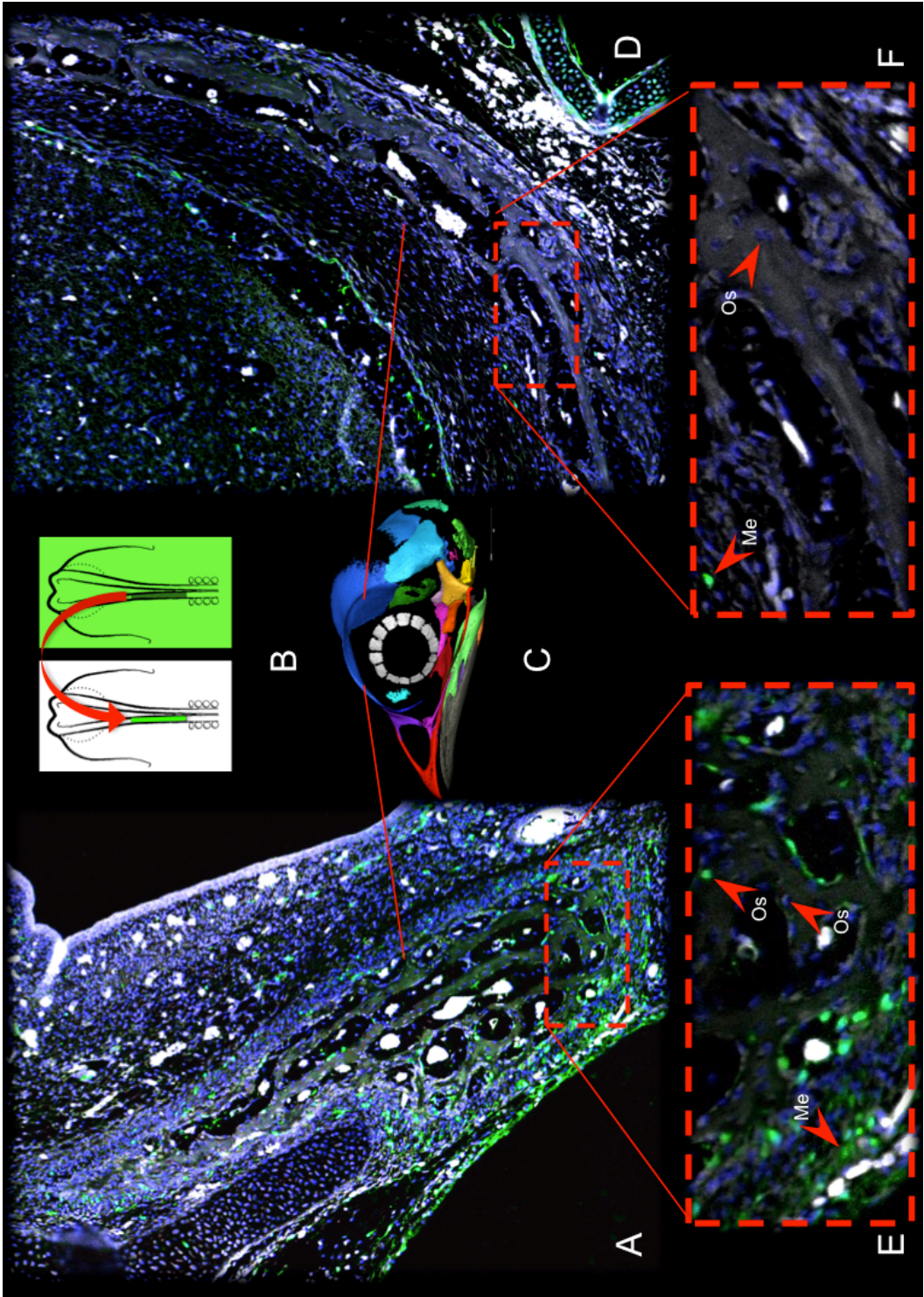


Fig. 27 (previous page) Transverse histological section of the head of a GFP-wt chicken chimera (embryo 27). A, anterior frontal bone region; **B**, schematic draw of the neural crest transplant performed. **C**, virtual segmentation of a micro-ct performed to a chicken embryo where each bone as a different color; **D**, posterior frontal region; **E** and **F**, enlargements of the area framed in **A** and **D** respectively. Images **A** and **D** are coplanar.

Abbreviations: Me, mesenchymal cell; Os, osteocyte encased in osteoid matrix.

Blue: DAPI. Green: GFP after subtraction of autofluorescence captured with RFP channel.

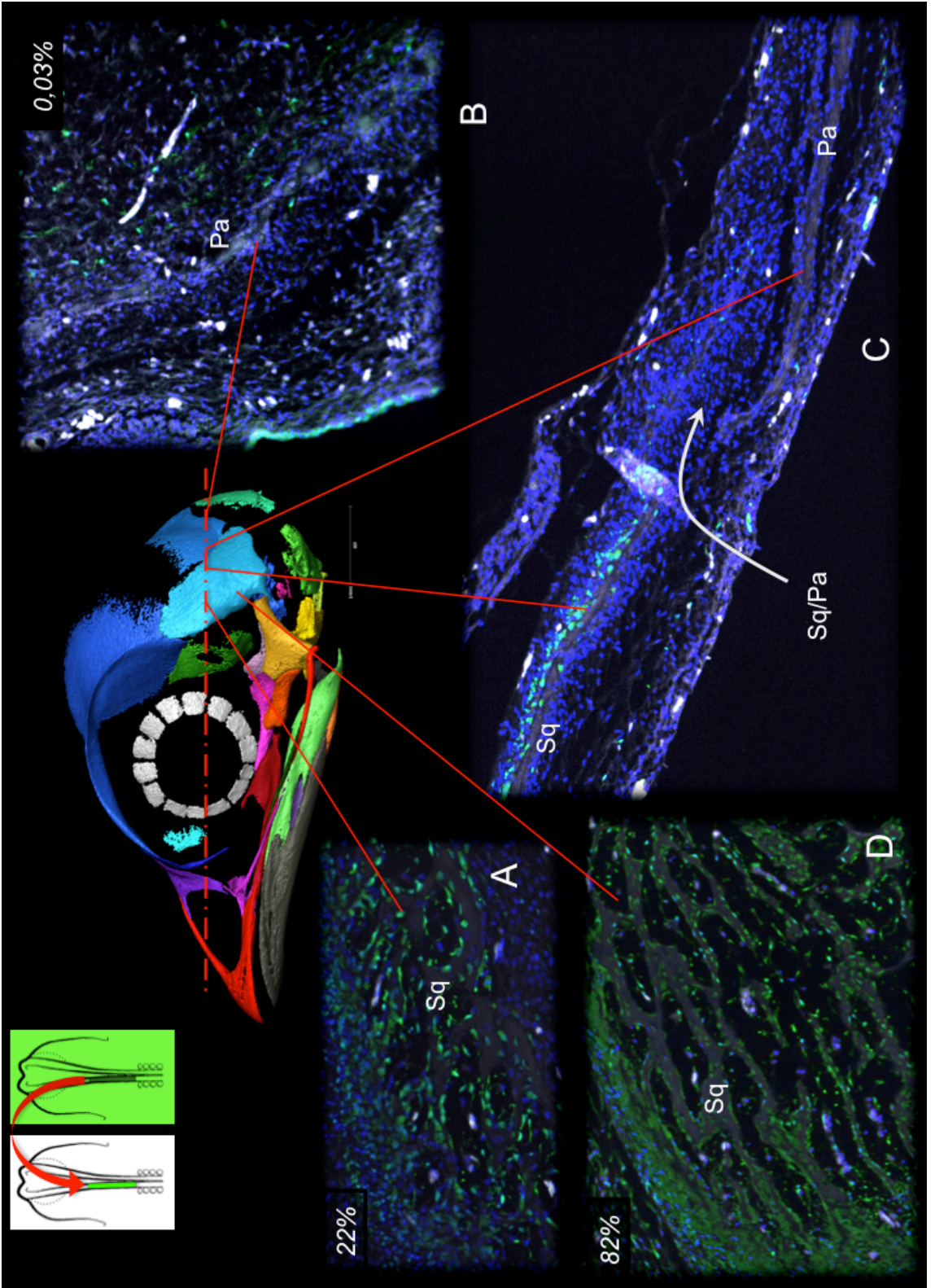


Fig. 28 (previous page) Transverse histological section of the head of a GFP-wt chicken chimera (embryo 27). A, anterior squamosal region; B, posterior parietal; C, squamosal-parietal suture; D, anterior squamosal region (ventral section). Upper left corner: schematic draw of the neural crest transplant performed plus virtual segmentation of a micro-ct performed to a chicken embryo where each bone as a different color.

Images **A-C** are coplanar (dashed line). Image **D** corresponds to a more ventral section.

Abbreviations: Pa, parietal; Sq, squamosal, Sq/Pa, squamosal-parietal suture.

Numbers indicate the percentage of GFP cells present in each bone at each level.

Blue: DAPI. Green: GFP after subtraction of autofluorescence captured with RFP channel.

Paraxial Mesoderm Transplants

Grafts of the Paraxial Mesoderm at the mesencephalic level

We transplanted 87 embryos ranging from 2 to 6 somite stage. From these, 37 survived until day 8 to 15^{1/2} and were fixed in buffered formaldehyde 4 % solution over night before being analyzed (see methods section for detailed protocol). These transplants are technically challenging and in order to have success only very few cells could be transplanted in each embryo.

All surviving embryos were photographed using a fluorescence microscope (examples can be see in Fig. 29 and 30). Only very weak signal was captured. In some embryos it was possible to see a small strip of GFP cells at the posterior region of the eye. After macroscopic analysis we selected and sectioned 3 embryos presenting GFP signal.

Each section presented very few GFP cells but all embryos showed GFP cells in structures known to be derived from mesoderm, namely vascular endothelium and striated muscle cells. There were no GFP cells resulting from mesoderm transplants crossing from one side to the other. The GFP cells tended to be in groups (e.g. in one or two muscles) rather than separated over many mesoderm derived tissues.

In one out of 3 embryos sectioned, we found some GFP cells present inside the frontal bone osteoid matrix and in the periosteum surrounding it (Fig. 31). The sections were made in the cryostat and had 40 μm in thickness and given that multiple layers of cells were overlapping the resolution was not as good as the paraffin sections that did not shown any GFP cells in the frontal bone.

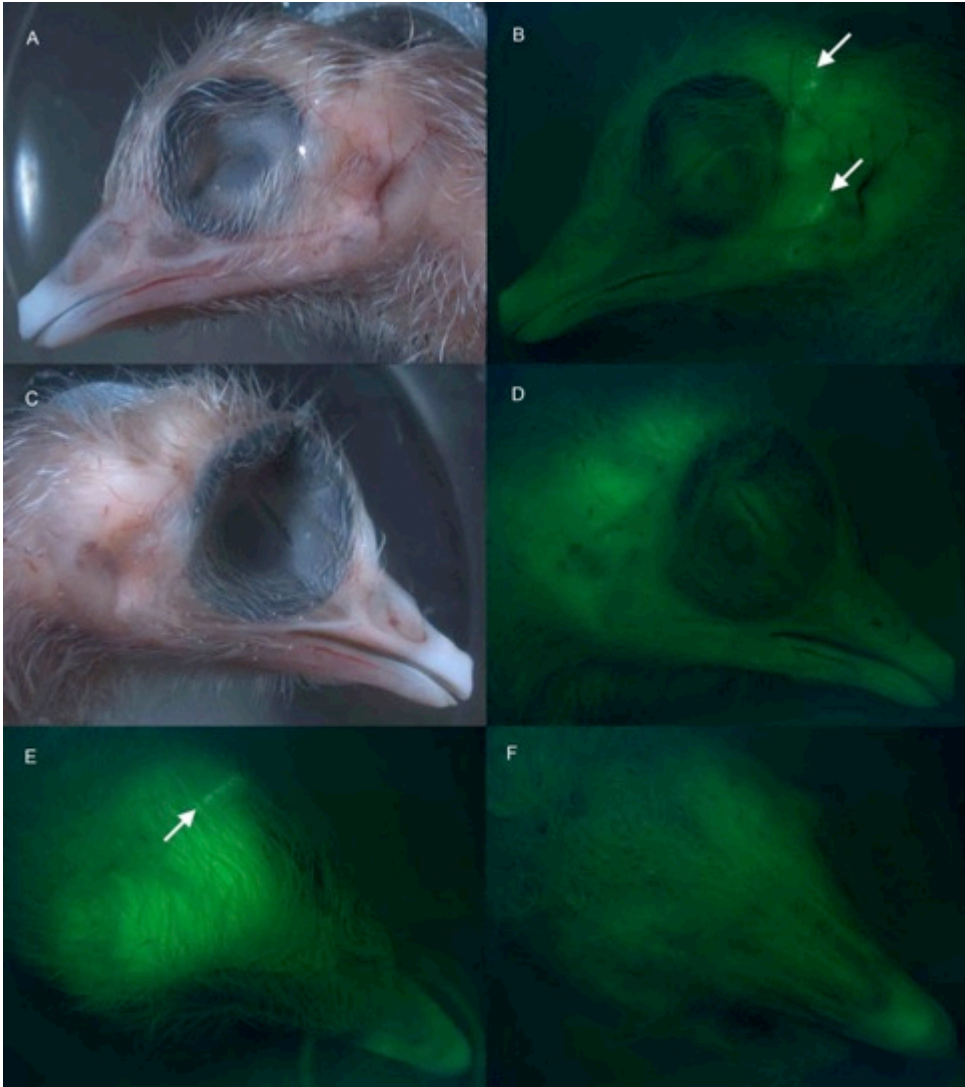


Fig. 29 Left side Paraxial Mesoderm transplant Chick GFP to Chick Wt. Embryo 154 (13 days of incubation). **A**, left lateral view under bright field. **B**, left lateral view under fluorescent light. **C**, right lateral view under fluorescent bright field. **D**, right lateral view under fluorescent light. **E**, dorsal view under fluorescent light (beak towards right inferior corner). **F**, ventral view under fluorescent light (beak towards right inferior corner). Arrows pointing to GFP cells.

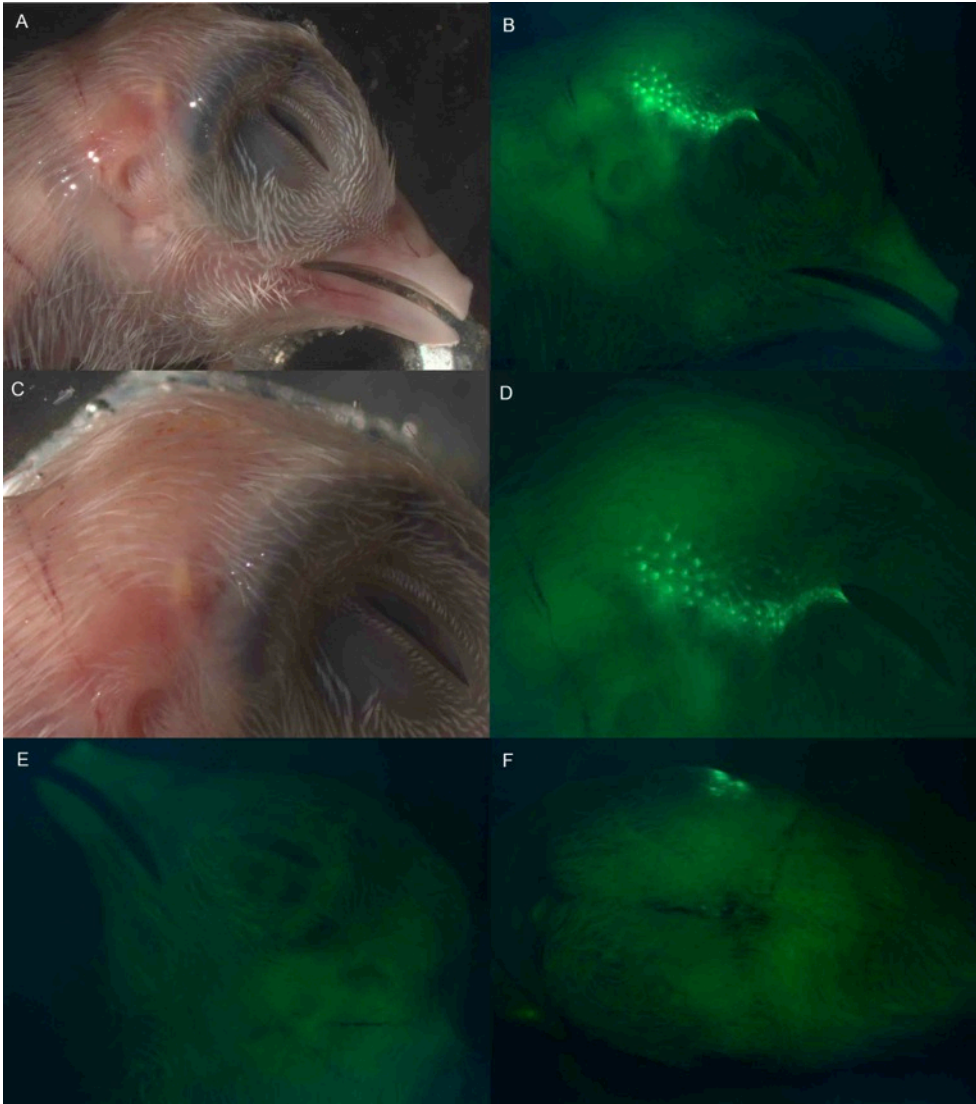


Fig. 30 Right side Paraxial Mesoderm transplant Chick GFP to Chick Wt. Embryo 128 (15 days of incubation). **A**, right lateral view under bright field. **B**, right lateral view under fluorescent light. **C**, zoom in the temporal region under bright field. **D**, zoom in the temporal region under fluorescent light. **E**, left lateral view under fluorescent light. **F**, Posterior view under fluorescent light (dorsal part towards left).

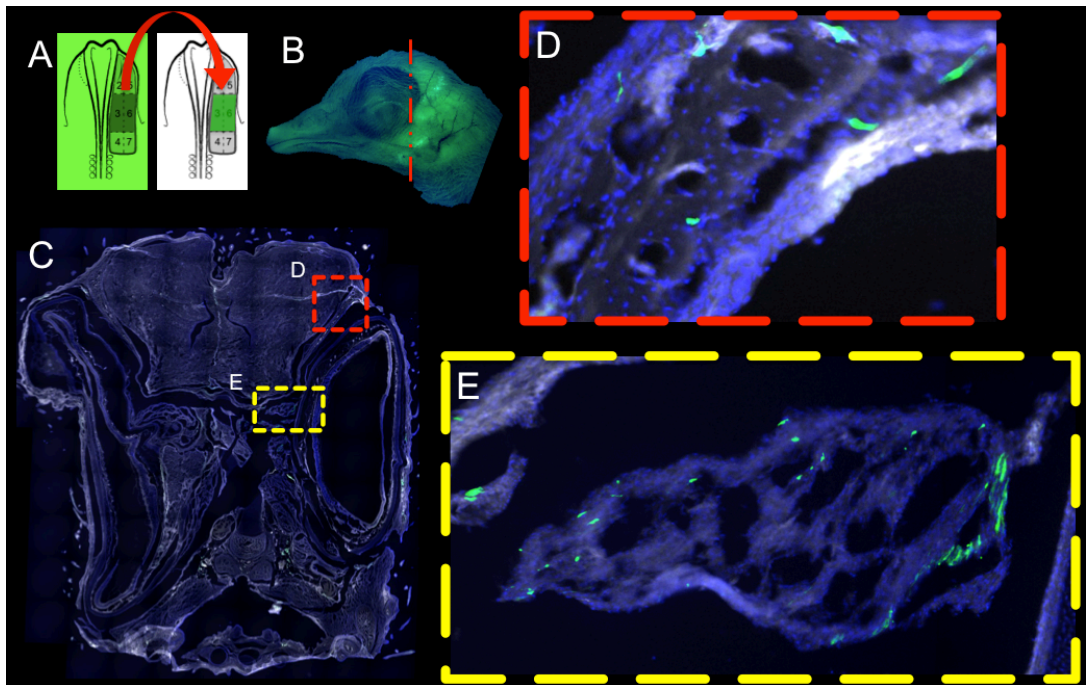


Fig. 31 Coronal histological section of the head of a GFP-wt chicken chimera. **A**, schematic draw of the mesoderm transplant performed; **B**, Head of the embryo with section plane marked by a dashed line; **C** Coronal histological section (dorsal towards top). **D**, Posterior region of the frontal with GFP cells inside osteoid matrix. **C**, Oculomotor muscle with GFP cells derived from donor origin. Green – GFP . Blue - DAPI.

OPT

After dissection it was possible to isolate and remove both frontal bones from one chicken embryo (4 somites) to which a piece of neural crest was transplanted (Fig. 32). We could measure the exact portion of neural fold transplanted. The graft had 685 μm in length and its anterior limit reached the posterior prosencephalic NC region while the caudal limit reached the boundary between r1:r2. It is difficult to determine if the anterior limit of the graft did or did not include part of the prosencephalic NC given that the best fate map made so far could not define the prosencephalon:mesencephalon boundary at 5 somite stages (Grapin-Botton et al. 1995). (Fig. 22) The embryo was sacrificed at 15 days of incubation and presented strong GFP signal under the binocular microscope in the anterior region of the head but also in the lower beak.

The isolated frontals were imaged using optical projection tomography (OPT) (for detailed protocol see methods section). The OPT resolution was not sufficient to distinguish between different cells but the GFP signal was clearly detected. Both GFP signal and the autofluorescence emitted were intense enough to produce a virtual volume of both frontals (see methods section). After digital subtraction of the autofluorescence signal we isolated the pure GFP signal.

The resulting 3D images show a strong GFP signal at the supraorbital region of the frontal. This pattern decreased in intensity anteriorly, almost until the most anterior tip of the frontal. Conversely, the posterior region of the frontal did not present any difference when compared to the control right frontal. This latter bone did present very faint GFP signal but only at the corresponding contralateral regions (not visible in Fig. 32). There was an evident frontier between the posterior region of the frontal and its anterior part where the GFP signal was

present. This segregation was abrupt and extremely visible in any angle of the 3D volume (Fig. 32).

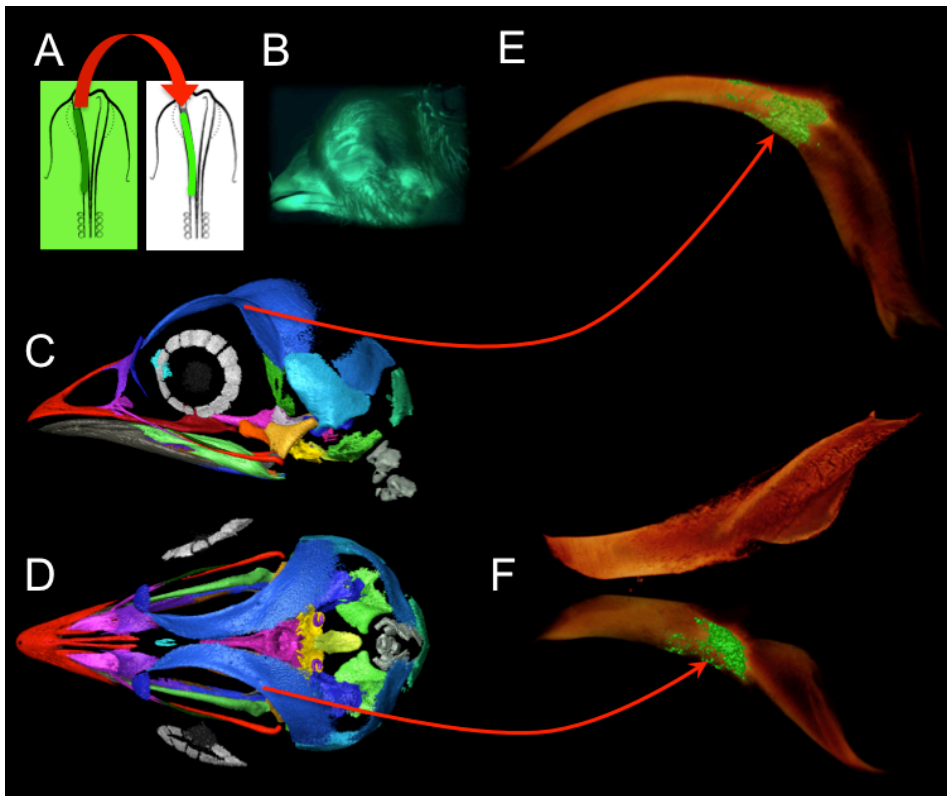


Fig. 32 Optical projection tomography image from the frontal bones of embryo 76. **A**, schematic draw of the neural crest transplant performed. **B**, Head in lateral view under florescence light. **C and D** left and dorsal view of a chicken embryo with all bones segmented in a different color. **E and F** left and dorsal view of the frontal bones of embryo 76. Red arrows point to the equivalent regions in the frontal. In **E** and **F**, GFP staining is represented by green smear while red brown color represents autofluorescence.

Discussion

Frontal ossification

The fact that the frontal bone of *Gallus gallus* shows, during its development a double center of ossification has been reported previously (Erdmann 1940). Erdmann described two centers formed synchronously with one being dorsolateral to the upper edge of the interorbital septum and another center posterior in what would form the caudal third portion of the adult frontal. Although Erdmann did not provide any sample data nor showed the dynamics of this process, this double ossification center pattern is consistent with what we found in the embryos that we examined. Other authors failed to confirm this observation (Thompson, Owens, and Wilson 1989) or, although citing Erdmann work, do not mention whether their observations agreed with those of Erdmann (Jollie 1957). In addition, different studies point to distinct starting points of ossification of the frontal bone, namely: 9 days of incubation (Erdmann 1940); 10 days (Thompson, Owens, and Wilson 1989); 11 days (Jollie 1957) and 12 days (Schinz and Zangerl 1937) in (Romanoff 1960; Thompson, Owens, and Wilson 1989). This discrepancy in results may be explained by differences in: a) conditions during incubation; b) chicken breeds; c) protocols used to access ossification and also difficulties in registering the starting point of incubation or even d) reduced sample numbers and time points.

Erdmann used two chicken breeds (Leghorn and Rhode Island) and registered some significant differences in the ossification onsets. For example, the frontal bone registered a delay of almost 6 hours between the two breeds (Leghorn 8 days and 23^{1/2} hours and Rhode Island 9 days and 5 hours). Although multiple time points were covered, it should be noted that Erdmann did not open eggs from both breeds at regular

and simultaneous periods, so this difference might be smaller. Jollie did not present exact incubation ages given that the starting point (and rate) of development could not be ascertained (Jollie 1957). He also points to the fact that his embryos with 10-11 days were equivalent in development to the ones describe by Erdmann at day 9. A simple difference of one or two degrees in the temperature at which the eggs were incubated can result in significant differences in rates of embryo development (French 1997). Given that only Thompson and colleagues describe the temperatures of incubation used (37.5 °C) it is hard to compare the onset of ossification between the different studies.

Our experiments were carried at 38°C which might explain why we find the ossification of the frontal at 9 day plus 3 hours. This is inline with Erdmann's experiments (between 8 days and 23^{1/2} hours and 9 days and 5 hours) but it is earlier than what Thompson and colleagues have reported (10 days). The latter authors used a lower incubation temperature. Furthermore, the fact that they did not register any embryo with a double center of ossification might be a result of a small sample bias, meaning that they might have collected embryos from outside of the 24h interval that the two centers take to fuse (i.e. embryos younger than 9D + 3h or older than 10 days + 3h). Although the temperature discrepancy might help to explain the difERENCE in the ossification onset the latter observation can be indicative that they might have opened few eggs or not at regular intervals. In any case, the published methodological description in all these works does not provide enough detail to clarify these questions (Schinz and Zangerl 1937; Erdmann 1940; Jollie 1957; Thompson, Owens, and Wilson 1989). However, our data shows that with all variables controlled a developmental time series can be rigorously established.

As noticed by Erdmann, the double center of ossification in the frontal suggests that the posterior center is homologous to the reptilian postfrontal bone. Given that there is no experimental work regarding the development of the postfrontal in other Archosauria (e.g. crocodylian) this hypothesis awaits empirical testing.

If the postorbital is found to be derived from neural crest (e.g. in other reptiles) and the fate maps produced by Couly and colleagues are correct, then the postorbital would be in a better position to claim the homology with the posterior center of ossification present in the frontal of birds.

If the reptile postorbital is shown to be derived from any other embryological origin and Couly fate maps are correct, then, it would be more parsimonious to assume that this bone was either lost during the evolutionary lines that originated the birds. At most, if still conserved, it is undergoing some vestigialization process as appears to be the case for the classical example of the pleurospenoid cartilage that some times ossifies at its postorbital region (Zusi 1993). In fact, *Struthio* does not present a ossified postorbital process of the pleurospenoid, instead the postorbital process develops in the posterolateral region of the frontal (Zusi 1993).

If instead the posterior portion of the bird frontal is derived from paraxial mesoderm (as our work seems to indicate), then the postorbital bone would be a good candidate to be homologized to that region in the frontal, in case it is proven to have the same origin (what is yet to be done). If not, it would be more parsimonious to assume that the postorbital bone was lost or is only conserved as part of the pleurospenoid. In any case, and given that there is no experimental evidence regarding the origin of the postorbital bone these hypotheses

are only speculative and cannot be accepted until further analyses are done. It would be important to perform fate map experiments in crocodylians, Squamata or even chelonian species given that all these groups possess well-developed postorbital bones. The resulting data could shade light into this debate.

Until now we have done sequential Alizarin-Red/Alcian-blue stainings in chicken, quail and duck embryos. We used a time window of 4 hours along the development of these three species. The results show that chicken and duck clearly present two centers of ossification in the frontal bone while the quail shows only a single ossification center. Few other bones (e.g. maxilla, dentary, sphenoid) ossify from multiple centers merging latter into one, none of which in the calvarium. In addition, all those bones present multiple rami, foramina and diverticula and it would be difficult to imagine a process that would form such complex shapes via a single ossification center. In any case, high morphological complexity should not be the only explanation and, above all, it should not prevent any additional effort to explain why and how these bones form and to speculate about possible evolutionary causes. Nonetheless, any detailed analysis about each one of these bones entails significant work that goes beyond the scope of this thesis.

Having this in mind, the general rule in vertebrate cranial osteogenesis is: one bone, one center of ossification. As is known, there are exceptions, and these exceptions must be elucidated. The frontal bone is one of these remarkable examples. As presented above, this bone is formed via a double center of ossification in chicken and duck but not in quail, crocodile and mouse.

Different ossification centers might suggest different embryological origins. Thus, as previously proposed, one possible explanation might be that the chicken anterior ossification center is homologous to the NC

derived frontal bone of the mammals and the posterior ossification center is homologous to the parietal PM derived bone of the mammals (Drew M. Noden and Trainor 2005).

The fact that in quail we only observe one OC might be due to: a) insufficient resolution in the staining technique (the embryos at this stage are smaller than the chicken ones and the resolution of the staining is tricky) or b) a secondary lost during evolution of the posterior OC. The former explanation seems less likely given the large replication of our experiments and consistent results pointing to the quail frontal being formed by a single ossification center. However, if the latter hypothesis is correct and if, as is known from other experiments important information regarding bone size and shape are already specified in the premigratory neural crest cells (Jennifer Fish and Schneider 2014), then we might just be observing different effects. Meaning that Noden retrovirus experiments and Couly chimeras would not be contradictory. For the transplants of quail NC via insertion in the excise orthotopic part might show the normal development of the only ossification center present in quails: the frontal anterior center, completely derived from NC. It is important to note that in any case this explanation does not resolve the contradictory results observed in the parietal. Most importantly it also does not explain the different results obtained by different works when using the same method (Le Lièvre 1978; D. M. Noden 1982; D. M. Noden 1984; Couly, Coltey, and Douarin 1992; Couly, Coltey, and Douarin 1993).

There are no complete fate maps published resulting from chicken (donor) to quail (host). These results could help to know if there is any significant interspecific variation influencing the results.

Another possible complementary experiment that could address this issue consists in the use of late NC or PM markers that are present in mesenchymal bone progenitor cells. The problem, though, is that there are no genetic markers that would be appropriate for this purpose. Some early neural crest markers as HNK1 or Wnt1 would be good candidates but they are no longer expressed once the mesenchymal stem cells start to differentiate into osteoblasts. It has been shown that neural crest and mesoderm-derived mesenchymal cells do present over 140 genes that exhibited statistically significant differential levels of expression but it would be challenging to use sets of genes to distinguish between these two cell types (Bhattacharjee et al. 2007). Thus, to the best of our knowledge, there are no molecular marker for mesenchymal bone progenitor cells that can distinguish between NC derived mesenchymal cells from those derived from mesoderm at comparable developmental stages. Although in mice the fate maps have been performed using different experimental approaches. Namely using transgenic mouse with a permanent neural crest cell lineage marker, Wnt1-Cre/R26R, Jiang and colleagues were able to detect the neural crest vs mesoderm components of the mouse cranial vault (Jiang et al. 2002). No equivalent transgenic experiment in chicken was ever produced and, given the difficulties of generating transgenic birds, there is little hope that comparable results will be available in the near future. In addition, Jiang and co-workers reported reduced development of the neural crest derived meninges in retinoic acid treated embryos. This occurs due to an inhibition of the parietal bone development without having any effect in frontal osteogenesis. It would be interesting to repeat this experiment in chicken embryos. This is particularly true because it is known that retinoic acid produces strong phenotypic effects in the avian skull but there is no data about the phenotypic alterations in the skull roof (Lee et al. 2001).

Finally, another approach to shed light over this debate was carried out in the present work and consisted of performing transplants using GFP chickens. Namely, tracing NC and PM cells in GFP-Chicken /wt chicken chimeras can remove any interspecific questions. Through a thorough histological sectioning, we analyzed two embryos. Our results, though preliminary given the low sample size, point to the idea that NC derived cells form the chicken frontal bone anteriorly. The posterior portion of the frontal and the parietal bone do present some few isolated GFP cells suggesting that the contribution of NC to this region of calvarial bones is small but probably not negligible.

An alternative interpretation can advocate that the isolated cells present at the parietal and posterior frontal are not but small contaminations or even systemic leakage normal in any living organism that do not carry any addition signal. If so we should be open to consider that there could be no contribution from neural crest derived cells to these regions.

In order to better understand the development of the ossification centers it would be interesting to perform another experiment. It would be important to see if the quail-chick and chick-quail chimeras present one or two ossification centers using standard Alizarin-red/Alcian-blue staining. This would, not only help to support or reject the previous hypothesis but also contribute to understand if the NC cells that will originate the calvaria represent an example of plasticity or prepatterning (Santagati and Rijli 2003).

Prefrontal/Lacrimal

This antorbital region of the skull is also very interesting since in other Archosauria the prefrontal contacts the lacrimal, ventrally. The latter is thought to have been lost during evolution although some authors prefer to use the term “lacrimal” when referring to the prefrontal (Erdmann 1940; Zusi 1993). It would be interesting to speculate about the evolutionary path of the prefrontal and the lacrimal. Given that both bones have been unambiguously attributed as derived from neural crest origin, and given that they both form via intramembranous ossification it is difficult to be sure if the two centers of ossification can be homologous to the prefrontal and lacrimal of other reptiles. Jollie discussed this hypothesis and points to the fact that the ventral part of the prefrontal (orbital process) has been homologized to the lacrimal by Erdmann (Jollie 1957). In any case, Jollie sustains that the position of the orbital process is not equivalent in reptiles and argues that, because in birds (except ratites) the lacrimal duct does not penetrate it, both ossification centers should be considered part of the prefrontal. Jollie concluded that the prefrontal bone in *Gallus* is more similar to the prefrontal in reptiles (than to the lacrimal) and opted to only use the former name. The same observation (that in ratites this bone is perforated by the lacrimal duct and sometimes contacts the jugal bar) was enough for other authors to consider it as a true lacrimal (Zusi 1993). In any case, only further research combining embryological and anatomical data could help to address this hypothesis properly.

Authors contributions

Conceived and designed the experiments: Rui Castanhinha, Élio Sucena and Joaquín Leon. Performed the experiments: Rui Castanhinha, Gabriel G. Martins, Joaquín Leon, and Gerard Couly. Analyzed the data: Rui Castanhinha. Contributed reagents/materials/analysis tools: Rui

Castanhinha, Joaquín Leon, Élio Sucena, Gabriel G. Martins, Vincent Fernandez, Paul Tafforeau, Nicole Le Douarin and Gerard Couly.

Acknowledgments

We are thankful to Fabian Wilde, Felix Beckmann, for proving the means to perform micro-ct to bird embryos. To Christine Köppl for providing owl eggs. To Marcelo Sanchez Villagra and Daisuke Koyabu for important critical inputs and discussion of ideas.

We are particularly thankful to all Histopathology Unit and Cellular Imaging Unit teams of IGC for all the patience and skill demonstrated in finding practical solutions to all challenges that we have created during the last years.

Chapter II

The first fossil Crocodylomorpha eggs with embryos: a preliminary description

Introduction

Extant reptiles comprise Chelonia, Lepidosauria, Aves and Crocodylia. Fossil ancestors of all these groups are common and represent some of the most studied vertebrates worldwide. Nevertheless, embryonic remains preserved in the fossil record are particularly rare, which is unfortunate given that fossilized embryos can give important insights into deep time ontogeny, reproductive behavior, paleoecology and evolution.

Multiple studies describe other reptilian or even archosaurian embryos, namely pterosaurs (Chiappe et al. 2004; Wang and Zhou 2004) and dinosaurs (Araújo et al. 2013; Reisz et al. 2013; Carpenter 1999 and references therein). Eggshell fragments, complete eggs, nests and juvenile specimens are relatively common, but some biological questions can only be properly addressed with access to fossil embryos (Sánchez-Villagra 2012). In Portugal, there are previous reports of eggs attributed to crocodylian type (Antunes, Taquet, and Ribeiro 1998) and multiple Upper Jurassic sites are known to present fossil assemblages containing diverse reptilian eggshells types (Castanhinha, Araujo, and Mateus 2009).

Over the last two decades, an increasingly amount of publications has been presenting new exquisitely preserved fossil embryos attributed to multiple amniote taxa (de Ricqlès et al. 2001; O'Keefe and Chiappe 2011; Chiappe et al. 1998; Chiappe et al. 2004; Piñeiro et al. 2012; Kundrát et al. 2008; Reisz et al. 2013; Reisz et al. 2005; Araújo et al. 2013). Nevertheless, there is no report of embryonic remains from one of the most widely distributed tetrapods and fundamental for their basal phylogenetic position: Crocodylomorpha.

Crocodylomorpha include a wide biodiversity (over 200 taxa) that lived during most of the Mesozoic and all Cenozoic (Oliveira et al. 2011). The first crocodylomorph fossils are found in 230 million years old strata, in the upper Carnian, Late Triassic (Irmis, Nesbitt, and Sues 2013). They occupied an extensive variety of terrestrial ecosystems and display a broad paleogeographical distribution, ranging from equatorial regions to high-paleolatitudes, being bipedal, quadruped and even marine (Irmis, Nesbitt, and Sues 2013).

Until now, only few eggs or eggshells have been attributed to Crocodylomorpha and the diagnostic features available do not allow refined taxonomical ascriptions of specimens found (Tanaka et al. 2010; Oliveira et al. 2011; Rogers 2001; Moreno-Azanza et al. 2013; Hirsch 1985; Hirsch and Kohring 1992). Generally, eggshells and eggs are described as “crocodiloid eggs” and are attributed to crocodylomorphs or crocodiliforms but without fossilized embryos inside eggs it is difficult to propose a definitive match between eggs and progenitor.

Even in the rare case when reptile embryos are found inside eggs it is challenging to correctly identify the taxon that laid the eggs. This is true because many of the fossil species are diagnosed based on fragmentary material and in the wide majority of cases authors are centered in trying to find differences. This can result in false positive taxonomical ascriptions ending in overestimation of paleobiodiversity (Horner and Goodwin 2009; Scannella and Horner 2010). When describing a new fossil taxon, diagnostic features should be conspicuous and stable. This means that diagnostic features should have in consideration variation at many different levels: intraspecific, ontogenetic, sexual dimorphism, pathological and diagenetic.

When describing fossil embryos, paleontologists need to be even more careful in order to relate a particular morphological feature (still under development) to an adult form. This can be done but the above mentioned criteria must be proven robust (e.g. (Araújo et al. 2013)).

As relevant as a correct and detailed taxonomical ascription can be, comparative anatomy of fossil embryos allows testing hypotheses involving macroevolutionary patterns difficult to assess by other means. For example, deep time conservation of ontogenetic trajectories can be estimated using recent animals but can only be verified by examining how extinct animal developed. When did some modern developmental patterns emerge regarding ossification sequences, evolutionary modules or even morphological heterochronies? When and how did certain evolutionary novelties appear?

Here we present a preliminary description of a new fossil clutch found in the Upper Jurassic of Portugal containing the first Crocodylomorpha embryos ever described. Using a morphometric analysis we compared the fossil embryos with different embryos from recent taxa and discuss the limits of testable ascriptions of fossil embryos to recent taxa.

Geology

The clutch was found near the seashore in the West coast of Portugal near a locality called Cambelas, approximately 50km north of Lisbon (Fig 33 A). This site belongs to the Assenta Member of the Lourinhã Formation, located in the central Lusitanian Basin, part of the rift system for the formation of a proto-Atlantic (Fig 33 A) (Carvalho et al. 2005). The Assenta Member is dominated by intercalations of mudstones and sandstones and is located above the Sr stratigraphic marker that divides the Kimmeridgian and Tithonian (Schneider, Fürsich, and Werner 2009) (152.1 ± 0.9 Ma (Cohen et al. 2013a)). The Assenta Member is Tithonian in age based on stratigraphic correlation of fossil vertebrates and invertebrates (chiefly bivalves and gastropods) biostratigraphy, and Sr-isotope chemostratigraphy using oyster shells (Schneider, Fürsich, and Werner 2009).

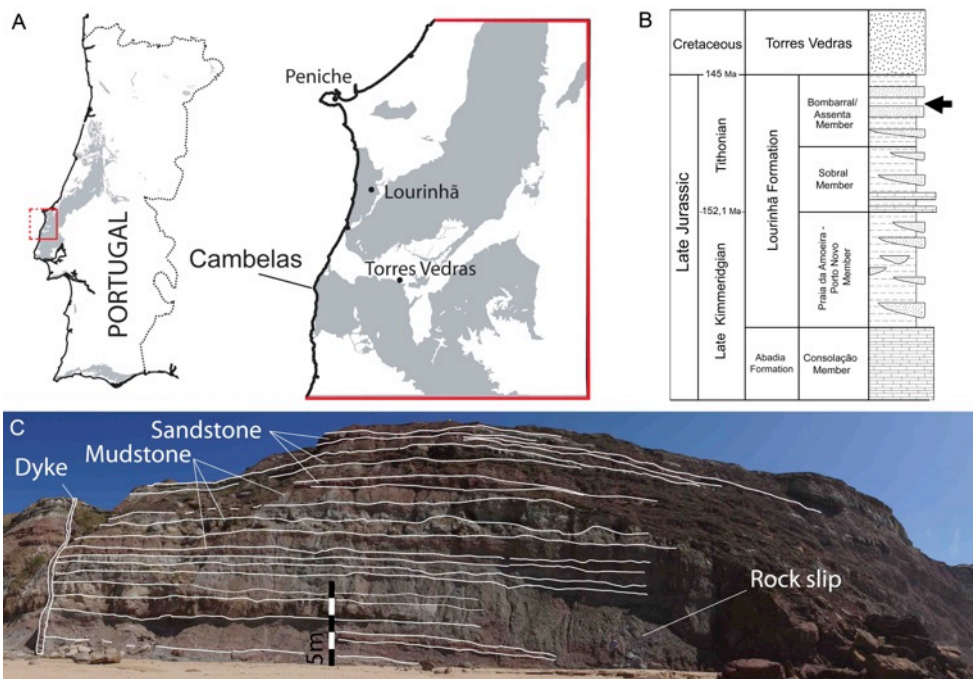


Fig. 33 Geographical and chronostratigraphic framework of ML 1582 site. A, Portugal map, grey patches represent areas containing

Mesozoic sedimentary rocks. **B**, Table relating main formations and members of the Lourinhã formation to a chronostratigraphic scale. Rectangles: limestone; dotted pattern: sandstone; dashed pattern: mudstone (adapted from (Araújo et al. 2013) and (Manuppella 1999)). Black arrow shows location of Cambelas strata. Ages in millions of year (Ma) according to (Cohen et al. 2013). **C**, location where ML 1582 was found.

Results

Clutch and Eggs

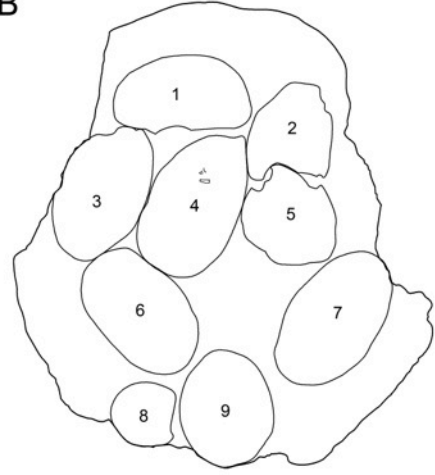
The clutch is composed of thirteen eggs displayed in a subcircular area (maximum diameter across the clutch is 113.33mm and 99.85mm perpendicularly). There are never more than two eggs stacked up forming a maximum thickness of 37.55mm. Four eggs are subvertically-oriented, whereas the rest are subhorizontally-oriented. The horizontally-oriented eggs do not seem to have any preferred alignment, ranging more than 150° relative to the major axis of the clutch diameter (Fig. 34).

The eggs are ellipsoidal (for detailed measurements see appendix). However, their real volumes are difficult to estimate, as most of them were crushed. Only one egg appears to have been partially destroyed prior to burial. This egg was found after preparation underlying another one and it is at the periphery of the clutch. Two other eggs were found partially destroyed but due to erosion.

A



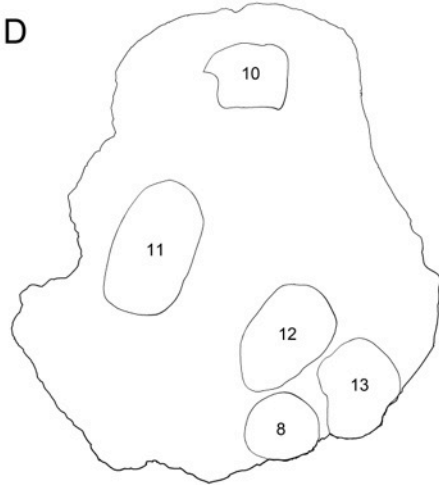
B



C



D



5 cm

Fig. 34 ML1852 (previous page) after preliminary preparation. **A** and **C**, two sides of the fossilized clutch. **B** and **D**, schematic draws of image **A** and **C** respectively. Each number corresponds to a different egg.

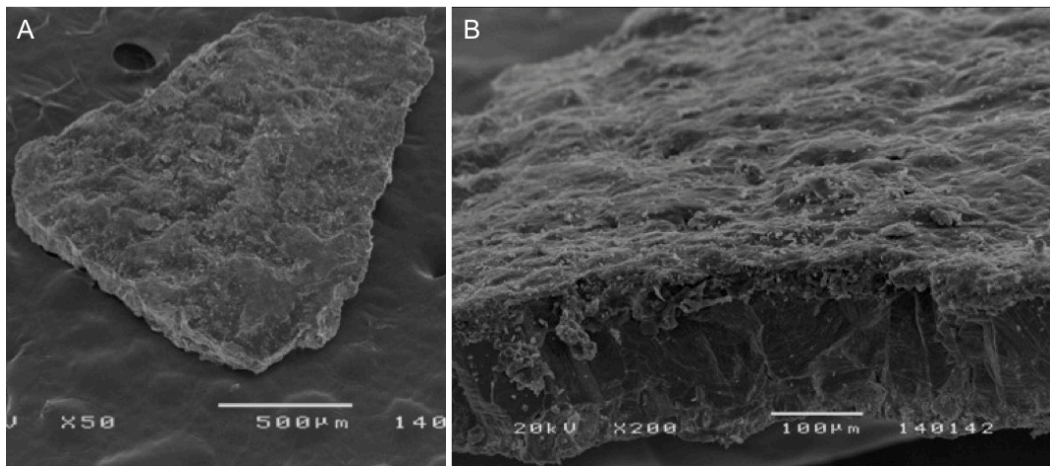


Fig. 35 SEM images of ML 1582 Eggshell morphology. **A**, external surface; **B**, transverse section.

Eggshells

The external morphology of the eggshells are composed of scattered subcircular bumps and irregularly-shaped islets (Fig.35). In radial-section the eggshells present wedge-shaped crystals made of tabular plates of calcite and without organic nucleation cores (Carpenter 1999). The pores are narrow and straight (i.e., angusticanaliculate pore

type) usually positioned between shell units. The shell units are trapezoidal being narrower at the base (egg internal surface).

Embryo Anatomy

Preliminary preparation of the block that contained the clutch exposed, inside two broken eggs, some bone fragments. It was not possible to identify any other anatomical detail rather than the fact that they seem to be long bones. The necessity to further describe and analyze these bones implied a challenging problem for any classical fossil preparation technique. Although fine preparation could have helped to expose some of the bones present, the risk of damaging these fragile embryonic remains was high. Thus, we opted to apply a new non-destructive technology.

Propagation phase contrast X-ray synchrotron microtomography (PPC-SR- μ CT) has been presented as a good solution to visualize the internal structures of fossils and particularly, fossil embryos (Fernandez et al. 2012). Like commercial microtomography, this technique requires an x-ray beam that will create a series of projections that can be used to reconstruct in a virtual space the different material in each sample (see methods section for further details). As any typical x-ray of microtomography, PPC-SR- μ CT is not invasive and does not destroy the sample under analysis. The optical resolution is not improved over commercial micro-CT machines. However, the “propagation phase contrast” enhances the density contrast detection since it provides a way to amplify small density differences (e.g. between bone and rock matrix) improving the final detail in the 3D reconstructions. The embryonic data here described is the result of the segmentation of each individual bone fragment present inside one single egg (egg 9). All other eggs were also scanned and a preliminary segmentation could retrieve other bone fragments at a similar developmental stage. This might indicate that the species that laid the eggs had a synchronous eclosion.

Over 250 fragments were virtually prepared and placed in anatomical position, using PPC-SR- μ CT data from a *Crocodylus niloticus* as reference (Fig.36). Besides this, we did not apply any correction or deformation to the fossil bones.

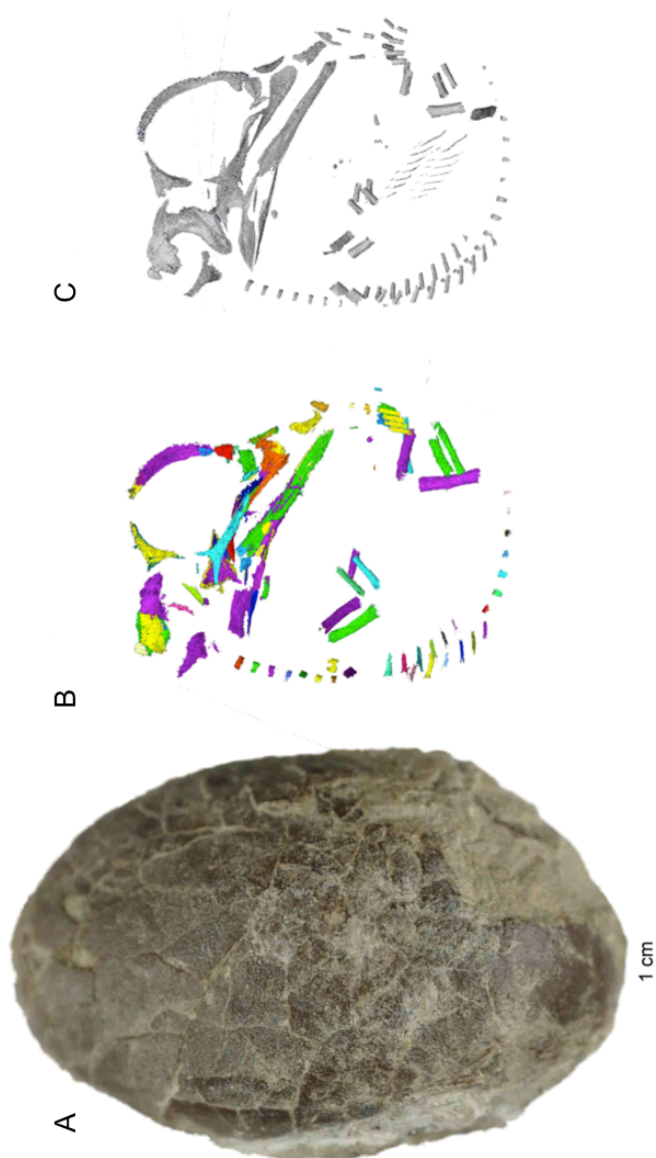


Fig. 36 (previous page) **A**, Egg 9 after final preparation; **B**, ML1582 (egg 9) bone fragments after reposition according to *C. niloticus* embryo (39D); **C**, Segmented bones from *C. niloticus* embryo (39D).

Dermatocranium

Premaxillae

The crescent-shaped left and right premaxilla ossification centers are formed by trabecular bone thoroughly pierced by vascular foramina. The right premaxilla is better preserved than its counterpart. The dorsal surface is convex whereas the ventral surface is concave. The dorsal surface slopes into a small hooked conical ascending process anteriorly and curves dorsally into another ascending process posteriorly. Two sharp ridges that meet posteriorly into the dorsal ascending process, border the concave ventral surface. The premaxilla is bean-shaped in ventral view. None of the alveolar process, palatal process, dorsomedial process, and dorsolateral process observed in extant adult crocodylia is formed at this stage.

Maxillae

The maxilla is composed by a large lamina that forms the ascending process and is connected to a thickened horizontally-oriented alveolar process. There is a reduced, medioventrally-oriented, palatal process on both maxillae. The anteroposterior length of the dorsal process is at least half of the alveolar process.

Although not entirely complete, the right maxilla is better preserved than the left one. On the former, a small posterodorsal part of the

ascending process is broken. In the left maxilla the alveolar process is also fragmented, nevertheless, it was possible to identify three pieces and articulate them in 3D. A large portion of the dorsal part of the ascending process of the same maxilla is missing and it is possible that one (or some) of the flat not-identified fragments of bone belong to the maxilla ascending process. Due to lack of a good 3D alignment of these fragments it was not possible to ascribe any fragment to this process.

The ascending process is thin and semi-elliptical in lateral view. In both maxillae the ascending process is slightly sigmoidal in anterior view.

The alveolar process is sub-triangular in cross-section. There is a groove extending along the alveolar process. This groove curves anteroposteriorly from the dorsal to the medial surface of the alveolar process and would possibly host neurovascular structures, such as the facial ramus of the trigeminal nerve (Leitch and Catania 2012). On the lateral surface of the alveolar process there is a slight excavation that extends to the posteriormost portion of the maxilla where the jugal abuts. On the alveolar process, ventral to the ascending process, there are seven tooth sockets that are not separated by interalveolar septa.

Nasals

The nasal is saddle-shaped with the lateral and medial margins lightly bent. The nasal has a bean-shape outline. The convex medial margin is more curved than the concave lateral margin. The posterior and anterior ends are more porous than the median portion. The lateral margin of the nasal is convex in *C. niloticus* whereas it is concave in the Cambelas embryos.

Lacrimals

The lacrimal is a highly porous bone with the two relatively mineralized lateral walls that converge anteriorly into an undifferentiated

mesh of trabeculae anteriorly. The lacrimal is pierced posterodorsally by a large elliptical lacrimal foramen funneling anteriorly. The facial lamina and the anterior or the descending processes seen in adults are not yet formed.

Prefrontals

The prefrontals are subtriangular in lateral view and mediolaterally narrow with a posterior curvature of the dorsal tip. The ventral border is straight, the posterior concave and the anterior convex. The prefrontals are medially concave and laterally convex. There is no evidence for the dorsal and orbital lamina, or any descending process at this stage.

Frontals

The left and right ossification centers of the frontals are formed by two curved fusiform strips of bone, opened dorsally. The medial margin of the frontal is convex and the ventral border is concave. The dorsal edge of the dorsal is composed of irregular trabecular bone, whereas the ventral edge is more smooth and compact. At mid-height there is a longitudinal groove pierced by a series of aligned, and regularly-spaced, nutrient foramina in lateral view. At about the same height a similar groove is visible medially.

Parietals

Do not seem to be preserved or ossified.

Squamosals

In *C. niloticus* 39D the squamosal is composed of a pointy anteriorly tapering process that opens into a proportionally large laterally convex sheet of bone. In the extinct form both left and right parietals present the anterior process broken but it was possible to reposition it. This process is present at the less pointy anterior tip but it also tapers anteriorly. On the posterolateral part of the squamosal there is a bulge of

bone that coincides with that of *C. niloticus*, although in the latter is positioned posterodorsally. Contrary to *C. niloticus* this budge is composed of many smaller protuberances. A groove excavates shallowly the medial side of the squamosal at about its ventral third. A similar groove is not present in *C. niloticus*. In the extinct form there is no evidence of the medial and posterior processes present in adult crocodyliformes.

Postorbitals

The postorbital is subtriangular thoroughly perforated by vascular canals. The left postorbital is better preserved with a more complete ventral and posterior processes. The postorbital is slightly curved, in dorsal view, with its medial side being concave and the lateral convex. The dorsal border is sigmoidal with a convexity on the anterior half, but it is straight in *C. niloticus*. The anterior and posterior borders are concave. The smooth anterior border contributes to the posterodorsal orbit margin. The three processes observed in adult crocodyliformes are already present in the embryos. These processes trifurcate from a central point near the posterodorsal corner of the orbit.

Quadratojugals

The dorsal portion of the right quadratojugal is preserved. The quadratojugal is a flat bone with a pointy dorsal process, which projects on the medial side of the bone. The medial border is straight. This bone is quite massive, thus it does not possess many vascular foramina, though it displays a line of regularly spaced foramina in its posterior margin.

Jugals

The jugal is a triradiated, trabecular bone. The dorsal process curves gently posteriorly, contributing to the posteroventral margin of the

orbit. A crest accompanies the anterolateral surface of the dorsal process of the jugal. The anterior process is about twice as large as the posterior process. The anterior process presents a sulcus laterally that tapers posteriorly and another one ventrally, for the articulation with the alveolar process of the maxilla. The posterior process presents two sulci, one laterally and another medially. If aligned by the dorsal process the extinct form has a longer anterior process than *C. niloticus*, yet shorter posterior process. *C. niloticus* embryos are also mediolaterally wider than those of ML1582. The three distinctive processes of the jugal are present both in the embryos and adult crocodyliformes forms.

Ectopterygoids

The ectopterygoid is a subrectangular sheet of bone whose medial half is somewhat torsioned clockwise in medial view. The dorsal and anterior margins are straight, whereas the posterior border is concave. *C. niloticus* ventral margin is straight whereas it is slightly curved in the ML1582. There is a well-developed descending (pterygoid) process and an incipient posterior process as in *C. niloticus* embryo and adult forms.



Fig. 37.(previous page) ML 1582 skull and *Alligator mississippiensis* embryos after digital segmentation. ML1582 in **a**, anterior; **d**, left lateral and **g**, dorsal views. *Alligator mississippiensis* skull (Ferguson Stage 21) in: **b**, anterior; **e**, left lateral and **h**, dorsal. *Alligator mississippiensis* skull (Ferguson stage 23) in: **c**, anterior; **f**, left lateral and **i**, dorsal.

Pterygoids

Although unpaired in adults, at the developmental stage of ML1582 there are two ossification centers for the pterygoid. The pterygoid is a somewhat saddle-shaped triangular bone. The pterygoid is concave laterally and is formed by a dorsal (ascending) process that continues into the anterior (palatal) process and, these processes develop ventrolaterally into a transverse process. On the posterior part of the medial part of the pterygoid body there is a subhorizontal medial crest, which is not preserved on the right one. This crest meets anteriorly with a dorsal bulge absent in *C. niloticus*. The ascending process is a posterolaterally-deflected sheet of bone that tapers posteriorly. It continues into the anterior process forming a straight dorsal margin, anteriorly. The palatal process is subtriangular and is perforated near its anterior apex by a foramen present both in the right and left pterygoids. The ventral border of the palatal process is smoothly concave terminating into a wide transverse process. The transverse process is a subrectangular lateral bone expansion with its anterior and ventral margins somewhat torsioned laterally in ventral view. There is no evidence of internal nares (choanae), which are typically contained within the pterygoid in adult crocodyliformes.

Palatines

The posterior half of the left palatine is preserved and the right one is almost complete. The palatine is a lanceolate bone, concave medially and presenting a horizontal crest laterally. It presents a posteriorly tapering sharp process, which forms a medially deep subtriangular sulcus and a convex surface laterally. Anteriorly the palatine presents round tip and is subtriangular in cross section. The dorsal margin is somewhat dorsally concave and the ventral margin is almost straight. As in *C. niloticus* 39D the palatine does not form the complete palate. The vertically oriented ascending process present in adult crocodyliformes is not present in ML1582.

Vomers

The vomers are completely preserved and formed by compact bone. The vomer is a relatively simple tubular of bone that opens medially with a ventrally-projecting flange. The tubular portion widens posteriorly, but terminates into an acute and short posterior process. The ventral flange curves medially, thus making the lateral side convex. The ascending process observed in adult *C. niloticus* is not preserved in the 39D embryos as well as in ML1582.

Dermal ossifications

Palpebrals and sclerotical ossicles

Do not seem to be preserved or ossified.

Chondrocranium

Laterosphenoids

Do not seem to be preserved or ossified.

Basisphenoid

As in *C. niloticus*, the basisphenoid is a small flat bone. The basisphenoid is subtriangular and highly trabecular.

Parasphenoids

Do not seem to be preserved or ossified.

Basioccipital

Do not seem to be preserved or ossified.

Supraoccipitals

In *C. niloticus* 39D, the supraoccipitals are two flat, small, subcircular and very dense ossifications. We have found one bone with these characteristics and dimensions. Thus we tentatively ascribe it as the supraoccipital although its shape does not match the exact shape of the two supraoccipitals of *C. niloticus* 39D.

Exoccipitals / Otoccipitals

Although in many crocodyliformes the exoccipital co-ossifies with the opisthotic, at the developmental stage only the exoccipital is present. The exoccipital is a triradiate bone formed by a posterior process, a lateral process and a ventral process. The exoccipital is a crescent-like shape in posterior view.

The medial process is a thin subtriangular sheet of bone pointing medioventrally at approximately 45° relative to the horizontal in posterior view. The medial process meets the ventral process at an approximately right angle. The ventral process is subrectangular and has a slightly concave ventral border. The posterior is subtriangular in cross-section

and tapers smoothly posteriorly with a pointy end. The medial border of the posterior process is the most ossified part of the exoccipital. The medial border of the posterior process is deeply excavated, and the anterior margin is straight. Contrary to the exoccipital of *C. niloticus* 39D there is no evidence of any foramen piercing the ventral process.

Opisthotics

Do not seem to be preserved or ossified.

Splanchnocranium

Ceratobranchials

As in *C. niloticus* 39d, only the median portion of the ceratobranchial is ossified. The ceratobranchial is a tubular kinked bone collar with its curvature pointing ventrally.

Stapedes

Do not seem to be preserved or ossified.

Epipterygoids

Do not seem to be preserved or ossified.

Quadrates

As in *C. niloticus* 39D, the right quadrate only preserved a hyperbolic shred of bone that ossifies at its posterior side but the left is more complete and includes also part of the lateral walls. The right quadrate can be assigned based on the somewhat more expanded ventral portion, also the medial portion is more ossified than the lateral counterpart. The left quadrate is hourglass shaped in lateral view with its ventral part more expanded than the dorsal one. In posterior view the lateral walls are parallel.

Articulars

Do not seem to be preserved or ossified.

Dermal bones of the jaw

Surangulars

In the *C. niloticus* embryo the surangular is composed of a sharp anterior process that expands into a sub-rectangular posterior portion. In ML1582, the right posterior portion is better preserved while in the left side it was only possible to identify a posterior fragment. The lateral side is ornamented with horizontal grooves whereas the medial side is smooth. As in *C. niloticus*, the dorsal margin is straight and slightly thickened relative to the rest of the posterior portion of the surangular. The anterior tip of the surangular is broken.

Angulars

Although fragmented, both angulars seem to be almost completely preserved. The angular is a U-shaped bone in cross section. The lateral wall is taller than the medial wall. The anterior portion presents longitudinal grooves at its ventral surface. The dorsal border of the angular posterior process slopes ventrally to meet the horizontally-oriented ventral margin. Especially the lateral walls of both angulars are thoroughly pierced by primary cavities.

Coronoids

The coronoid is composed by two ossification centers; this trait is only visible at *C. niloticus* 45D. The dorsal ossification center is similar to the ectopterygoid but much smaller. It presents concave posterior and anterior margins and a straight ventral margin that contacts the ventral ossification center. It bifurcates dorsally forming a U-shaped sulcus for

the articulation with the anterior process of the surangular. The curved posterior margin forms dorsally an isolated spur, immediately before the dorsal margin.

The ventral ossification center is a simple tapering splint of bone that contacts anterodorsally with the dorsal ossification center, like in the *C. niloticus* 45 D.

Splenials

Only the right splenial is present. It is a hemicylindrical bone with a thin vertical deflection. The anterior tip appears to be missing. The posterior margin is smoothly convex. The splenial is convex medially and filled with nutrient foramina. The dorsal and ventral margins are sub-parallel converging gently anteriorly.

Dentaries

The dentaries are anteroposteriorly long subrectangular bones, laterally convex. The dentaries are thick, heavily trabecular anteriorly and thin posteriorly. The dorsal and ventral margins smoothly converge anteriorly. The dentary is deeply excavated at the symphysis, becoming shallower posteriorly. At the last third of the dentary there is a horizontally-oriented elliptical foramen, coincident to the one seen in *C. niloticus* 39D. Near the symphysis, the dentary forms a relatively flat area ventrally which is also highly trabecular, whereas towards the dorsal margin the bone is much more compact. The dentaries symphysis is parallel to the anteroposterior axis of the skull.

Inner ear ossifications

Otoliths

The otoliths are massive hourglass-shaped bones, similar to the curved torus in *C. niloticus*. The otoliths shape corresponds to an almost

complete torus with deep depressions on the dorsal and ventral sides bordered by a thick lip that opens laterally.

Utriculi

The utriculus otolith is a flat massive bone with a D-shape outline in dorsal view. The utriculus has a medial bend on the anterior margin. The utriculus in *C. niloticus* 39D is relatively smaller, subrectangular but possesses a similar sized medial bend.

Sacculi

The sacculus is a flat massive bone with a sigmoid shape with its margin slightly rimmed. It presents medially a deep notch and point end ventrally. The major difference with *C. niloticus* 39D is that ML1582 possesses a subtriangular ventral projection.

Other ossifications

Egg tooth

At the ossification stage of 39D in *C. niloticus* there are only small speckles of bone, however the surrounding cartilage is cordiform. In the extinct form the eggtooth is also cordiform, with the apex pointing dorsally and a small posterior excavation. There are two small swellings located ventrally on the anterior side of the eggtooth.

Postcrania

Scapulae

Both scapulae are preserved but one presents half of its bone collar collapsed. The scapula is a tubular bone in the postcrania with an ellipsoid cross-section. Its elongation ratio (diameter/length) is 93%.

Propodia and Zeugopodia

Due to the similar anatomy of propodial and zeugopodial elements at an early developmental stage, it is hard to distinguish all the different elements. All long bones are preserved as tubular elements (bone collars) with no epiphyses, and the medulla is hourglass shaped if the bones are sectioned longitudinally. The synchrotron micro CT does not allow detection of primary or secondary fossilized spongiosa. By superimposing in 3D the fossil bones with the bones from *C. niloticus* at three developmental stages (39D; 45D; 55D) it was possible to identify each one of the fossil bones. Although the skull bones size corresponds to the *C. niloticus* at 39 days the size and shape of the propodia and zeugopodia bones closely matches the *C. niloticus* at 45 days.

All the elements are preserved with the exception of one ulna and one tibia.

Femora

The two femora are differently preserved making one slightly smaller than the other due to an incomplete preservation of the periosteum. The femora diaphyses are preserved as bone collars with a slight hourglass shape. The surface of the femora presents some longitudinal grooves and symmetrical oval nutrient foramina dispersed along its length. As in the *C. niloticus* (stage 45 days) the distal end of the femoral bone collar is an ellipse while the proximal end is approximately circular, in cross section.

Humeri

One of the humeri has a well-preserved periosteum on which it is possible to observe several nutrient foramina along its entire length. The humeri are nearly the same thickness throughout their length and are only slightly curved. Assuming the position of the *C. niloticus* 39D

embryo, the lateral side is convex and the medial side concave. The proximal and the distal ends of the humeri are approximately symmetric ovals in cross section.

Tibia

The tibia bone collar is not well-preserved, yet it is pierced by several nutrient foramina throughout the surface. The tibia is straight and uniformly thick along its length.

Fibulae

One of the fibulae has a well-preserved periosteum showing in its external surface a longitudinal groove ending on a foramen in the mid-diaphysis. Both fibulae present a somewhat sigmoidal outline. The proximal end of the bone collar is elliptical while the distal end is subcircular, in cross section.

Ulna

The only ulna present is poorly preserved missing some fragments. It is transversely compressed which makes it difficult to assess its cross-sectional shape, yet, it may be considered a straight bone.

Radii

The two radii are well-preserved, but one of them is deformed in the proximal end. The radii are more expanded on the proximal end and both present a large nutrient foramen, distally. The proximal cross-section is oval shaped and the distal one is circular.

Autopodia

There are 13 autopodial elements preserved. There are two different morphotypes of autopodial elements a group of 8 metacarpal or metatarsal elements that are about five times longer than a group of

carpal or tarsal elements. The metacarpals/metatarsals were found in three groups of associated elements, a group of four and two other separate pairs. The metacarpals/metatarsals were preserved in articulation, parallel to each other along the same plane. The metacarpals/metatarsals have approximately the same length, are straight and preserve the same transverse thickness. The diameter of the metacarpal/metatarsal elements varies up to approximately 40%. The elongation ratio of these elements is ~19% (diameter/length).

The carpals/tarsals are ring-like elements (bone collars) that have approximately the same length and cross-sectional diameter. Two of them were found in close association, oriented parallel to each other on the same plane. The cross-section is subcircular. One of the autopodial elements has a smaller diameter than the rest and has a higher elongation ratio than the rest of the elements (35% diameter/length).

Vertebrae

We have found fifteen vertebral centra. In *C. niloticus* the vertebrae start to ossify from one or two ossification centers ventrodorsally. This ventrodorsal pattern of ossification is not shared by other reptiles (e.g. gekkonoids (Werner 1971; Winchester and Bellairs 1977)) nor mammals (e.g. mouse (Hautier et al. 2014)). The ossification centers are initially ovate and become crescent-like when fused ventrally. They start to ossify ventrally and invade the periphery of the vertebral centrum laterally forming a cuff of periosteal bone until they fused dorsally forming the bone collar. At day 39, the *C. niloticus* vertebral ossification centers can be seen, but none of the vertebrae have yet fused dorsally as in the *C. niloticus* 45 D. The more developed vertebrae are (at 39D) the first six cervicals and the second half of the dorsals. The less developed are the first five thoracic and the caudals, that (at 39D) seem

not to be ossified. Within the cervicals the ossification is progressively more developed starting with the first to the sixth vertebrae.

The preserved 14 to 15 fossil vertebrae were not found in articulation, thus they were positioned using *C. niloticus* (39D) as a model. They seem to be slightly more developed than those of the extant species because they present a more developed cuff of periosteal bone almost completely fused dorsally. Although the diameter is similar, they present a higher height/diameter ratio than in *C. niloticus*. Some of the ossification centers were found isolated but can be positioned into similar sized pairs. They are concave in dorsal view and are formed by a thin sheet of D-shaped bone.

Ribs

There are 12 ribs preserved at different developmental stages. All ribs have a curved tubular shape with a marked costal groove. They are a subtriangular proximally and subcircular distally in cross section. The ribs are all slightly curved and expand proximally with a marked projection in the more developed ones, forming the tuberculum primordium.

Gastralia

Do not seem to be preserved or ossified.

Procrustes analysis

The anatomical description above is qualitative. In order to perform a quantitative analysis of the fossil specimen further tests are needed. We performed a morphometric analysis comparing ML 1582 embryos with data from three different extant species at multiple stages in development: *Crocodylus niloticus* (n=7), *Tyto alba* (n=4), *Centrochelys sulcata* (n=8). We analyzed four bones in total: jugal, dental, maxilla and pterygoid. In order to sustain a taxonomic ascription of ML 1582 to Crocodylomorpha the results should be more similar (=less dissimilar) to the extant Crocodylia taxa than to any of the two other reptiles. Embryos were ordered according its correspondent incubation day with the exception of *Tyto alba*. The latter embryos were ordered using the staging tables produced by Köppl and colleagues (Köppl et al. 2005). None of the embryological sequence was normalized.

In all bones analyzed the dissimilarity index was smaller between the fossil embryo and the *Crocodylus niloticus* than with any of the other two compared species, at all developmental stages. Only the maxilla retrieved a similar difference between the fossil and the turtle embryo when compared with the fossil versus the extant crocodile (Fig 38 to 41).

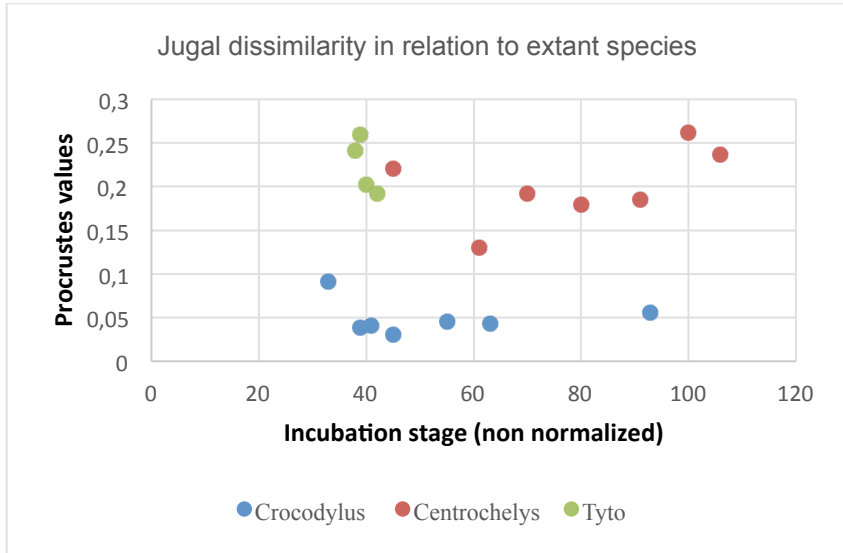


Fig. 38

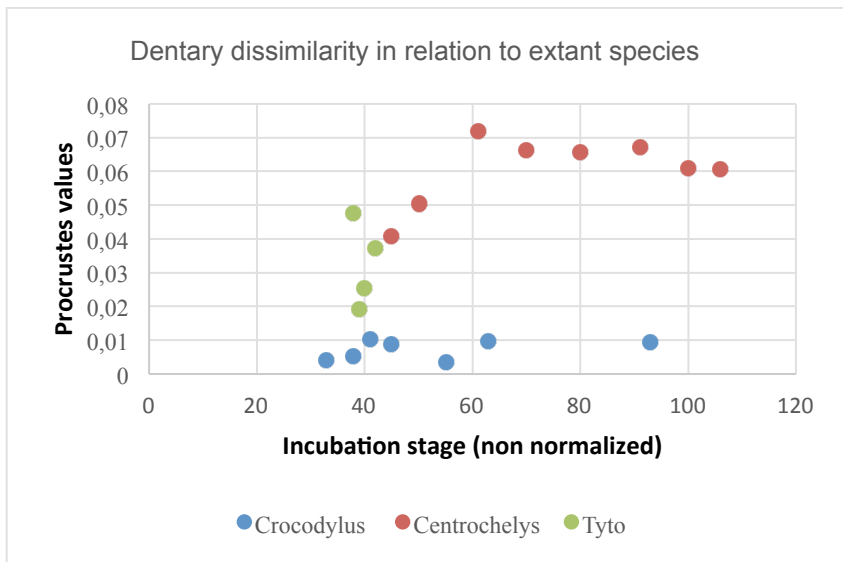


Fig. 39

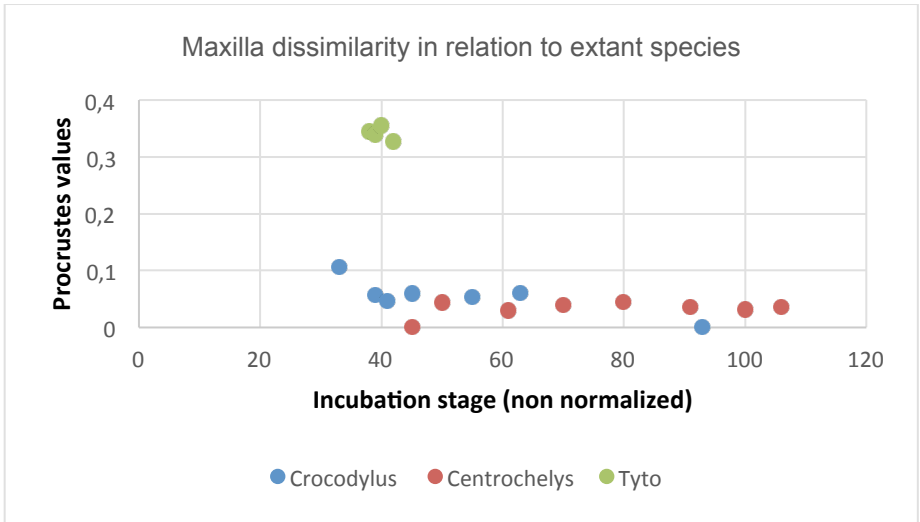


Fig. 40

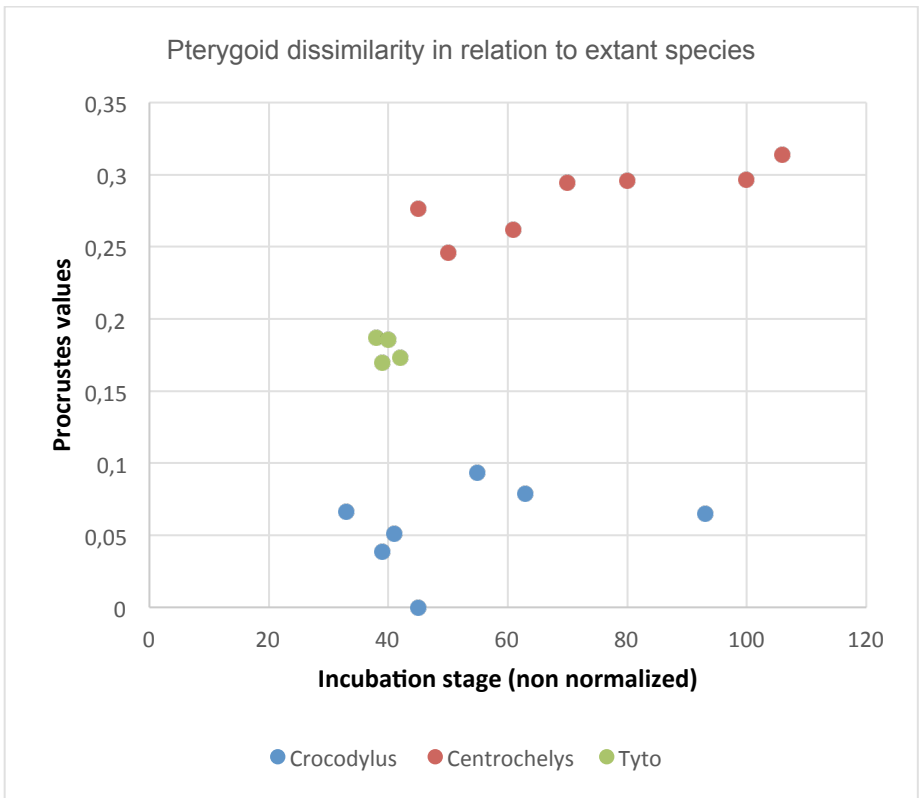


Fig 41

Discussion

As in almost all fossil embryos, definitive taxonomic ascription is hard to produce given that morphological characters are still under development. However the almost complete correspondence of the segmented fossil bones with the 3D volumes of an extant crocodile taxon confirms our ascription as a Crocodylomorpha.

It is clear that the fossil embryo is much more similar to the two forms of extant crocodiles than to the *Tyto alba* or *Centrochelys sulcata* embryos.

The similarities found between both extant crocodile embryos and the fossil embryo make it extremely hard to determine if ML 1582 is (or is not) a Crocodylia. There is no form to compare with other extinct Crocodylomorpha given the total absence of these fossils. As it is obvious, the chance of discovering a Crocodylia embryo in the Upper Jurassic is remote (according to Martin et al 2010, they are only found in the late Cretaceous) but it is also hard to exclude this hypothesis.

So where shall the line be drawn? What should be considered necessary and sufficient to observe in a fossil embryo to accept (or refute) the hypothesis that ML1582 embryos are Crocodylia? And how could we test this?

There are obvious strategies to consider. For instance, showing that the fossil specimens present a diagnostic feature (i.e. one, or a set, of synapomorphies) of Crocodylia. At the same time for obvious reasons, this putative trait (or set of traits) cannot vary ontogenetically.

Nesbitt described 19 synapomorphies for Crocodylomorpha (a more inclusive taxa than Crocodylia) 7 of those are in the post-cranial skeleton which very poorly developed in ML 1582 impairing any attempt

to code these characters (Nesbitt 2011). The remaining 12 synapomorphies are also extremely difficult to identify in the fossil embryo ML 1582. For instance character 1 described as “Posterodorsal process of the premaxilla less than or about the same as the anteroposterior length of the premaxilla”. The premaxilla of the fossil embryo is well developed and similar to a *Crocodylus* or *Alligator* premaxilla at the same stage but it is impossible to know how it would be in an adult specimen. This type of problems rule out the usage of many (in this case all) characters classically considered when classifying fossils of adult forms.

As an alternative, it would be interesting to verify that the fossil embryo here described (at his particular stage) is morphologically closer to Crocodylia than to any non-crocodylia Crocodyliforms embryos.

This can only be done indirectly given that we cannot compare a fossil embryo with other extinct "non-crocodylia crocodyliforms" embryos simply because they were not found. Nevertheless, it should be possible to test this hypothesis in a different way. This could be done by mapping the morphological variation in a number of embryological traits within each modern group of Crocodylia and testing if the fossil embryo morphology would fall inside the variation of one of these extant groups. If it did not, then ML1582 could not be considered a Crocodylia, but if it did, then we could not exclude the hypothesis that we would be facing a Crocodylia embryo from to Jurassic. In any case, this would imply to map a wide sample of recent crocodiles at different developmental stages and compare run the analysis.

Having said this, as tempting as might be to speculate about what could be the exact species that laid the eggs in the Jurassic period, without any further data, any definitive conclusion would be merely

speculative. No synapomorphies could be identified in the embryo and the procrustes analyses (with three different Sauropsida species) showed that ML 1582 is more similar to *Crocodylus niloticus* than to bird (*Tyto alba*) or turtle (*Centrochelys sulcata*) embryos. At this point, and until more data is available or new methodological techniques are applied, our best ascription of ML 1682 is: Crocodylomorpha.

Authors contributions

Conceived and designed the experiments: Rui Castanhinha, Gabriel G. Martins and Ricardo Araújo. Performed the experiments: Rui Castanhinha, Ricardo Araújo, Gabriel G. Martins, Nelson Martins, Rui Martins, Vincent Fernandez and Paul Tafforeau. Analyzed the data: Rui Castanhinha, Ricardo Araújo, Gabriel G. Martins, Nelson Martins. Contributed reagents/materials/analysis tools: Rui Castanhinha, Ricardo Araújo, Rui Martins, Gabriel G. Martins, Élio Sucena, Joaquín Leon, Vincent Fernandez and Paul Tafforeau.

Acknowledgments

We are thankful to the GEAL - Museu da Lourinhã for all the support during these years. Alexandra Tomás performed dedicated effort and skill to prepare ML 1582. It would be also important to acknowledge all volunteers that have been collaborating with us in many different ways. They represent the continuous driving force in our Museu da Lourinhã.

We discovered the specimen here described (ML1582) during fieldwork financed in 2008 by a Jurassic Foundation award attributed to Rui Castanhinha and Ricardo Araújo under the project “*Dinosaur Eggs and Embryos of the Lourinhã Formation (Upper Jurassic, Portugal)*”.

General Discussion

This thesis was dedicated to complementary areas. In the first part we used experimental evidence to better understand if the avian frontal bone was originated from the fusion of two bones present in the ancestors of living birds. A bone is a complex tissue made of different cell types and extracellular matrix. Moreover, bones present a complex dynamic morphology with constant remodeling via degradation (osteoclasts) and secretion of osteoid matrix (osteoblast). This osteoid matrix encases osteocytes and is perforated by blood vessels (Hall 2005). In this context, it seems obvious that the identification of homologous structures might be more complex than usually thought.

In addition, in order to identify homologous structures between two taxa, one needs to trace the same character to the common ancestor and be sure that the trait is the same that is present in the two taxa under comparison. This can be properly addressed analyzing fossil sequences in combination with new data from embryological experimental work. As can be seen in Fig. 38 the evolution in numbers and contacts in calvarial bones of Archosauriformes is complex. Assuming that a bone is an individual isolated calcified structure present in an adult skull (classical usage of this term), we can observe fewer bones in the more derived taxa relative to the basal forms. Two hypotheses can explain this pattern, either bones are not formed because they disappeared during evolution or they exist as distinct elements early in development that fuse along the ontogeny of each species. The two processes are not mutually exclusive and each of these processes may be applicable to different bones within the same species or lineage.

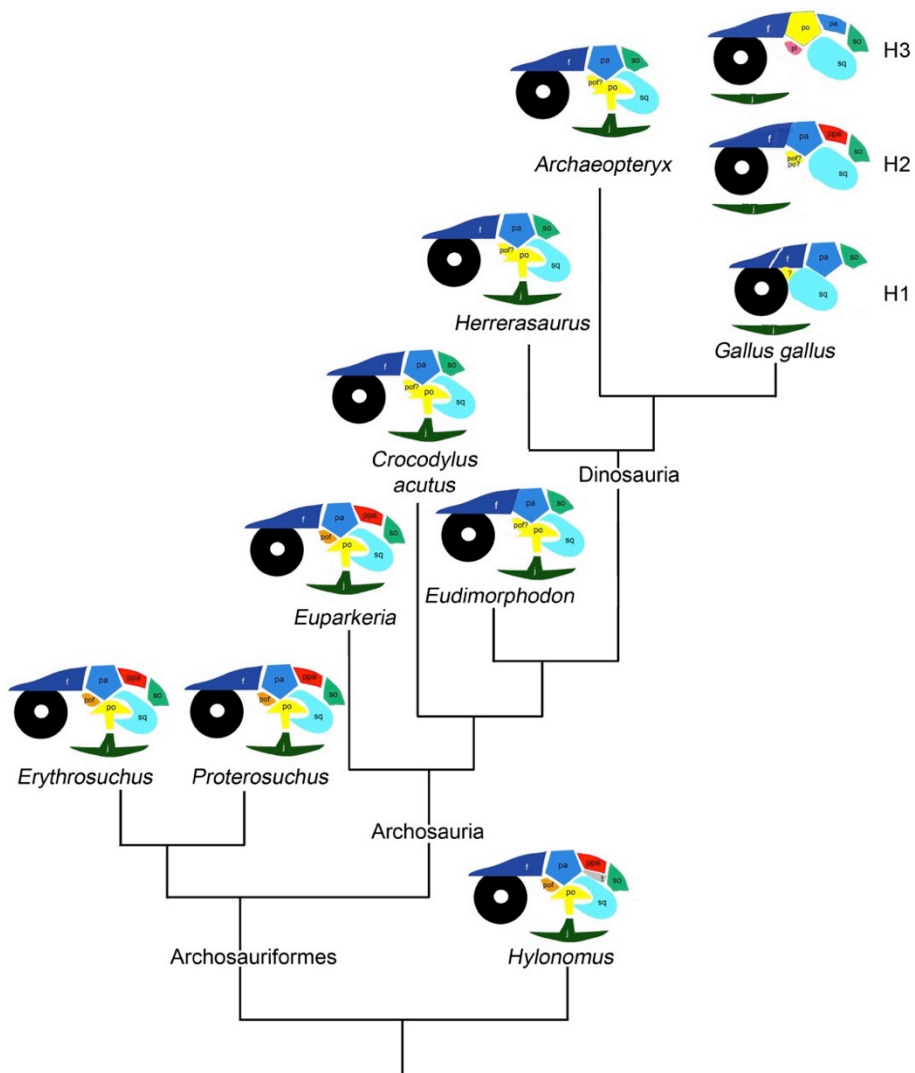


Fig. 38 Different calvarial bones mapped over Archosauriformes phylogeny (tree pruned from Nesbitt 2011). f, frontal; j, jugal; pa, parietal; po, postorbital; pof, posfrontal; ppa, postparietal; so, supraoccipital; sq, squamosal; t, tabular. **H1, H2, H3** three different hypotheses for the calvarial bones in birds.

Our experiments shown that the frontal bone in birds presents two ossification centers in chick and duck and only one in quail embryos. It also shows (in chicken) that the interval when the two centers are present lasts approximately 24h and this is clearer if rigorously controlled experimental conditions are met. Duck development is slightly different given that the double ossification center is present for a longer interval showing that the two centers are not formed simultaneously (the anterior center forms first). The quail embryology strongly indicates that there is only one center of ossification and it is not clear of the quail lost the anterior center of the posterior. It would be interesting to know if the mesenchyme that will form the frontal bone in quail by secreting osteoid matrix is also a single continuous population of cells or, if on the contrary, there is also two clear populations that start ossification so synchronously that only one ossification center can be discerned.

Previous studies have presented contrasting results regarding the embryological origins of the avian frontal and parietal bones. Some attribute to the neural crest the responsibility to form the two bones while others propose that only the anterior part of the frontal bone is derived from neural crest and all the rest is formed from mesoderm derived cells (Gross and Hanken 2008b and references therein).

In addition to the discussion already presented at the end of the first chapter there is a supplementary comment that should me made at this point. One possible difficulty in interpreting some classical experiments involving quail-chick chimeras is precisely the fact that all transplants are from quail (donor) to chick (host). For the quail might have lost the posterior (PM origin) center of ossification of the frontal and thus might be that the quail frontal is entirely derived from the anterior ossification center (NC derived) and this is why previous experiments show an entire frontal formed by cells derived from NC in chimeric embryos. In addition, there are no complete fate maps published

resulting from chicken (donor) to quail (host). These results could help to know if there is any significant interspecific variation influencing the results.

We performed new experiments that did not imply mixing cells from different species. Moreover, our approach did not involve injections of retrovirus, thus avoiding problems with reduced precision when labeling cell populations.

Using transplants of GFP chickens to wt chickens, we showed that, not only the technique worked but that our preliminary histological analysis of few embryos could provide a solution to this long-standing debate.

Our results showed that when transplanting the neural fold, the percentage of osteocytes present at the anterior region of the frontal is significantly smaller than the proportion of these cells on the posterior part of the same bone. The percentage of GFP cells present in the parietal are even less than the surrounding bones. In addition when transplanting paraxial mesoderm at the mesencephalic level (at 4 somite stage) there are GFP cells in the posterior region of the frontal after two weeks of incubation.

It is important to refer that these observations are only based in histological sections made in two embryos (one resulting from a NC and another from a mesoderm transplant) and one dissection and imaged embryo in OPT (NC transplant). We performed successful transplants in over 60 embryos and further detailed analysis and repetition of results is required prior to achieve any definitive conclusion. It would also be interesting to identify which cells are expressing GFP in these transplants. For instance, in the mesoderm transplants the few GFP cells present in the frontal are only in the periosteum and only a handful is encased in osteoid matrix. For this, it would be important to use molecular markers of osteoblasts and osteocytes to correctly identify

which cells are expressing GFP. This would allow a necessary refinement in the identification of the cell types that form such a complex and fascinating structure as the bone.

Regarding the evolutionary implications of this work, we could define more clearly hypotheses for the evolution of the some skull elements across amniotes. Our fine developmental characterization sets new standards and refines alternative evolutionary scenarios and homology relationships. This has the fundamental heuristic consequence of producing clear experimental suggestions for further testing and consequent clarification of the evolutionary history of the skull over the past 500 million years.

One such experiment, important for the proper clarification of the origin and evolution of the calvarium bones, involves the generation of a thorough ontogenic description of the *Crocodylia* skull. Unfortunately, we did not perform such experiments but we have taken this task from the other end. Indeed, we were lucky enough to have found and described the first (incomplete) embryonic series of a *Crocodylomorpha* from the Upper Jurassic. This is of fundamental importance in permitting to establish the general ontogenic features of the ancestral state of this group.

In the second chapter, we presented a preliminary anatomical description and morphometric analysis of this new clutch containing complete embryos ascribed to *Crocodylomorpha*. After fine preparation, we performed a propagation phase contrast X-ray synchrotron microtomography scan of one egg. The data allowed us to segment the scattered bone elements inside this egg. After anatomical comparison with ct-scans from embryos of extant *Crocodylus niloticus* and *Alligator mississippiensis* we could identify each bone and replace it according the anatomy of the reference embryo *Crocodylus* (39D).

We placed landmarks in four different bones (jugal, dental, pterygoid and maxilla) in three different species: one bird (*Tyto alba*), one turtle (*Centrochelys sulcata*) and one crocodile (*Crocodylus niloticus*). We run a procrustes analysis and the results confirmed our interpretation. For the embryonic fossil is more similar to the crocodile at any developmental stage in any bone comparison (exception made to the maxilla). The maxilla results need to be further investigated given that the most similar animal retrieved by the analysis was the *Centrochelys*. Both our fossil and the turtle embryos do possess a somewhat comparable maxilla and these results might suggest some constrain in the developmental program of turtles and crocodiles. In any case only further analysis can bring light to this debate.

It will be important to complete this morphometric analysis with a wider sample of embryos. Particularly by increasing the amount of crocodile embryos we could test for relevant questions regarding conservation of developmental patterns. Crocodiles are extremely interesting animals given that they share a conserved morphology and ecology but their ancestors were much more diverse. Questions about is the developmental patterns observed in recent crocodiles were also present in the Mesozoic and if they were how conserved were these patterns when compared with other groups?

Using a combination of multiple lines of evidence, many other questions can now be addressed in different and complementary ways.

Importantly, we have tried in this thesis to approach the reconstruction of evolutionary history from both ends. On one end, using paleontology to determine ancestral states, on the other, by using ontogenic data as a more robust source of information regarding the mechanisms generating adult form. Pursuing this fusion and complementary approaches is at the core of our research programme as indeed we hope that a true paleo-evo-devo field will blossom to

contribute effectively to uncovering the mysteries of these *endless forms
most beautiful and most wonderful*.

References

- Antunes, M. T., P. Taquet, and V. Ribeiro. 1998. "Upper Jurassic Dinosaur and Crocodile Eggs from Paimogo Nesting Site (Lourinha-Portugal)." *Mem. Acad. Ciênc. Lisb* 37: 83–100.
- Araújo, Ricardo, Rui Castanhinha, Rui M. S. Martins, Octávio Mateus, Christophe Hendrickx, F. Beckmann, N. Schell, and L. C. Alves. 2013. "Filling the Gaps of Dinosaur Eggshell Phylogeny: Late Jurassic Theropod Clutch with Embryos from Portugal." *Scientific Reports* 3 (May). doi:10.1038/srep01924.
- Bhattacharjee, Vasker, Partha Mukhopadhyay, Saurabh Singh, Charles Johnson, John T. Philipose, Courtney P. Warner, Robert M. Greene, and M. Michele Pisano. 2007. "Neural Crest and Mesoderm Lineage-Dependent Gene Expression in Orofacial Development." *Differentiation* 75 (5): 463–77. doi:10.1111/j.1432-0436.2006.00145.x.
- Bomfleur, Benjamin, Stephen McLoughlin, and Vivi Vajda. 2014. "Fossilized Nuclei and Chromosomes Reveal 180 Million Years of Genomic Stasis in Royal Ferns." *Science* 343 (6177): 1376–77. doi:10.1126/science.1249884.
- Borue, Xenia, and Drew M. Noden. 2004. "Normal and Aberrant Craniofacial Myogenesis by Grafted Trunk Somitic and Segmental Plate Mesoderm." *Development* 131 (16): 3967–80. doi:10.1242/dev.01276.
- Botelho, João Francisco, Luis Ossa-Fuentes, Sergio Soto-Acuña, Daniel Smith-Paredes, Daniel Nuñez-León, Miguel Salinas-Saavedra, Macarena Ruiz-Flores, and Alexander O. Vargas. 2014. "New Developmental Evidence Clarifies the Evolution of Wrist Bones in the Dinosaur–Bird Transition." *PLoS Biol* 12 (9): e1001957. doi:10.1371/journal.pbio.1001957.
- Brigandt, Ingo. 2003. "Homology in Comparative, Molecular, and Evolutionary Developmental Biology: The Radiation of a Concept." *Journal of Experimental Zoology Part B: Molecular and Developmental Evolution* 299B (1): 9–17. doi:10.1002/jez.b.36.
- Čapek, Daniel, Brian D. Metscher, and Gerd B. Müller. 2014. "Thumbs down: A Molecular-Morphogenetic Approach to Avian Digit Homology." *Journal of Experimental Zoology*

- Part B: Molecular and Developmental Evolution* 322 (1): 1–12. doi:10.1002/jez.b.22545.
- Carpenter, Kenneth. 1999. *Eggs, Nests, and Baby Dinosaurs: A Look at Dinosaur Reproduction*. Indiana University Press.
- Carvalho, J., H. Matias, L. Torres, G. Manupella, R. Pereira, and L. Mendes-Victor. 2005. “The Structural and Sedimentary Evolution of the Arruda and Lower Tagus Sub-Basins, Portugal.” *Marine and Petroleum Geology* 22 (3): 427–53. doi:10.1016/j.marpetgeo.2004.11.004.
- Castanhinha, Rui, Ricardo Araujo, and Octavio Mateus. 2009. “Dinosaur Eggshell and Embryo Localities in Lourinhã Formation, Late Jurassic, Portugal.” In *Journal of Vertebrate Paleontology*, 29:76A – 76A. SOC VERTEBRATE PALEONTOLOGY 60 REVERE DR, STE 500, NORTHBROOK, IL 60062 USA.
- Chen, Lei, Shuhai Xiao, Ke Pang, Chuanming Zhou, and Xunlai Yuan. 2014. “Cell Differentiation and Germ-Soma Separation in Ediacaran Animal Embryo-like Fossils.” *Nature* advance online publication (September). doi:10.1038/nature13766.
- Chiappe, Luis M., Laura Codorniú, Gerald Grellet-Tinner, and David Rivarola. 2004. “Palaeobiology: Argentinian Unhatched Pterosaur Fossil.” *Nature* 432 (7017): 571–72. doi:10.1038/432571a.
- Chiappe, Luis M., Rodolfo A. Coria, Lowell Dingus, Frankie Jackson, Anusuya Chinsamy, and Marilyn Fox. 1998. “Sauropod Dinosaur Embryos from the Late Cretaceous of Patagonia.” *Nature* 396 (6708): 258–61. doi:10.1038/24370.
- Cohen, K. M., S. C. Finney, P. L. Gibbard, and J. X. Fan. 2013a. “The ICS International Chronostratigraphic Chart.” *Episodes* 36 (3): 199–204.
- . 2013b. “The ICS International Chronostratigraphic Chart.” *Episodes* 36 (3): 199–204.
- Coons, Albert H., Hugh J. Creech, and R. Norman Jones. 1941. “Immunological Properties of an Antibody Containing a Fluorescent Group.” *Experimental Biology and Medicine* 47 (2): 200–202. doi:10.3181/00379727-47-13084P.
- Couly, G. F., P. M. Coltey, and N. M. Le Douarin. 1992. “The Developmental Fate of the Cephalic Mesoderm in Quail-Chick Chimeras.” *Development* 114 (1): 1–15.

- . 1993. “The Triple Origin of Skull in Higher Vertebrates: A Study in Quail-Chick Chimeras.” *Development* 117 (2): 409–29.
- Creuzet, Sophie, Christine Vincent, Gérard Couly, and others. 2005. “Neural Crest Derivatives in Ocular and Periocular Structures.” *Int J Dev Biol* 49 (2-3): 161–71.
- Dahdul, Wasila M., James P. Balhoff, David C. Blackburn, Alexander D. Diehl, Melissa A. Haendel, Brian K. Hall, Hilmar Lapp, et al. 2012. “A Unified Anatomy Ontology of the Vertebrate Skeletal System.” *PloS One* 7 (12): e51070.
- De Beer, Sir Gavin. 1937. “The Development of the Vertebrate Skull.” <http://www.sidalc.net/cgi-bin/wxis.exe/?IsisScript=FCL.xis&method=post&formato=2&cantidad=1&expresion=mfn=000141>.
- De Ricqlès, Armand, Octávio Mateus, Miguel Telles Antunes, and Philippe Taquet. 2001. “Histomorphogenesis of Embryos of Upper Jurassic Theropods from Lourinhã (Portugal).” *Comptes Rendus de l'Académie Des Sciences - Series IIA - Earth and Planetary Science* 332 (10): 647–56. doi:10.1016/S1251-8050(01)01580-4.
- Douarin, Nicole Le, and Chaya Kalcheim. 1999. *The Neural Crest*. Cambridge University Press.
- Erdmann, Kurt. 1940. “Zur entwicklungsgeschichte der knochen im schädel des huhnes bis zum zeitpunkt des ausschlüpfens aus dem ei.” *Zeitschrift für Morphologie und Ökologie der Tiere* 36 (3): 315–400. doi:10.1007/BF00406236.
- Etchevers, H. C., C. Vincent, N. M. Le Douarin, and G. F. Couly. 2001. “The Cephalic Neural Crest Provides Pericytes and Smooth Muscle Cells to All Blood Vessels of the Face and Forebrain.” *Development* 128 (7): 1059–68.
- Evans, Darrell J.R., and Drew M. Noden. 2006. “Spatial Relations between Avian Craniofacial Neural Crest and Paraxial Mesoderm Cells.” *Developmental Dynamics* 235 (5): 1310–25. doi:10.1002/dvdy.20663.
- Ferguson, M. W. J. 1987. “Post-Laying Stages of Embryonic Development for Crocodilians.” *Wildlife Management: Crocodiles and Alligators*, 427–44.
- Fernandez, Vincent, Eric Buffetaut, Eric Maire, Jérôme Adrien, Varavudh Suteethorn, and Paul Tafforeau. 2012. “Phase Contrast Synchrotron Microtomography: Improving

- Noninvasive Investigations of Fossil Embryos In Ovo.” *Microscopy and Microanalysis* 18 (01): 179–85.
doi:10.1017/S1431927611012426.
- Feulgen, R., and H. Rossenbeck. 1924. “Mikroskopisch-Chemischer Nachweis Einer Nukleinsäure von Typus Der Thymonukleinsäure Und Die Darauf Beruhende Elektive Färbung von Zellkernen in Mikroskopischen Präparaten.” *Zeitschrift Physiology Chemistry* 135: 203–48.
- French, N. A. 1997. “Modeling Incubation Temperature: The Effects of Incubator Design, Embryonic Development, and Egg Size.” *Poultry Science* 76 (1): 124–33.
doi:10.1093/ps/76.1.124.
- Gans, Carl, and R. Glenn Northcutt. 1983. “Neural Crest and the Origin of Vertebrates: A New Head.” *Science* 220 (4594): 268–73. doi:10.1126/science.220.4594.268.
- Grapin-Botton, A., M. A. Bonnin, L. A. McNaughton, R. Krumlauf, and N. M. Le Douarin. 1995. “Plasticity of Transposed Rhombomeres: Hox Gene Induction Is Correlated with Phenotypic Modifications.” *Development* 121 (9): 2707–21.
- Gross, Joshua B., and James Hanken. 2008a. “Review of Fate-Mapping Studies of Osteogenic Cranial Neural Crest in Vertebrates.” *Developmental Biology* 317 (2): 389–400.
doi:10.1016/j.ydbio.2008.02.046.
- . 2008b. “Review of Fate-Mapping Studies of Osteogenic Cranial Neural Crest in Vertebrates.” *Developmental Biology* 317 (2): 389–400. doi:10.1016/j.ydbio.2008.02.046.
- Gualda, Emilio J., Tiago Vale, Pedro Almada, José A. Feijó, Gabriel G. Martins, and Nuno Moreno. 2013. “OpenSpinMicroscopy: An Open-Source Integrated Microscopy Platform.” *Nature Methods* 10 (7): 599–600.
- Gualda, Emilio, Nuno Moreno, Pavel Tomancak, and Gabriel G. Martins. 2014. “Going ‘Open’ with Mesoscopy: A New Dimension on Multi-View Imaging.” *Protoplasma* 251 (2): 363–72.
- Hall, Brian K. 2005. *Bones and Cartilage: Developmental and Evolutionary Skeletal Biology*. Academic Press.
<http://www.google.com/books?hl=en&lr=&id=y-RWPGDONiIC&oi=fnd&pg=PR2&dq=hall+bone+and+cartilage&ots=tlicrMKiGF&sig=WgdXOFoJFm2NmW72TgNjRwunJu4>.

- Hamburger, Viktor, and Howard L. Hamilton. 1951. "A Series of Normal Stages in the Development of the Chick Embryo." *Journal of Morphology* 88 (1): 49–92.
- Hautier, Lionel, Cyril Charles, Robert J. Asher, and Stephen J. Gaunt. 2014. "Ossification Sequence and Genetic Patterning in the Mouse Axial Skeleton." *Journal of Experimental Zoology Part B: Molecular and Developmental Evolution* 322 (8): 631–42. doi:10.1002/jez.b.22590.
- Hirsch, Karl F. 1985. "Fossil Crocodylian Eggs from the Eocene of Colorado." *Journal of Paleontology* 59 (3): 531–42.
- Hirsch, Karl F., and Rolf Kohring. 1992. "Crocodylian Eggs from the Middle Eocene Bridger Formation, Wyoming." *Journal of Vertebrate Paleontology* 12 (1): 59–65.
- His, Wilhelm. 1868. *Untersuchungen Über Die Erste Anlage Des Wirbelthierleibes*. Vogel.
http://www.google.com/books?hl=en&lr=&id=4SEUAAAAQAAJ&oi=fnd&pg=PR1&dq=his+1868&ots=6Baf_Te0yV&sig=SXyEtmfh8WKjPZj5mT0t0AwlEXI.
- Horner, John R., and Mark B. Goodwin. 2009. "Extreme Cranial Ontogeny in the Upper Cretaceous Dinosaur *Pachycephalosaurus*." *PLoS ONE* 4 (10): e7626. doi:10.1371/journal.pone.0007626.
- Irmis, Randall B., Sterling J. Nesbitt, and Hans-Dieter Sues. 2013. "Early Crocodylomorpha." *Geological Society, London, Special Publications* 379 (1): 275–302. doi:10.1144/SP379.24.
- Jennifer Fish, Richard A. Schneider, and Richard A. Schneider. 2014. "Neural Crest-Mediated Tissue Interactions During Craniofacial Development: The Origins of Species-Specific Pattern." In *Neural Crest Cells Evolution, Development and Disease*, 102–15. Academic Press.
- Jiang, Xiaobing, Sachiko Iseki, Robert E. Maxson, Henry M. Sucov, and Gillian M. Morriss-Kay. 2002. "Tissue Origins and Interactions in the Mammalian Skull Vault." *Developmental Biology* 241 (1): 106–16. doi:10.1006/dbio.2001.0487.
- Jollie, Malcolm T. 1957. "The Head Skeleton of the Chicken and Remarks on the Anatomy of This Region in Other Birds." *Journal of Morphology* 100 (3): 389–436. doi:10.1002/jmor.1051000302.

- Ke, Meng-Tsen, Satoshi Fujimoto, and Takeshi Imai. 2013. "SeeDB: A Simple and Morphology-Preserving Optical Clearing Agent for Neuronal Circuit Reconstruction." *Nature Neuroscience* 16 (8): 1154–61.
- Klembara, J. 2001. "Postparietal and Prehatching Ontogeny of the Supraoccipital in Alligator *Mississippiensis* (Archosauria, Crocodylia)." *Journal of Morphology* 249 (2): 147–53.
- Köppl, Christine, Eva Futterer, Bärbel Nieder, Ralf Sistermann, and Hermann Wagner. 2005. "Embryonic and Posthatching Development of the Barn Owl (*Tyto Alba*): Reference Data for Age Determination." *Developmental Dynamics* 233 (4): 1248–60. doi:10.1002/dvdy.20394.
- Koyabu, Daisuke, Wolfgang Maier, and Marcelo R. Sánchez-Villagra. 2012. "Paleontological and Developmental Evidence Resolve the Homology and Dual Embryonic Origin of a Mammalian Skull Bone, the Interparietal." *Proceedings of the National Academy of Sciences* 109 (35): 14075–80. doi:10.1073/pnas.1208693109.
- Kundrát, Martin, Arthur R. I. Cruickshank, Terry W. Manning, and John Nudds. 2008. "Embryos of Therizinosauroid Theropods from the Upper Cretaceous of China: Diagnosis and Analysis of Ossification Patterns." *Acta Zoologica* 89 (3): 231–51. doi:10.1111/j.1463-6395.2007.00311.x.
- Kuratani, Shigeru. 2005. "Craniofacial Development and the Evolution of the Vertebrates: The Old Problems on a New Background." *Zoological Science* 22 (1): 1–19. doi:10.2108/zsj.22.1.
- Le Douarin, Nicole M. 1973. "A Feulgen-Positive Nucleolus." *Experimental Cell Research* 77 (1–2): 459–68. doi:10.1016/0014-4827(73)90600-9.
- Le Douarin, N. M. 1969. "Particularités Du Noyau Interphasique Chez La Caille Japonaise (*Coturnix Coturnix Japonica*). Utilisation de Ces Particularités Comme 'marquage Biologique' Dans Les Recherches Sur Les Interactions Tissulaires et Les Migrations Cellulaires Au Cours de L'ontogenèse." *Bull. Biol. Fr. Belg* 103: 435–52.
- Le Douarin, N. M., and Chaya Kalcheim. 1982. "The Neural Crest." Cambridge University Press. Cambridge, UK.
- Lee, S.-H., K. K. Fu, J. N. Hui, and J. M. Richman. 2001. "Noggin and Retinoic Acid Transform the Identity of Avian Facial

- Prominences.” *Nature* 414 (6866): 909–12.
doi:10.1038/414909a.
- Le Lièvre, Christiane S. Le. 1978. “Participation of Neural Crest-Derived Cells in the Genesis of the Skull in Birds.” *Journal of Embryology and Experimental Morphology* 47 (1): 17–37.
- Long, John A., Elga Mark-Kurik, Zerina Johanson, Michael S. Y. Lee, Gavin C. Young, Zhu Min, Per E. Ahlberg, et al. 2014. “Copulation in Antiarch Placoderms and the Origin of Gnathostome Internal Fertilization.” *Nature* advance online publication (October). doi:10.1038/nature13825.
- Lumsden, A., N. Sprawson, and A. Graham. 1991. “Segmental Origin and Migration of Neural Crest Cells in the Hindbrain Region of the Chick Embryo.” *Development (Cambridge, England)* 113 (4): 1281–91.
- Luo, Zhe-Xi. 2011. “Developmental Patterns in Mesozoic Evolution of Mammal Ears.” *Annual Review of Ecology, Evolution, and Systematics* 42 (1): 355–80. doi:10.1146/annurev-ecolsys-032511-142302.
- Malpighi, Marcello. 1672. *M. Malpighii ... Dissertatio Epistolica de Formatione Pulli in Ovo*.
- . 1675. “Appendix, Repetitas Auctasque De Ovo Incubato Observationes Continens. (Malpighi, Marcello: Anatomie Plantarum. Appendix.) | Malpighi, Marcello.” *Europeana*. http://www.europeana.eu/portal/record/09428/permalink_2010_01_katkey_267160.html.
- Manuppella, Giuseppe. 1999. *Carta Geológica de Portugal, Notícia Explicativa Da Folha 30-A: Lourinhã Escala 1:50000*. 2nd ed. Lisboa: Instituto Geológico e Mineiro. Departamento de Geologia.
- Moreno-Azanza, Miguel, Blanca Bauluz, José I. Canudo, Eduardo Puértolas-Pascual, and Albert G. Sellés. 2013. “A Re-Evaluation of Aff. Megaloolithidae Eggshell Fragments from the Uppermost Cretaceous of the Pyrenees and Implications for Crocodylomorph Eggshell Structure.” *Historical Biology* 26 (2): 195–205.
doi:10.1080/08912963.2013.786067.
- Müller, Johannes, Torsten M. Scheyer, Jason J. Head, Paul M. Barrett, Ingmar Werneburg, Per G. P. Ericson, Diego Pol, and Marcelo R. Sánchez-Villagra. 2010. “Homeotic Effects, Somitogenesis and the Evolution of Vertebral Numbers in

- Recent and Fossil Amniotes." *Proceedings of the National Academy of Sciences* 107 (5): 2118–23.
doi:10.1073/pnas.0912622107.
- Nesbitt, Sterling J. 2011. "The Early Evolution of Archosaurs: Relationships and the Origin of Major Clades." *Bulletin of the American Museum of Natural History*, April, 1–292.
doi:10.1206/352.1.
- Noden, D. M. 1982. "Patterns and Organization of Craniofacial Skeletogenic and Myogenic Mesenchyme: A Perspective." *Progress in Clinical and Biological Research* 101: 167–203.
- . 1984. "The Use of Chimeras in Analyses of Craniofacial Development." In *Chimeras in Developmental Biology*, 241–80. London: Academic Press.
- . 1990. "Origins and Assembly of Avian Embryonic Blood Vessels." *Annals of the New York Academy of Sciences* 588 (1): 236–49. doi:10.1111/j.1749-6632.1990.tb13214.x.
- . 1991a. "The Development of Craniofacial Blood Vessels." In *Development of the Vascular System.*, Feinberg RN, Sherer G, Auerbach R, 1–24. Basel: Karger.
- . 1991b. "Origins and Patterning of Avian Outflow Tract Endocardium." *Development* 111 (4): 867–76.
- Noden, Drew M., and Paul A. Trainor. 2005. "Relations and Interactions between Cranial Mesoderm and Neural Crest Populations." *Journal of Anatomy* 207 (5): 575–601.
doi:10.1111/j.1469-7580.2005.00473.x.
- O'Keefe, F. R., and L. M. Chiappe. 2011. "Viviparity and K-Selected Life History in a Mesozoic Marine Plesiosaur (Reptilia, Sauropterygia)." *Science* 333 (6044): 870–73.
doi:10.1126/science.1205689.
- Oliveira, Carlos E. M., Rodrigo M. Santucci, Marco B. Andrade, Vicente J. Fulfaro, José a. F. Basílio, and Michael J. Benton. 2011. "Crocodylomorph Eggs and Eggshells from the Adamantina Formation (Bauru Group), Upper Cretaceous of Brazil." *Palaeontology* 54 (2): 309–21.
doi:10.1111/j.1475-4983.2010.01028.x.
- Owen, Richard. 1848. *On the Archetype and Homologies of the Vertebrate Skeleton*. van Voorst.
<http://www.google.com/books?hl=en&lr=&id=L1Bg6KFMw34C&oi=fnd&pg=PA1&dq=On+the+archetype+and+homologi>

es+of+the+vertebrate+skeleton.&ots=b5V3TGf70H&sig=mqXQccXfd0-XxF2zTppqJdufg-Q.

- Owen, Richard, and William White Cooper. 1843. *Lectures on the Comparative Anatomy and Physiology of the Invertebrate Animals : Delivered at the Royal College of Surgeons, in 1843 / By Richard Owen ; From Notes Taken by William White Cooper and Revised by Professor Owen*. London : Longman, Brown, Green, and Longmans,.
<http://www.biodiversitylibrary.org/bibliography/6788>.
- Panchen, Alec L. 1999. "Homology—history of a Concept." *Homology*, 5–17.
- Pander, Christian Heinrich. 1817a. *Beiträge Zur Entwicklungsgeschichte Des Hühnchens Im Eye*.
http://www.google.com/books?hl=en&lr=&id=QRFBAAAACA&oi=fnd&pg=PA1&dq=pander+1817&ots=dRogx4Huzb&sig=bG-6B1gO7ffh_KF04R0XMEIsU9c.
- . 1817b. *Dissertatio Inauguralis Sistens Historiam Metamorphoseos, Quam Ovum Incubatum Prioribus Quinque Diebus Subit*. Typis Nitribitt.
http://www.google.com/books?hl=en&lr=&id=3CJbAAAACA&oi=fnd&pg=PA1&dq=pander+1817&ots=biiUT6cLiz&sig=YyNWfc33jIU4AjDbq_iKBRjw8Us.
- Parker, William Kitchen. 1890. "On the Morphology of the Duck and the Auk Tribes." In . Royal Irish Academy.
- Piñeiro, Graciela, Jorge Ferigolo, Melitta Meneghel, and Michel Laurin. 2012. "The Oldest Known Amniotic Embryos Suggest Viviparity in Mesosaurs." *Historical Biology* 24 (6): 620–30. doi:10.1080/08912963.2012.662230.
- Raff, Rudolf. 1996. *The Shape of Life: Genes, Development, and the Evolution of Animal Form*. University Of Chicago Press.
<http://www.amazon.ca/exec/obidos/redirect?tag=citeulike09-20&path=ASIN/0226702669>.
- Rasband, W. S. 1997. "ImageJ, US National Institutes of Health." *Bethesda, Maryland, USA* 2012.
- Reisz, Robert R. 1997. "The Origin and Early Evolutionary History of Amniotes." *Trends in Ecology & Evolution* 12 (6): 218–22. doi:10.1016/S0169-5347(97)01060-4.
- Reisz, Robert R., Timothy D. Huang, Eric M. Roberts, ShinRung Peng, Corwin Sullivan, Koen Stein, Aaron R. H. LeBlanc, et al. 2013. "Embryology of Early Jurassic Dinosaur from

- China with Evidence of Preserved Organic Remains.” *Nature* 496 (7444): 210–14. doi:10.1038/nature11978.
- Reisz, Robert R., Diane Scott, Hans-Dieter Sues, David C. Evans, and Michael A. Raath. 2005. “Embryos of an Early Jurassic Prosauropod Dinosaur and Their Evolutionary Significance.” *Science* 309 (5735): 761–64. doi:10.1126/science.1114942.
- Riedl, Rupert. 1978. *Order in Living Organisms: A Systems Analysis of Evolution*. New York: Wiley.
<http://library.wur.nl/WebQuery/clc/140930>.
- Rieppel, Olivier. 1994. “Homology, Topology, and Typology: The History of Modern Debates.” *Homology: The Hierarchical Basis of Comparative Biology*, 63–100.
- Rocek, Zbynek. 1988. “Origin and Evolution of the Frontoparietal Complex in Anurans.” *Amphibia-Reptilia* 9 (4): 385–403.
- Rogers, Jack V. 2001. “A Complete Crocodyloid Egg from the Lower Cretaceous (Albian) Glen Rose Formation, Central Texas.” *Journal of Vertebrate Paleontology* 20 (4): 780–83. doi:10.1671/0272-4634(2000)020[0780:ACCEFT]2.0.CO;2.
- Romanoff, A. L. 1960. “The Avian Embryo. Structural and Functional Development.” xvi+1305 pp.
- Romer, Alfred Sherwood. 1956. “Osteology of the Reptiles.” *XXI, 772 Pp., 248 Figs.*
- Sánchez-Villagra, Marcelo. 2012. *Embryos in Deep Time*. University of California Press.
<http://mwbdvjh.muse.jhu.edu/books/9780520952300/9780520952300-17.pdf>.
- Santagati, Fabio, and Filippo M. Rijli. 2003. “Cranial Neural Crest and the Building of the Vertebrate Head.” *Nature Reviews Neuroscience* 4 (10): 806–18. doi:10.1038/nrn1221.
- Scannella, John B., and John R. Horner. 2010. “Torosaurus Marsh, 1891, Is Triceratops Marsh, 1889 (Ceratopsidae: Chasmosaurinae): Synonymy through Ontogeny.” *Journal of Vertebrate Paleontology* 30 (4): 1157–68. doi:10.1080/02724634.2010.483632.
- Schinz, Hans Rudolf, and Rainer Zangerl. 1937. *Beiträge Zur Osteogenese Des Knochensystems Beim Haushuhn, Bei Der Haustaube Und Beim Haubensteissfuss*. Fretz.
- Schneider, Simon, Franz T. Fürsich, and Winfried Werner. 2009. “Sr-Isotope Stratigraphy of the Upper Jurassic of Central Portugal (Lusitanian Basin) Based on Oyster Shells.”

- International Journal of Earth Sciences* 98 (8): 1949–70.
doi:10.1007/s00531-008-0359-3.
- Serbedzija, G. N., M. Bronner-Fraser, and S. E. Fraser. 1992.
“Vital Dye Analysis of Cranial Neural Crest Cell Migration in
the Mouse Embryo.” *Development* 116 (2): 297–307.
- Sookias, Roland B., and Richard J. Butler. 2013. “Euparkeriidae.”
Geological Society, London, Special Publications 379 (1):
35–48. doi:10.1144/SP379.6.
- Standen, Emily M., Trina Y. Du, and Hans C. E. Larsson. 2014.
“Developmental Plasticity and the Origin of Tetrapods.”
Nature 513 (7516): 54–58. doi:10.1038/nature13708.
- Stern, Claudio D. 2005. “The Chick: A Great Model System
Becomes Even Greater.” *Developmental Cell* 8 (1): 9–17.
doi:10.1016/j.devcel.2004.11.018.
- Tanaka, Kohei, Darla K. Zelenitsky, Thomas Williamson, Anne
Weil, and François Therrien. 2010. “Fossil Eggshells from
the Upper Cretaceous (Campanian) Fruitland Formation,
New Mexico.” *Historical Biology* 23 (1): 41–55.
doi:10.1080/08912963.2010.499171.
- Thompson, T J, P D Owens, and D J Wilson. 1989.
“Intramembranous Osteogenesis and Angiogenesis in the
Chick Embryo.” *Journal of Anatomy* 166 (October): 55–65.
- Topper, Timothy P., Lars E. Holmer, and Jean-Bernard Caron.
2014. “Brachiopods Hitching a Ride: An Early Case of
Commensalism in the Middle Cambrian Burgess Shale.”
Scientific Reports 4 (October). doi:10.1038/srep06704.
- Tuinen, Marcel van, and Elizabeth A. Hadly. 2004. “Error in
Estimation of Rate and Time Inferred from the Early
Amniote Fossil Record and Avian Molecular Clocks.”
Journal of Molecular Evolution 59 (2): 267–76.
doi:10.1007/s00239-004-2624-9.
- Van der Plas, A., and P.j. Nijweide. 1992. “Isolation and
Purification of Osteocytes.” *Journal of Bone and Mineral
Research* 7 (4): 389–96. doi:10.1002/jbmr.5650070406.
- Von Baer, Carl-Ernst. 1828. *Über Entwicklungsgeschichte Der
Thiere. Beobachtung Und Reflexion.-Königsberg, Gebrüder
Bornträger 1828-1837*. Vol. 1. Gebrüder Bornträger.
<http://www.google.com/books?hl=en&lr=&id=HxBUAAAACAAJ&oi=fnd&pg=PA3&dq=%C3%9Cber+Entwicklungsgesichte+der+Thiere.+Beobachtung+und+Reflexion+Borntr%C3>

%A4ger&ots=UplTfBvsTf&sig=ZLlkBo2UPhnUjVhjigi_354fK
Dw.

- Wagner, Günter P. 1989. "The Biological Homology Concept." *Annual Review of Ecology and Systematics*, 51–69.
- . 2014. *Homology, Genes, and Evolutionary Innovation*. Princeton ; Oxford: Princeton University Press.
- Wagner, Günter P., and Jacques A. Gauthier. 1999. "1,2,3 = 2,3,4: A Solution to the Problem of the Homology of the Digits in the Avian Hand." *Proceedings of the National Academy of Sciences* 96 (9): 5111–16. doi:10.1073/pnas.96.9.5111.
- Wang, Xiaolin, and Zhonghe Zhou. 2004. "Palaeontology: Pterosaur Embryo from the Early Cretaceous." *Nature* 429 (6992): 621–621. doi:10.1038/429621a.
- Werner, Yehudah L. 1971. "The Ontogenic Development of the Vertebrae in Some Gekkonoid Lizards." *Journal of Morphology* 133 (1): 41–91. doi:10.1002/jmor.1051330104.
- Wilson, Laura A. B. 2013. "The Contribution of Developmental Palaeontology to Extensions of Evolutionary Theory." *Acta Zoologica* 94 (3): 254–60. doi:10.1111/j.1463-6395.2011.00539.x.
- Winchester, Lesley, and A. d'A. Bellairs. 1977. "Aspects of Vertebral Development in Lizards and Snakes." *Journal of Zoology* 181 (4): 495–525. doi:10.1111/j.1469-7998.1977.tb03259.x.
- Wissowsky, A. 1876. "Ueber Das Eosin Als Reagens Auf Hämoglobin Und Die Bildung von Blutgefässen Und Blutkörperchen Bei Säugethieren und Hühnerembryonen." *Arch Mikr Anat* 3: 479–96.
- Zusi, RICHARD L. 1993. "Patterns of Diversity in the Avian Skull." *The Skull* 2: 391–437.

Appendix A

Methods

Whole-mount Alizarin red and Alcian Blue staining

The protocol described below was used in embryos from: chicken (*Gallus gallus*) provided alive (fertilized eggs) by Sociedade Agrícola Quinta da Freiria; domestic duck (*Anas platyrhynchos domesticus*, Pekin Duck breed) provided alive (fertilized eggs) by Marinhas; quail (*Coturnix coturnix*) provided alive (fertilized eggs) by Interaves; crocodile (*Crocodylus niloticus*) provided dead (frozen) by Granja de Cocodrilos Kariba and mouse (*Mus musculus*) provided dead by Luciana Moraes (Disease Genetics Lab, IGC).

All bird embryos were incubated in a ventilated humid incubator at 38 °C at arrival or stored at 16 °C for no more than a week before incubation start.

Dissection. Embryos were dissected removing all extraembryonic membranes. In addition the crocodile embryos were skinned prior to the staining. All information regarding the arrival of the eggs, incubation time, developmental stage, dissector or any other notes were registered.

Skinning (crocodile embryos only). The embryos were removed from the egg and placed in a styrofoam plate and nailed using sterile needles. The skin and visceral content was removed using forceps and a small scissor.

Fixation. The embryos were numbered and placed in ethanol 96% ethanol inside individual wells in hand-made trays containing up to 50 numbered wells. These trays allow: a quicker exchange of solutions, a

more homogeneous dispersal of the standing dyes, preserves individual tagging of each embryo with reduced damaging for the specimens and reduces solution spilling.

The trays were kept on an automatic shaker using gentle agitation (rotating plate) at room temperature. The ethanol was replaced at least once during a 24-48h period. Some embryos were maintained in this step during longer periods (up to one month) without producing any visible differences in the final staining results.

Alcian blue staining. The embryos were incubated in a solution of 150 mg/l alcian blue 8 GX (A3157) 80% ethanol, 20% acetic acid for a variable amount of time, from 12h up to two days according to the size of the embryos (bigger embryos were maintained for longer periods for proper alcian blue penetration).

To improve results, the alcian blue staining intensity was checked periodically under a stereo microscope before advancing to the next step.

Post-fixation. The embryos were rinsed in 96% ethanol for 24h up to 48h. The ethanol was changed at least once in the first 24h. Some embryos were maintained in this step during longer periods (up to one month) without producing any visible differences in the final staining results.

Initial KOH clearing. The samples were incubated in KOH 0.5% to 2% (in milliQ or distilled water) during 30 min up to 6h depending of their size (bigger embryos were maintained for longer periods using higher concentrations) until the embryos start to become transparent.

After this step, due to its fragility, the embryos were transferred, from the trays to closed individual vials. The vials were also maintained on an automatic shaker using gentle agitation (rotating plate) at room temperature.

The KOH initial clearing dissolves the embryos tissues making them extremely fragile. Thus, in all subsequent steps the solutions were changed by a combination of pouring the liquids and aspirating carefully the remaining with a pipette.

Alizarin red staining. The embryos were incubated in a solution of Alizarin Red S (A5533 Sigma)) 50 mg/l in KOH 0,5 or 1% in distilled water from 2h up to 8h (bigger embryos were maintained for longer periods). The alizarin red staining intensity was checked under a stereo microscope periodically before advancing to the next step.

Final clearing. Depending on its developmental stage, the embryos were incubated in KOH from 0,1% to 2% (milliQ water) until the skeletal elements and visible (bigger embryos were maintained in higher concentrations). The bones lost some of the red staining while in KOH solution, making the timing of this step crucial to adjust the correct saturation of the alizarin red staining. The solution was changed several times in some of the more developed embryos. The less developed embryos were only maintained in this step for short periods (some less than 30 min). The timing was controlled by periodical observations under a stereo microscope.

Stopping clearing reaction. The KOH solution was replaced by distilled water to rinse the embryos and stopping the reaction. The embryos were kept in water for approximately 1h.

Glycerol storage. The embryos were transferred to a solution of glycerol 25% (in water) with azide. Then they were transferred stepwise into 50%, 75% glycerol solutions with azide and maintained up to 1 or 2 days in each concentration, until the embryos sink. Finally, they were store in 100% glycerol + azide.

Histological techniques

Cryopreservation and sectioning

The embryos destined to be sectioned were dissected and fixed in 4% PFA in PBS for at least over night (bigger samples were fixed during 48h), at 4 °C. After, the Quail-Chick chimera specimens were dehydrated in ethanol series and included in paraffin to be sectioned in coronal symmetrical slices using a microtome. The GFT Chick – wt Chick chimera embryos were inserted in a 15 % sucrose solution in PBS during at least 48 h. They were included in a mold were we poured OCT (Compound for Cryostat Sectioning, Tissue-Tek). The samples were fast-frozen by dipping in liquid nitrogen for a few seconds. The Quail-Chick chimeras were sectioned at 6 µm in a manual microtome (Leica RM 2135) while the GFP Chick-wt Chick chimeras were sectioned at 40 µm using a cryostat (Leica I). The latter slides were maintained in the dark at 4 °C until being used in any experiment.

Hematoxylin Eosine staining

Hematoxylin and eosin stain (HE stain) is probably the most widely used histological staining method in routine microscopy and histopathology studies. It was developed in the XIX century by Wissowsky (Wissowsky 1876) and still presents one big advantage for it works well, enhancing a wide range of cellular features, even under

many different fixatives. Hematoxylin stains nucleic acids with a blue-purple color while Eosin presents a red-pink color staining proteins nonspecifically. Thus, basophilic structures (e.g. nuclei) are stained blue-purple while eosinophilic structures (e.g. cytoplasmic content) appear in variable shades of red-pink color.

Protocol

The slides were placed in xylene during 10 minutes and again in clean xylene during 5 minutes. After they passed twice through ethanol 100%, one time in ethanol 95% and once in ethanol 70% (2 minutes each ethanol wash). The sections were washed using tap water during 2 minutes and then stained with Harris hematoxylin during 8 minutes. After this, the slides were rinsed in running tap water and dipped 4 times in 0,5% chloridric alcohol in 70% ethanol and immediately washed in warm running tap water for 8 minutes. The slides were then placed during 2 minutes in ethanol 95% and then in eosin during 2 minutes. The sections were dehydrated by a double passage through ethanol 100% and another double passage in xylene before mounting with GLCTM Mounting Medium (Sakura, cat no1408).

Feulgen – Rossenbeck staining

This histological technique, firstly described by Feulgen and Rossenbeck in 1924 (Feulgen and Rossenbeck 1924) involves HCl hydrolysis of DNA allowing a specific staining of this nucleic acid. The free aldehyde groups of DNA that are produced by the acidic hydrolysis react with pararosaniline present in Schiff reagent and stains the cells with magenta color, particularly in the nuclei. This allows a quantification of the DNA present in each nucleus allowing a differentiation of the quail cells in relation to the chicken. Quail cells interphase nuclei present a

condensed mass of heterochromatin. On the contrary, in chicken cells the heterochromatin is dispersed in small chromocenters (N. L. Douarin and Kalcheim 1999).

Rehydration. The sections were brought to water through sequential passages in 20 min in Toluene (twice), 5 min in Ethanol 100%, 2 min in Collodion (0,2% colloidine in a solution of Ethanol 50% / Ether 50%), 2 min Ethanol 85% / Formol 15%, a passage through Ethanol 96%, 15 min in running water and one passage in distilled water.

Acidic hydrolysis. The sections were placed in HCL 5N for 32 minutes.

Wash. The sections were washed in running water during 15 minutes and then laced in distilled water.

Magenta staining. The sections were submerged in Schiff reagent during 90 minutes at 4 °C.

Clearing non-specific staining. The sections were washed with a solution of 0,5% $\text{Na}_2\text{S}_2\text{O}_5$ in water during 1 minute followed by 3 minutes in the same fresh solution.

Wash. The sections were washed in running water during 15 minutes and placed in distilled water.

Counter stain. To improve contrast the sections were stained with 1% light green in 1% acetic acid 40 sec.

Dehydration. The slides were passed three times through ethanol 100 during 30 minutes each and then placed in Toluene twice.

Imaging and Storage. Given that the staining loses intensity with time, the sections were immediately observed and imaged or stored at 4 °C and analyzed as soon as possible.

Optical Projection Tomography (OPT)

In order to image large size embryos in three dimensions (3D), Sharpe and others develop recently a new visualization technique entitled Optical Projection Tomography (Sharpe et al. 2002). Its imaging principles are similar to classic CT scans (Computed Tomography). In a CT scan the specimen is placed in a center of rotation axis and multiple images are taken at a defined number of angles (usually one image every fraction of degree) but instead of penetrating the sample with x-rays, OPT uses visible light. The resulting projections can be used to 3D reconstruct the whole volume of the imaged sample via a procedure known as back-projection reconstruction. We used a prototypical scanner built with open source soft&hardware, known as OPenT (E. Gualda et al. 2014; E. J. Gualda et al. 2013). This scanner acquires a sequence of 1600 projections of each embryo and the image sequences are then post-processed using ImageJ (Rasband 1997) and the software NRecon (SkyScan). The OPenT can also operate in light-emitting mode, in which case it is possible to image fluorescently labeled samples. This is accomplished by illuminating with blue light (470nm) and using an emission filter which only allows the capture of GFP signal. In addition, OPT works better if light passes through the sample without scattering, which implies that the embryos must be cleared prior to imaging. Typically embryos are dehydrated and embedded in a solution with high-refractive index (e.g. a mixture of Benzyl-Alcohol / Benzyl Benzoate) however this does not allow imaging of GFP, which is quenched under these conditions. To circumvent this problem, we impregnated the embryos with a saturated solution of Fructose (~85%) for several days.

This protocol entitled SeeDB (Ke, Fujimoto, and Imai 2013), effectively raises the refractive index of the sample without significantly affecting the fluorescence of GFP.

Immunohistochemistry

Firstly developed by Albert H. Coons in 1941 (Coons, Creech, and Jones 1941), this technique has been widely used to detect specific molecules in tissues of interest. The affinity of an antibody to a specific antigen allows a tagging of particular molecules in many different situations, including *in vivo*. Whole embryos and dissected heads were fixed over night in 4% PFA (freshly made) or commercial buffered formaldehyde 4 % solution (VWR # 9713.1000), at 4 °C.

Solutions needed

PBS = Phosphate buffered saline

PBS-T = PBS with Triton (0,05%)

PBS-G-T = PBS + Gelatin (2gr/L) and Triton (0,25%)

PBS-G-L = 9mL PBS-G-T + 1mL Lys 1M (=10mL PBS-G-T-Lys
0,1M)

H2O2 (0,5%)

Protocol

Day 1

Sectioning. The embryonic heads were sectioned in the cryostat according to the protocol described in “Cryopreservation and sectioning” section.

From this point onwards (except if indicated otherwise) all steps were made in the dark and at room temperature.

Wash. The sections (stored at -20 C°) were left at RT during 5 minutes and then were washed in PBS-T during approximately 15 minutes.

Inactivation of the endogenous peroxidases (optional). The slides were placed in a solution of H₂O₂ 0,5% in PBS-T for 30 minutes.

Wash. The slides were washed twice with PBS-G-T during 15 min each wash.

Blocking. In order to block nonspecific sites, each slide was covered with 500 µl of PBS-G-T-Lys for at least 1h. This step was done placing the slides inside a wet chamber.

Primary Ab. After draining, the slides were covered with the primary antibody diluted (with a concentration according to manufacture instructions) in 100 µl of PBS-G-T, over night at 4°C. This step was done placing the slides inside a wet chamber. In order to avoid dehydration, each slide was covered by a small rectangle of Parafilm M(R).

Day 2

First Wash. The slides were washed with PBS-T, three times during 10 min each wash.

Second Wash. The slides were washed once with PBS-G-T during 10 min.

Secondary Ab. After draining, the slides were incubated in a solution containing the secondary antibody diluted (concentration according to manufacture, usually Alexa 546 1:100) in 100 to 200 μ l of PBS-G-T, over night at 4°C. This step was done placing the slides inside a wet chamber. In order to avoid dehydration, each slide was covered by a small rectangle of Parafilm M(R).

Day 3

First Wash. The slides were washed three times with PBS-T during 10 min each wash.

Nuclei Stain. The slides were covered with a solution of DAPI 1:10000 (in PBS) during 5 minutes.

Second Wash The slides were washed three times with PBS-T during 10 min each wash.

Mount. The final coverslip mounting was done using Vectashield (#H-1000) directly and by sealing the coverslip with commercial nail polish.

Storage. The slides were storage at 4 °C until being observe an imaged in a microscope.

The Immunohistochemistry experiments were done using the following monoclonal antibodies:

- QCPN concentration 1:1 or 1:2. This MAb was developed by Carlson, B. and Carlson, J. and was obtained from the Developmental Studies Hybridoma Bank, created by the NICHD of the NIH and maintained at The University of Iowa, Department of Biology, Iowa City, IA 52242)
- OCG4 (ab13421), Mouse monoclonal to Osteocalcin 1:170
- OB7.3 concentration 1:20. This MAb (van der Plas and Nijweide 1992) was kindly sent by Cor Semeins, ACTA, Orale Celbiologie, Amsterdam.

In vivo manipulation techniques

Transplants of Neural Crest Cells

Quail – Chicken Chimeras

All containers, instruments, benches and any other material involved in the experiment was previously washed with ethanol 70% or, when possible, autoclaved. Dissection instruments were sterilized in a dry oven (at least 1h at 200°C). All incubators used were previously washed with commercial bleach (sodium hypochlorite) diluted in water. Right before the start of this protocol my hands were disinfected using ethanol 70%. The Neural Crest transplants were performed between embryos in the same HH stage and, at most, with only one somite of difference.

Except if indicated otherwise all steps were made at room temperature.

Incubation. We incubate quail and chick eggs with their long axis horizontal during 28-34h in order to obtain embryos between stages 7 to

9 (Hamburger and Hamilton 1951). The top of each egg was marked using a permanent marker or a pencil.

Albumen removal. Using the tip of a forceps, a small hole was made near the narrowest pole of each egg. After, using a sterile 10 ml syringe with a needle we carefully aspirated approximately 3 ml of albumen per egg. During this process the syringe needle was inserted in the hole previously made and directed away from the fluctuating yolk. This step creates some space between the blastoderm and the eggshell membrane. The hole was covered with a small piece of adhesive tape (around 2 cm²).

Windowing eggs. Using a small curved scissor we cut a small rounded window on the marked part (upper part) of each egg. Usually the blastoderm was visible, but when it was not in the central part of the window we increased the opening in order to center it. This guarantees that the embryo is available to manipulation.

Contrasting. By injecting beneath the endoderm a solution of 1% Indian ink (Pelikan, black 17) in PBS with penicillin and streptomycin the embryos were made visible and the contrast was highly enhanced. The Indian ink solution was made fresh and filtered every day before injection through Millipore filters (0,2 µm). In order to inject the ink solution we used a glass micropipette attached to a rubber tube for mouth aspiration (Sigma A5177-5EA).

Donor (Quail) Embryo Removal. All embryos used as donors were cut from the egg with spring scissors and, using a perforated spoon, placed in a petri dish with PBS to remove any yolk residues and then transferred to another cleaned PBS solution in a petri dish (with its base cover by black silicone) and nailed using Austerlitz insect pins.

Excision of donor neural crest. Using a microscalpel made with an Austerlitz insect pin with its tip bended at approximately 90° we made a transverse cut on the posterior part of the right neural crest (in some cases the left side was the one transplanted). Then a longitudinal slit was made laterally through the ectoderm. Another slit was made on the medial part of the right Neural Crest. Ultimately, in order to detach the piece of Neural Crest, a final transverse cut was made in the anterior region, uniting the two anterior tips of the longitudinal slits freeing a small piece of neural crest.

Excision of host (Chicken) neural crest (*in ovo*). With a microscalpel we made a small cut in the vitelline membrane over the site where the neural crest needed to be transplanted. Then, using the procedure described in the previous step it was possible to free, in the same region, an equivalent fragment of Neural Crest, leaving the contralateral Neural Crest intact. The freed rectangular piece of Neural Crest was pushed away creating a gap in the Neural Crest region of interest (where the donor fragment was grafted). Contrary to the previous step, this operation was made through a window in a chicken egg. Thus, every time the egg was not being operated the window was covered with a small piece of sterilized glass and the lights were turned off to prevent desiccation.

Grafting. The donor (quail) neural crest piece was transplanted to the host (chicken) embryo using a glass micropipette and placed in the gap produced by the host excision. The donor antero-posterior and dorso-ventral orientation of the Neural Crest piece was respected.

At this step, the diameter of the micropipette is crucial. The width of the Neural Crest piece should have approximately the same size as the diameter of the glass micropipette. Too narrow micropipettes will

fragment the Neural Crest piece when suction occurs, while too wide diameters will let the Neural Crest pieces escape.

We used two stereo microscopes side by side, to reduce the time during the transplant, one focused on the donor embryo and another on the host. This not only reduced the time need to replace and refocus the samples bellow the objective but also freed the hands to hold the micropipette and transplant the fragments in seconds.

Sealing. Once the transplanted fragment was placed the egg was numbered, the window was covered with adhesive tape and the egg was immediately placed inside an incubator at 38 °C.

The transplanted eggs were monitored daily and every eggs presenting a dead embryo was removed and, when considered justified, fixed for further analysis.

GFP Chicken – wt Chicken Chimeras

All containers, instruments, benches and any other material involved in the experiment was previously washed with ethanol 70% or, when possible, autoclaved. Dissection instruments were sterilized in a dry oven (1h at 130°C). The operation room was left under U.V. lights over the night previous to the experiments. All incubators used were previously washed with commercial bleach (sodium hypochlorite) diluted in water. Right before the start of this protocol my hands were disinfected using ethanol 70%.

Except if indicated otherwise all steps were made at room temperature.

Incubation. We incubate fertilized GFP chicken and wt chick eggs with their long axis vertically, placing the narrowest pole facing down.

The eggs were incubated during 28-34h in order to obtain embryos between stages 7 to 9 (Hamburger and Hamilton 1951).

Albumen removal. Using the tip of a forceps, a small hole was made near (but not exactly at) the narrowest pole of each egg. After, using a sterile 10 ml syringe with a needle we carefully aspirated approximately 3 ml of albumen per egg. During this process the syringe needle was inserted in the hole previously made and directed away from the fluctuating yolk. This step increases the usual space occupied by the air chamber separating the blastoderm and the eggshell membrane. The hole was covered with a small piece of adhesive tape (around 2 cm²).

In order to reduce time consumption, this step was usually made sequentially to 3 or 4 eggs.

Windowing eggs. Same as in “Quail – Chicken Chimeras”.

Contrasting. The embryos were made visible and the contrast was highly enhanced by injecting beneath the endoderm a solution of 2% Indian ink (Pelikan, black 17) in PBS. This solution was autoclaved on the day before and before the experiment we added penicillin and streptomycin. In order to inject the ink solution we used a 1 ml syringe with its needle bent in “Z” to facilitate the ink injection.

Donor (GFP Chicken) Embryo Removal. All embryos used as donors were cut from the egg with spring scissors and, using a perforated spoon, placed in a petri dish with PBS to remove any yolk residues and then transferred to another cleaned PBS solution in a petri dish (with its base cover by black silicone) and nailed using Austerlitz insect pins.

Excision of donor neural crest. Using a microscalpel made with an Austerlitz insect pin with its tip bended at approximately 90° we made a transverse cut on the posterior part of the right neural crest (in some cases the left side was the one transplanted). Then a longitudinal slit was made laterally through the ectoderm. Another slit was made on the medial part of the right Neural Crest. Ultimately, in order to detach the piece of Neural Crest, a final transverse cut was made in the anterior region, uniting the two anterior tips of the longitudinal slits freeing a small piece of neural crest.

Excision of host (wt Chicken) neural crest (*in ovo*). With a microscalpel we made a small cut in the vitelline membrane over the site where the neural crest needed to be transplanted. Then, using the procedure described in the previous step it was possible to free, in the same region, an equivalent fragment of Neural Crest, leaving the contralateral Neural Crest intact. The freed rectangular piece of Neural Crest was pushed away creating a gap in the Neural Crest region of interest (where the donor fragment was grafted). Contrary to the previous step, this operation was made through a window in a chicken egg. Thus, every time the egg was not being operated the window was covered with a small piece of sterilized glass and the lights were turned off to prevent desiccation.

Grafting. The donor (GFP Chicken) neural crest piece was transplanted to the host (wt Chicken) embryo using a glass micropipette and placed in the gap produced by the host excision. The donor antero-posterior and dorso-ventral orientation of the Neural Crest piece was respected.

At this step, the diameter of the micropipette is crucial. The width of the Neural Crest piece should have approximately the same size as

the diameter of the glass micropipette. Too narrow micropipettes will fragment the Neural Crest piece when suction occurs, while too wide diameters will let the Neural Crest pieces escape.

We used two stereo microscopes side by side, to reduce the time during the transplant, one focused on the donor embryo and another on the host. This not only reduced the time need to replace and refocus the samples bellow the objective but also freed the hands to hold the micropipette and transplant the fragments in seconds.

Sealing. Once the transplanted fragment was placed the egg was numbered, the window was covered with adhesive tape and the egg was immediately placed inside an incubator at 38 °C.

The transplanted eggs were monitored daily and every eggs presenting a dead embryo was removed and, is justified, fixed for further analysis.

Transplants of Paraxial Mesoderm Cells

All containers, instruments, benches and any other material involved in the experiment was previously washed with ethanol 70% or, when possible, autoclaved. Dissection instruments were sterilized in a dry oven (1h at 130°C). The operation room was left with U.V. on, over the night previous to the experiments. All incubators used were previously washed with commercial bleach (sodium hypochlorite) diluted in water. Right before the start of this protocol my hands were disinfected using ethanol 70%.

Except if indicated otherwise all steps were made at room temperature.

Incubation. Same as in “GFP Chicken – wt Chicken Chimeras” section.

Windowing eggs. Same as in “GFP Chicken – wt Chicken Chimeras” section.

Contrasting. Same as in “GFP Chicken – wt Chicken Chimeras” section.

Donor (GFP Chicken) Embryo Removal. Same as in “GFP Chicken – wt Chicken Chimeras” section.

Excision of donor ectoderm. Using a microscalpel made with an Austerlitz insect pin (with its tip bended at approximately 90°) we made one long longitudinal cut on the ectoderm over the site where the mesoderm eventually removed. In addition it were made two small cuts in the ectoderm, one anterior tip and another of the posterior tip of the longitudinal slit previously made. This “U” shaped cut allowed a exposition of the mesoderm to a better aspiration in step “Excision of donor mesoderm”.

Excision of host (wt Chicken) mesoderm (*in ovo*). Using a microscalpel we made a very small transverse cut on the vitelline membrane and ectoderm over the site where the mesoderm was transplanted. Then we inserted very gently the tip of the micropipette and aspirate carefully some mesoderm cells.

Excision of donor mesoderm. After cleaning the micropipette by sucking and blowing a few times some cleaned PBS, we aspirated some mesoderm cells from the corresponding location.

Grafting. We inserted very gently the tip of the micropipette and blow out carefully the GFP mesoderm cells into the site of interest.

Sealing. Same as in “GFP Chicken – wt Chicken Chimeras” section.

Microscopy techniques

Confocal

Immunohistochemical stainings were imaged using a confocal microscope.

Florescent Stereo Microscope

For imaging whole embryos or dissected heads resulting from GFP to wt chicken transplants, we used a florescent stereo microscope Zeiss Lumar V12. The specimens were observed and imaged while submerged in PBS (30% sucrose with azide). Both white and florescent lights were used to image the embryos, depending on the type of image of interest.

All GFP Chick-wt Chick embryos were imaged at 9,6X magnification in 6 orthogonal views: anterior, posterior, dorsal, ventral, left and right. Additional details and particular views were also photographed, if considered relevant.

The software ImageJ was used to analyze and post-process the resulting images.

Computed Tomography

Synchrotron radiation-based micro-computed tomography

The eggs were scanned using a microtomography (μ CT) set-up on the beamline ID17 and ID19 of the European Synchrotron Radiation Facility (ESRF, Grenoble, France). After an unsatisfactory test consisting of scanning the whole nest structure, we aimed for scanning eggs individually, as far as physical preparation would allow it. The first test on

egg 9 was performed on ID19 using filtered white beam (Wiggler 150B with a 55 mm gap; filters: Al= 2.8 mm, Cu= 1.2 mm) with an energy of 108 keV. The experimental set-up included a sample-detector distance of 13 m for propagation phase contrast synchrotron radiation μ CT (PPC-SR- μ CT); an optical instrument (with a 750 μ m thick LuAG scintillator) associated to a FReLoN.2k ccd camera generating images with a pixel size of 12.63 μ m; the size of the beam adjusted with slits to the optical instrument, giving a image of 600 pixels in vertical and 2048 pixels in horizontal. The center of rotation was shifted by about 5 mm, adding 800 pixels in horizontal field of view to the reconstructed tomography (i.e., half-acquisition geometry protocol). Given the limited vertical field of view (\sim 7.6 mm), several scans were needed to cover the height of the egg. The sample was moved by 3 mm in vertical between each scan, the important overlap being used to reduce ring artifacts and attenuate differences in spectrum and power along the beam vertical profile (Pierce et al., 2013). The acquisition of each scans consisted of 4998 projections of 0.15 seconds each, over 360 degrees. All other eggs were scanned on the ID17 beamline with a relatively similar protocol: monochromatic beam (bent double-Laue Si 111 crystals) of 100 keV; sample-detector distance of 10 m for PPC-SR- μ CT; FReLoN.2k camera with an optical instrument recording images with a pixel size of 13.63 μ m (750 μ m LuAG scintillator); beam size adjusted to record images of 500 pixel in vertical by 2048 pixel in horizontal; centre of rotation shifted by 800 pixels for half-acquisition protocol; displacement of 3.5 mm in vertical direction between each scans. The acquisition of each scan consisted of 4998 projections of 0.2 seconds each, over 360 degrees.

The tomographic reconstruction was done using the PyHST2 code (Mirone et al., 2014) with a single distance phase retrieval procedure (Paganin et al., 2002). The resulting EDF stack was converted to a TIF

stack by stretching the 32-bit range of raw gray values into a full range of 16-bit values. The final TIF stack was generated from the concatenation of all scans for a given sample, to which we applied a ring artifact filter (Lyckegaard et al., 2008).

Segmentation of the data for three-dimensional rendering was performed following the procedure introduced by Ni et al. (2012).

Tomography Data Processing

Data processing was done with Amira V5.3 software (Visualization Sciences Group, France) and included: (i) manual segmentation of different bones, either by using the “magic wand”, or “lasso”, or “brush” tools (ii) surface reconstruction of the individual segmented bones, using constrained smoothing with a minimal edge length of 0.4, and (iii) superimposition of each bone onto the skeleton of *Crocodylus niloticus* at 39 days of incubation stage (39D).

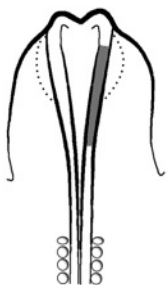
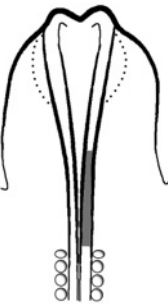
For *Crocodylus niloticus* the grayscale values of bone and eggshell are markedly higher from those of any other structure of the specimen. Firstly, we removed the eggshell (with a binary masking tool in Amira) so that when thresholding the grayscale values of the eggshell they would not be confounded with those of bone. The segmentation mask threshold used for isolating the bone in the scans of *C. niloticus* was calculated using the minimum grayscale value between the thresholds calculated by the algorithms “RenyiEntropy” (Kapur et al. 1985) from auto threshold tool in Fiji. “RenyiEntropy” (Kapur et al. 1985) are ranked among the best image thresholding algorithms by Sezgin and Sankur (2004). However, when we used the RenyiEntropy thresholding algorithm in *C. niloticus* 33d, due to the very early ossification stage, thus lack of contrast with the surrounding matrix, we opted to segment the embryonic bones manually to obtain the correct bone morphology.

We made three measurements for each variable using the 3D measurement tool and the surface cut option to calculate bone thicknesses for example.

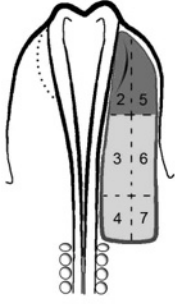
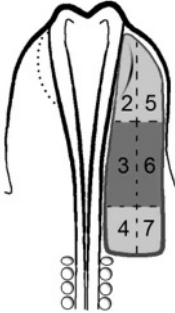
Appendix B

Chapter I supplementary data

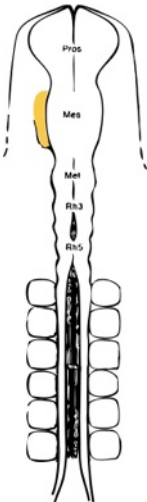
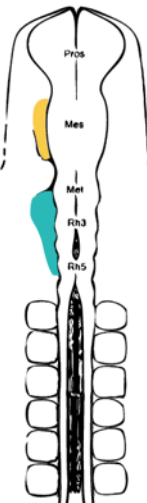
Neural crest

Graft	GFP (somites)	Wt (somites)	Age of sacrifice	Embryo code
	4-5	4-5	8D + 15h	45
	n.r.	n.r.	14D aprox	68
	7	7	9D + 6h	69
	4	4	15D aprox	76
	5	5	11D + 6h	1*
	8	8	10D + 16h	4
	8	8	10D + 16h	5
	5	6	10D + 2h	11
	5	5-6	10D + 8h	12
	8-9	11	10D + 17h	13
	5	5	10D + 17h	16
	7	7-8	13D + 16h	21
	10-11	8	14D + 15h	26
	3	4	13D + 16h	27
	5	5	8D + 17h	29
	5	5	8D + 17h	30
	8	8	9D + 20h	36
	7	7	9D + 20h	37
	4	4	8D + 15h	42
	4-5	4	8D + 15h	50
	7	7	9D + 6h	57
	10	9	7D + 13h	62
	9	8	9D + 6h	66
	7	7	15D aprox	73
	4	4	15D aprox	74
	4	4	15D aprox	76
	4	5	8D + 9h	79*
6	6	15D + 10h	86	
6	6	3D + 18h	103	

Mesoderm (first part)

Graft	GFP (somites)	Wt (somites)	Age of sacrifice	Embryo code
	4/5	4	15D + 8h	133
	4	4	7D + 8h	158*
Couly 2/5				
	5	6	9D + 6h	70
	4	4	14D aprox	71
	6	6	9D + 13h	84
	4	4	9D + 13h	89
	5	5	19D + 11h	94
	6	6	14D aprox	97
	5	5	14D aprox	98
	5	5	8D aprox	99
	4	4	3D + 18h	103
	5	5	3D + 18h	105
	5	5	16D + 11h	108*
	2	7-8	12D + 9h	130*
	2	2	16D + 9h	131
	3	3	10D + 8h	140*
	3	3	15D + 8h	145
	4	4	15D + 8h	146
	4	4	14D aprox	151**
	4	4	14D aprox	152*
	4	3	10D + 8h	156*
	4-5	5-6	11D + 8h	157*
	4	5	7D + 8h	159*
	5	5	13D + 8h	170
	3	3	10D + 8h	171*
	4	4	13D + 8h	172
	4	4	13D + 8h	173
				
Couly 3/6				

Mesoderm (second part)

Graft	GFP (somites)	Wt (somites)	Age of sacrifice	Embryo code
 <p>Noden FZ</p>	6	6	16D + 9h	124
	6	6-7	8D + 9h	125*
	5	5	16D + 9h	128*
	4	4	15D + 8h	146
	6-7	6	13D + 8h	137*
	5	5	8D + 8h	168*
 <p>Noden FZ + PZ</p>	6	6	9D + 9h	126*
	6	6	8D + 9h	127*
	6	6-7	14D + 8h	154
	5	5	8D + 8h	167*
	5	5	6D + 8h	169*

* Age of sacrifice might be overestimated since these embryos were collected dead at egg opening (but were alive 24h before).

**Transplant was made at Couly zone 4/7 and not 3/6.

n.r. – not registered.

Chapter II supplementary data

Table showing measures of eggs corresponding to ML 1582.

Egg #	Major axis (μm)	Minor axis (μm)
Egg 1	39157	24379
Egg 2	N.A.	N. A.
Egg 3	43281	25597
Egg 4	41939	25352
Egg 5	40848	27301
Egg 6	40385	27179
Egg 7	43629	24605
Egg 8	30256	23458
Egg 9	43456	28534
Egg 10	N.A	N.A
Egg 11	38646	19524
Egg 12	42107	25306
Egg 13	38251	26670
Average	40178	25264
Standard Deviation	3809	2409

Table showing measures of appendicular bones in ML 1582 and *Crocodylus niloticus*.

Measurement (μm)	Extinct	<i>C. niloticus</i> 39d Scaled to extinct	<i>C. niloticus</i> 45d Absolute measures
Femur Length #1	2671	1586	3680
Measurement # 2	2726	1615	3772
Measurement # 3	2785	1547	3610
Average	2727	1583	3687
Standard deviation	57	34	81
Femur Midshaft Diameter #1	507	434	642
Measurement # 2	488	370	809
Measurement # 3	491	389	691
Average	495	398	714
Standard deviation	10	33	86
Femur midshaft bone thickness #1	160	91	129
Measurement # 2	144	81	106
Measurement # 3	107	68	201
Average	137	80	145
Standard deviation	27	12	50
Humerus Length #1	2227	1231	3456
Measurement # 2	2178	1198	3345
Measurement # 3	2220	1137	3307
Average	2208	1189	3369
Standard deviation	27	48	77
Humerus Midshaft Diameter #1	420	370	750
Measurement # 2	406	326	665
Measurement # 3	406	369	724
Average	411	355	713
Standard deviation	8	25	44
Humerus midshaft bone thickness #1	117	102	120
Measurement # 2	51	98	57
Measurement # 3	126	45	50
Average	98	82	76
Standard deviation	41	32	39

